

Electronic Thesis and Dissertation Repository

---

3-9-2020 2:15 PM

# The effects of Chronic Inflammatory Demyelinating Polyneuropathy on the Neuromuscular System in Humans

Kevin J. Gilmore, *The University of Western Ontario*

Supervisor: Charles, Rice, *The University of Western Ontario*

A thesis submitted in partial fulfillment of the requirements for the Doctor of Philosophy degree in Kinesiology

© Kevin J. Gilmore 2020

Follow this and additional works at: <https://ir.lib.uwo.ca/etd>



Part of the [Medicine and Health Sciences Commons](#), and the [Neuroscience and Neurobiology Commons](#)

---

## Recommended Citation

Gilmore, Kevin J., "The effects of Chronic Inflammatory Demyelinating Polyneuropathy on the Neuromuscular System in Humans" (2020). *Electronic Thesis and Dissertation Repository*. 6921. <https://ir.lib.uwo.ca/etd/6921>

This Dissertation/Thesis is brought to you for free and open access by Scholarship@Western. It has been accepted for inclusion in Electronic Thesis and Dissertation Repository by an authorized administrator of Scholarship@Western. For more information, please contact [wlsadmin@uwo.ca](mailto:wlsadmin@uwo.ca).

## Abstract

Chronic Inflammatory Demyelinating Polyneuropathy (CIDP) is an inflammatory autoimmune peripheral nerve disorder. CIDP is associated with demyelination, slow motor nerve-conduction velocity, and distal muscle weakness. CIDP is under-recognized due to its heterogeneous presentation and the limitations of clinical diagnostic criteria. Using a combination of electrophysiology and muscle imaging techniques the four studies outlined in this thesis systemically investigate the impacts of this demyelinating disease on motor nerves and their innervated muscles.

The first two studies examine the neuronal consequences of demyelination caused by CIDP and the following two studies investigate how skeletal muscle is affected by these neuronal complications. Specifically, the purpose of study 1 was to investigate whether patients with CIDP demonstrate motor unit loss, and to determine the neuromuscular transmission stability of motor units. Results showed patients with CIDP have reduced motor unit number estimates (MUNEs), in addition to motor unit instability and transmission blocking in the tibialis anterior (TA) muscle. The purpose of study 2 was to investigate modifications to motor unit discharge characteristics of affected motor units. The results indicate CIDP leads to axonal or neuromuscular block and abnormally high motor unit firing rates of early recruited motor units as a compensatory mechanism to mitigate the frank neuronal loss in the TA.

The purpose of studies 3 and 4 was to assess the consequences of peripheral axon loss and motor unit instability on muscle quality and quantity in patients with CIDP. It is critical to investigate whether these neuronal changes precipitate uniform alterations in

musculature. Study 3 showed that patients with CIDP have less overall muscle mass and more non-contractile tissue infiltration in the TA of the anterior leg compartment. Study 4, demonstrated that muscles in the posterior leg compartment, that differ functionally from the TA and are innervated by a different portion of the sciatic nerve undergo similar morphological changes to the TA. In combination, these neuronal deficits and skeletal muscle structural abnormalities likely lead to muscle weakness and functional impairment seen in patients with CIDP. Together these studies form a foundational understanding of how CIDP impacts both nervous and muscle tissue at a systems level.

## Keywords

Chronic Inflammatory Demyelinating Polyneuropathy (CIDP); peripheral nervous system; muscle; human; weakness; motor unit; electromyography (EMG); magnetic resonance imaging (MRI).

## Summary for Lay Audience

Chronic inflammatory demyelinating polyneuropathy (CIDP) is an ultra rare immune mediated neurological disorder in which there is inflammation of peripheral nerves and destruction of the fatty protective covering (myelin sheath) surrounding the nerves, which affects how fast the nerve signals are transmitted to their attached muscles. This causes weakness, paralysis and/or impairment in motor function, especially of the arms and legs. Sensory disturbance may also be present. The motor and sensory impairments usually affect both sides of the body (symmetrical), and the degree of severity and the course of disease may vary greatly among individuals. Tests that can be of diagnostic help include nerve conduction testing and electromyography that demonstrate slow nerve conduction velocities, lumbar puncture with evidence of elevated spinal fluid protein and magnetic resonance imaging (MRI) of the nerve roots looking for enlargement and signs of inflammation. Despite this there is a lack of awareness and knowledge surrounding a specific cause and disease mechanism in CIDP making diagnosing the disease very difficult.

To date no studies have systematically investigated the neuronal and musculoskeletal consequences of this nerve disease. Therefore, it is critical to study the function of the peripheral nerves in this inflammatory disorder as well as their connection to skeletal muscle. In this work I investigated two main phenomenon related to CIDP. The first two studies of this thesis quantify the loss of motor nerves as well the health of the remaining motor nerves in response to the demyelinating process. The two subsequent studies investigate the repercussions of motor unit loss on the amount and quality of the muscles attached to these unhealthy nerves. The findings from this work demonstrate that patients

with CIDP not only have fewer motor units; the remaining motor units are very unhealthy. This reduction of motor units in combination with the poor connection these motor units have with their attached muscle leads to major losses in the amount and quality of muscle tissue. Overall, this work provides compelling evidence for the reasoning behind the functional strength decrements patients exhibit with CIDP.

## Co-Authorship Statement

This thesis contains material from published manuscripts (Chapters 2, 4, and 5). On all manuscripts, Kevin J Gilmore was the first author and, Dr. Kurt Kimpinski, Dr. Timothy J. Doherty and Dr. Charles L. Rice were co-authors. Eric Kirk was a co-author on Chapter 3 and Jacob Fanous was a co-author on Chapter 5. All experimental data in Chapters 2, 3 and 4 presented in this thesis were collected, analyzed, and interpreted by Kevin J Gilmore. With oversight, Jacob Fanous analyzed all control and patient MRI data in Chapter 5 that were originally collected and subsequently interpreted by Kevin J. Gilmore.

## Acknowledgments

First and foremost I want to thank my doctoral supervisor, mentor, and friend, Dr. Charles Rice, for your guidance and supportive role throughout my research studies. Your humble and active approach to mentoring has been a valuable influence on my graduate student training and research and I cherish the times spent in the Neuromuscular Laboratory.

A special thank you to my PhD advisory committee: Dr. Kurt Kimpinski, Dr. Brian Allman, and Dr. Tim Doherty for your valuable insights, and overall guidance with regard to my research interests. Kurt Kimpinski and Tim Doherty played a critical clinical role as physicians in the success of my thesis projects. Kurt was the lead clinician scientist during my PhD studies and played a vital role in patient recruitment and without this relationship these studies would not have been possible.

To the current and past members of the Neuromuscular Laboratory Matti, Colin, Eric, Dave, Kalter, and Jacob, thank you all for your valuable insights, and support over my years of study. You all make for a successful learning environment.

I would also like to thank my family, friends and partner for their unwavering and caring support throughout my studies.

Lastly, none of this work would have been possible without the patient and control participants. Thank you to all involved

*“Biology cannot go far in its subjects without being met by mind.”*  
- **Sir Charles Sherrington**

# Table of Contents

Abstract.....	ii
Summary for Lay Audience.....	iv
Co-Authorship Statement.....	vi
Acknowledgments.....	vii
Table of Contents.....	viii
List of Tables.....	xii
List of Figures.....	xiii
List of Appendices.....	xiv
List of Abbreviations.....	xv
Chapter 1.....	1
1 General Introduction.....	1
1.1 The Neuromuscular System Anatomy/Physiology and the Motor Unit in Humans.....	1
1.1.1 Neuromuscular System.....	1
1.1.2 The Motor Unit.....	2
1.2 Schwann Cells, the Myelin Sheath and Saltatory Conduction.....	5
1.3 Chronic Inflammatory Demyelinating Polyneuropathy (CIDP).....	7
1.3.1 Clinical Diagnosis.....	8
1.3.2 Differential Diagnosis.....	9
1.3.3 Pathology of CIDP.....	10
1.3.4 Treatment of CIDP.....	12
1.3.5 Functional Consequences of CIDP.....	13
1.4 Motor Unit Number Estimations (MUNE) Using Decomposition-based Quantitative Electromyography (DQEMG).....	14



1.5	Intramuscular Needle Electromyography .....	18
1.6	Magnetic Resonance Imaging (MRI).....	19
1.7	Purposes and Hypotheses.....	21
1.8	References.....	23
Chapter 2.....		32
2	<sup>1</sup> Electrophysiological And Neuromuscular Stability Of Persons With Chronic Inflammatory Demyelinating Polyneuropathy (CIDP).....	32
2.1	Introduction.....	32
2.2	Methods.....	35
2.2.1	Subjects.....	35
2.2.2	Dorsiflexor Strength and Tibialis Anterior DQEMG Data Acquisition ...	36
2.2.3	Data Analyses .....	38
2.2.4	Near-fiber Parameters .....	39
2.2.5	Statistics .....	40
2.3	Results.....	41
2.4	Discussion.....	47
2.5	Conclusion .....	50
2.6	References.....	51
Chapter 3.....		58
3	<sup>1</sup> Abnormal Motor Unit Firing Rates In Chronic Inflammatory Demyelinating Polyneuropathy .....	58
3.1	Introduction.....	58
3.2	Methods.....	60
3.3	Subjects.....	60
3.3.1	Patient Electrodiagnostic Criteria .....	60
3.3.2	Strength and Experimental Set-up .....	61

3.3.3	Electromyography.....	61
3.3.4	Data Analysis and Statistics.....	63
3.4	Results.....	65
3.5	Discussion.....	72
3.6	Conclusion.....	75
3.7	References.....	77
4	<sup>1</sup> Reductions In Muscle Quality And Quantity In CIDP Patients Assessed By Magnetic Resonance Imaging.....	80
4.1	Introduction.....	80
4.2	Methods.....	82
4.2.1	MRI Measures.....	83
4.2.2	TA Total Volume, Muscle Composition, and T2 Relaxation Times.....	84
4.2.3	Strength Assessment.....	85
4.2.4	Statistics.....	86
4.3	Results.....	86
4.4	Discussion.....	92
4.5	References.....	96
Chapter 5	.....	100
5	<sup>1</sup> Nerve Dysfunction Leads To Muscle Morphological Abnormalities In Chronic Inflammatory Demyelinating Polyneuropathy Assessed By MRI.....	100
5.1	Introduction.....	100
5.2	Methods.....	102
5.2.1	Strength Assessment.....	103
5.2.2	MRI Measures.....	104
5.2.3	Triceps Surae Total Volume, Muscle Composition, and T2 Relaxation Times.....	105

5.2.4	Statistics .....	106
5.3	Results.....	107
5.4	Discussion.....	114
5.5	References.....	119
6	General Discussion and Summary .....	125
6.1	General Discussion .....	125
6.2	Limitations .....	129
6.3	Future Directions .....	132
6.4	Summary and Significance .....	134
6.5	References.....	135
	Appendices.....	140
	Curriculum Vitae .....	144

## List of Tables

Table 2.1 Participant characteristics .....	42
Table 2.2 CIDP clinical classification .....	43
Table 2.3 Dorsiflexor strength and tibialis anterior MUP and MUNE parameters. ....	44
Table 2.4 Neuromuscular transmission stability and near-fiber parameters.....	45
Table 3.1 Subject characteristics.....	67
Table 3.2 CIDP clinical features.....	68
Table 3.3 Motor unit data.....	69
Table 4.1 Participant characteristics .....	87
Table 4.2 CIDP clinical features.....	88
Table 4.3 Strength, electrophysiology, and imaging parameters.....	90
Table 5.1 Participant characteristics .....	108
Table 5.2 CIDP clinical classification .....	109

## List of Figures

Figure 1.1 The motor unit .....	3
Figure 1.2 Saltatory conduction .....	7
Figure 1.3 Axonal damage in CIDP .....	11
Figure 2.1 Motor unit potential train raster plots .....	46
Figure 3.1 Example of tungsten needle recording during a contraction .....	70
Figure 3.2 Scatter plot of MUFR .....	71
Figure 3.3 Histograms of MUFR means .....	72
Figure 4.1 MRI cross section of left leg .....	91
Figure 4.2 T2 relaxation times .....	91
Figure 4.3 T2 maps .....	92
Figure 5.1 Total muscle volume of triceps surae .....	110
Figure 5.2 Total contractile volume triceps surae .....	111
Figure 5.3 T2 relaxation times of triceps surae .....	112
Figure 5.4 MRI T1 cross section of triceps surae .....	113
Figure 5.5 MRI T2 cross section of triceps surae .....	113

## List of Appendices

Appendix A: CIDP Ethics approval.....	140
Appendix B: License terms and conditions .....	141

## List of Abbreviations

APs - action potentials

AIDP - acute inflammatory demyelinating polyradiculoneuropathy

ALS - amyotrophic lateral sclerosis

BMI – body mass index

CSF - cerebrospinal fluid

CIDP - chronic inflammatory demyelinating polyneuropathy

CMAP - compound muscle action potentials

CT - computerized tomography

CV - conduction velocity

DQEMG - decomposition-based quantitative electromyography

EFNS - the European Federation of Neurological Societies

EMG – electromyography

EAN - experimental autoimmune neuritis

GBS - Guillain-Barré syndrome

ITT - interpolated twitch technique

INDs – internodes

IVIG - intravenous immunoglobulin

JXP – juxtaparanodes

LG - lateral gastrocnemius

LMN - lower motoneuron

MRI - magnetic resonance imaging

MTR- magnetization transfer ratio

MVC - maximal voluntary contraction

MG - medial gastrocnemius

MUAPs - motor unit action potentials

MUAPTs - motor unit action potential trains

MUNE - motor unit number estimate

MU – motor unit

MUNIX - motor unit number index

MUFR - motor unit firing rates

MS - multiple sclerosis

NF - near-fiber

NMJ - neuromuscular junction

ONLS - overall neuropathy limitations scale

PNJ - paranodal junction

PNS - peripheral nervous system

PE - plasma exchange

RF - radio frequency

ROI- region of interest

SNAP - sensory nerve action potentials

SFEMG - single fiber EMG

SL - soleus

SMUP - surface motor unit potential

sEMG - surface electromyography

TA - tibialis anterior



TR - repetition time

TE - time to echo

UMN – upper motorneuron

# Chapter 1

## 1 General Introduction

Beginning in the early eighteenth century, neurobiologists attempted to discover a link between electricity and how nerves function. Luigi Galvani took the first steps in laying the foundation of modern electrophysiology by demonstrating the presence of electricity in dissected frogs<sup>1</sup>. Julius Bernstein and Emil du Bois-Reymond, in 1843 were the first to accurately describe a phenomenon called the action potential<sup>2,3</sup>. Throughout the next half-century, others went on to show that nerve and muscle tissues generate electrical transients that accompany this nervous excitation. Although the field of neuroscience has progressed immensely our comprehension of numerous components within neuromuscular physiology continue to elude our understanding. Specific amongst these, are inquiries concerning the influences disease has on nerves and what consequences these nerve abnormalities have on connected muscle. A more comprehensive appreciation regarding neuromuscular disease processes may ultimately lead to early diagnosis or enhanced treatment options allowing individuals with nerve diseases the opportunity to mitigate the devastating consequences of muscle atrophy.

### 1.1 The Neuromuscular System Anatomy/Physiology and the Motor Unit in Humans

#### 1.1.1 Neuromuscular System

The neuromuscular system, composed of nerves and muscles, provides humans with the means to coordinate movement and is essential in controlling posture and gait.

Specifically, the neuromuscular system is responsible for transmitting signals from the central nervous system (brain and spinal cord) to skeletal muscle and is comprised of a

circuit of motor neurons and skeletal muscles. Electrical impulses elicited in the motor neuron's cell body propagate along the motor axon and result in the release of the neurotransmitter, acetylcholine, from the motor nerve terminal at a synaptic connection, termed the neuromuscular junction. The neurotransmitter molecules of acetylcholine diffuse across this neuromuscular junction and bind acetylcholine receptors on the muscle fiber. The binding results in the opening of ion channels within the muscle fiber, thus altering the muscle membrane potential. This muscle membrane depolarization then triggers a release of internal calcium ions that leads to a cascade of events resulting in skeletal muscle contraction<sup>4</sup>. The neuromuscular system is substantially more complex than outlined above and many questions remain unanswered. Investigation of modifications to nerves and muscles due to disease (e.g. demyelinating polyneuropathies) can provide useful insight into basic neuromuscular pathophysiology and the mechanisms responsible for the functional limitations seen in patients. Of most interest to the study of neuromuscular diseases and the focus of this dissertation is this vital connection between the nerves and their accompanied muscle.

### 1.1.2 The Motor Unit

A single motor unit is composed of an individual motor axon called an  $\alpha$ -motor neuron, and all skeletal muscle fibres innervated by this distinct axon. In humans there are two major types of motor units: type I and type II. Fundamentally, small motor units have smaller axon diameters, fewer fibers that make up the complete unit, and are more resistant to fatigue. These motor nerves innervate slower muscle fibers and are referred to as type I motor units. Large motor nerves innervate larger, faster muscle fibers that are less resistant to fatigue and are referred to as type II motor units. The number of muscle

fibers in a specific motor unit is directly correlated to the size of the motor neuron for that unit<sup>5</sup>. The size of a motor unit is defined by the number of muscle fibres it innervates and varies significantly in different motor units from dozens of muscle fibres per unit to thousands of muscle fibres per unit (Figure 1.1)<sup>6</sup>.

A small motor unit's cell body located in the ventral horn of the spinal cord has a low excitation threshold to cause an action potential. Therefore, less excitation input is required for small cell bodied neurons and a motor unit that has a smaller cell body also has a smaller nerve fiber that innervate fewer muscle fibers when activated. For this reason specifically, smaller, type I motor units are more easily discharged and are also more impervious to fatigue. Conversely, larger type II motor units can activate hundreds of muscle fibers collectively with a single action potential from a motor neuron<sup>7</sup>. Due to their direct relationship, muscle fibers are commonly referred to by their motor unit type.

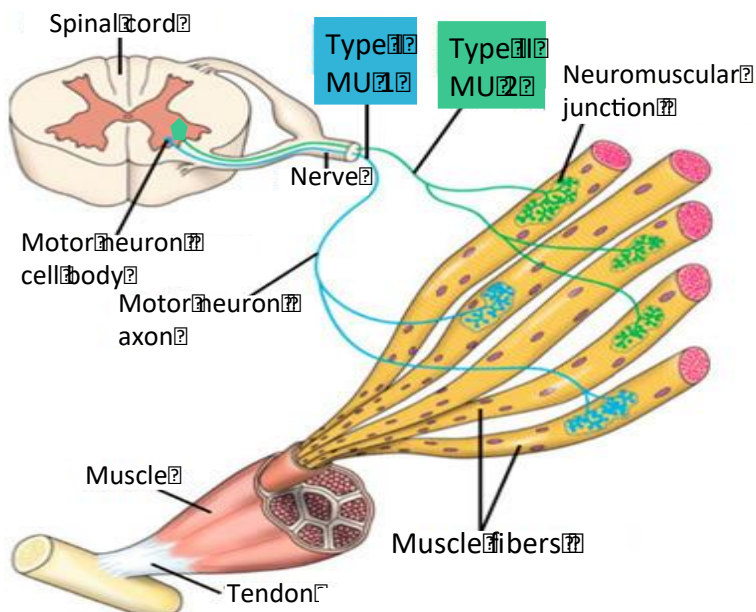


Figure 1.1 The motor unit

Two separate motor units are depicted (Type I and Type II).  $\alpha$ -motor neuron cell bodies are located in the ventral horn of the spinal cord. The axon exits the ventral horn into the periphery and synapses with their respective muscle fibers at the neuromuscular junction. Each motor unit is composed of an individual  $\alpha$ -motor neuron and all attached muscles fibers. Adapted from: Ko 2001 <sup>4</sup>

Skeletal muscles composed of smaller motor units are capable of finer, more accurate control. This would be advantageous for small muscles required for refined movements such as muscles in the hand. Alternatively, motor nerves innervate larger muscles responsible for gross or powerful movements <sup>8,9</sup>. The force exerted by a muscle during a voluntary contraction depends on the number of motor units that are activated and the rates at which these motor units discharge action potentials. These two properties of voluntary contractions are known as recruitment and rate coding. At low levels of voluntarily muscle contraction, smaller type I motor units are generally recruited prior to larger type II motor units, a concept referred to as the Henneman size principle <sup>6,8</sup>. The Henneman size principle states that the recruitment of motor units within a muscle proceeds from small motor units to large motor units. Small motor units have low thresholds of activation and are recruited first. Larger motor units with higher thresholds of activation follow are recruited later <sup>10</sup>.

In contrast, rate coding refers to the modulation of motor unit action potentials whereby the force of a muscle fibre is modified by increasing or decreasing the frequency at which motor neurons discharge to their coupled muscle fibres <sup>11</sup>. Experimental evidence suggests that recruitment is the more significant factor at low forces, whereas rate coding is more responsible for changes in muscle force at intermediate and high forces <sup>10</sup>.

## 1.2 Schwann Cells, the Myelin Sheath and Saltatory Conduction

Schwann cells are derived from neural crest cells, and are of two types: myelinating or non-myelinating Schwann cells. Myelinating Schwann cells form a tightly wrapped lipid bilayer that surrounds the motor axon composed of specialized protein constituents and is structurally and electrically critical for the propagation of nerve impulses and axonal maintenance<sup>12</sup>. Schwann cells also play a pivotal role in maintaining the nervous system and are vital in motor axon regeneration. The presence of myelin along the length of the  $\alpha$ -motor neuron is essential to maintain conduction velocity; its loss or damage can lead to significantly slower conduction or conduction block. In certain peripheral neuropathies, electrical propagation blockade may be the preliminary event in the cascade of events leading to the loss of Schwann cells in a process called demyelination<sup>14</sup>. Along the length of an  $\alpha$ -motor neuron the myelin sheath formed by Schwann cells is interrupted at regular intervals (nodes of Ranvier) where the axon membrane containing voltage gated sodium channels is exposed to the extracellular environment<sup>14</sup>. The propagation of action potentials along the length of motor axons relies on the collaborative action of these membrane-spanning selectively permeable ion channels<sup>15</sup>. Specifically, myelinated  $\alpha$ -motor neurons feature an extremely organized distribution of voltage-gated ion channels, with a characteristic clustering of Na<sup>+</sup> channels at the nodes of Ranvier. Saltatory conduction in myelinated axons refers to the rapid propagation of the electrical waveform from each node to the next. In this process myelinated axons only permit action potentials to transmit at the unmyelinated nodes of Ranvier. This ionic restriction allows saltatory conduction to propagate an action potential along the motor axon at rates significantly higher than would be achievable in the absence of myelination.

As sodium rushes into the node it creates an electrical diffusion gradient, which drives the ions contained within the axon's cytoplasm <sup>16</sup>. This rapid conduction of ionic signaling reaches the next node and generates another action potential, thus revitalizing the electrical signal (Figure 1.2). In this manner, saltatory conduction allows electrical nerve signals to be propagated along the axon length almost instantaneously without any degradation of the signal <sup>16,17,18</sup>. Focal disruption (segmental demyelination) of the myelin sheath can lead to failure of impulse conduction in the denuded axon segments (termed conduction block) in part because of a paucity of voltage-gated sodium ion channels between the nodes of Ranvier. Conduction block is a feature of many demyelinating conditions.

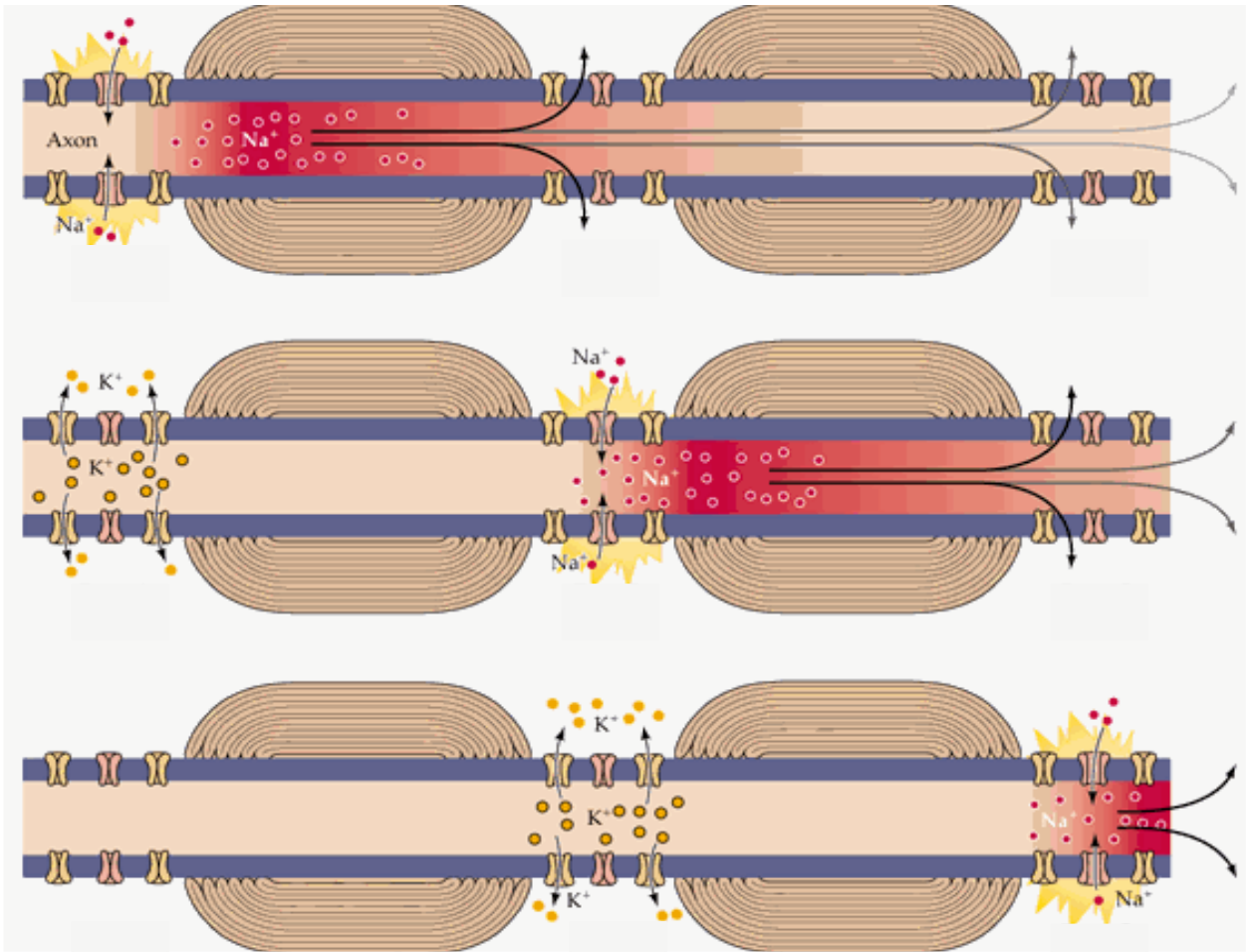


Figure 1.2 Saltatory conduction

Schematic depicts an action potential propagation down the length of an axon by method of saltatory conduction. As sodium rushes into the node it creates an electrical force that pushes on positively charged ions already inside the axon. This rapid conduction of electrical signal reaches the next node and creates another action potential refreshing the action potential. Saltatory conduction allows electrical nerve signals to be propagated at high rates, long distances. Adapted from: Rash et al 2016 <sup>18</sup>

### 1.3 Chronic Inflammatory Demyelinating Polyneuropathy (CIDP)

Chronic inflammatory demyelinating polyneuropathy (CIDP) is a rare neurological disorder characterized by inflammation of nerve roots and peripheral nerves and destruction of the myelinating Schwann cell covering the axon. The reported prevalence



of CIDP ranges from 0.7 to 10.3 cases per 100,000 people <sup>19</sup>. CIDP primarily affects adults and the incidence rises with advancing age. Although not well established there seems to be a male predominance and an age of onset is not known. No specific predisposing factors for CIDP have been identified <sup>20</sup>. There is heterogeneity in clinical phenotypes in CIDP, and it may not be a discrete disease entity but rather a spectrum of discrete albeit related conditions. Commonly reported phenotypes of CIDP include motor and sensory nerve dysfunction, with motor deficits reported in up to 94% of patients and sensory deficits in up to 89% <sup>21</sup>. The prognosis of CIDP is variable and is reminiscent of multiple sclerosis in its heterogeneity. Some patients (20-65%) <sup>22</sup> follow a relapsing remitting course, others a more progressive course. Over time, most patients without associated confounding conditions respond to treatment.

### 1.3.1 Clinical Diagnosis

The diagnosis of CIDP depends on a combination of clinical and electrophysiological criteria. The European Federation of Neurological Societies (EFNS)/Peripheral Nerve Society (PNS) guidelines were developed for clinical and research use <sup>22</sup>. The EFNS criteria combine clinical features in combination with electrophysiological evidence to define CIDP. In addition to the guidelines, supportive criteria include: elevated cerebrospinal fluid (CSF) protein, gadolinium enhancement of nerve roots or plexus on magnetic resonance imaging (MRI) in addition abnormal nerve biopsy findings provide complementary diagnostic evidence. In abnormal nerve biopsies thinly myelinated large axons are most frequently observed. Importantly, electrodiagnostic evidence of peripheral nerve demyelination specifically in motor nerves is required for diagnosis. Segmental demyelination and remyelination are also hallmarks of CIDP and repetitively over time

lead to onion bulb formations by proliferation of Schwann cell processes covering motor axons.

For a definitive diagnosis of CIDP the following electrophysiological indications must be identified in at least two nerves: latency prolongation, reduction of motor conduction velocity, prolongation of F-wave latency reduced compound muscle action potentials (CMAPs), and partial motor conduction block <sup>22</sup>. The features of CMAPs and conduction block and how they pertain to CIDP will be discussed in greater detail below. Clinical patient workup includes muscle strength evaluation (MRC 0-5 scale), Overall Neuropathy Limitations Scale (ONLS) score, ataxia score and 10-m walk test. Other tests and functional scales are used depending on symptoms (grip test, nine-hole peg test, and Inflammatory Neuropathy Cause and Treatment Sensory Sum Score). Although, other diagnostic guideline criteria have been suggested the EFNS/PNS criteria have demonstrated sensitivity and specificity for CIDP diagnosis and are currently the most commonly used <sup>23, 24</sup>.

### 1.3.2 Differential Diagnosis

CIDP is distinguished from acute inflammatory demyelinating polyradiculoneuropathy (AIDP) in that it is a monophasic disorder with nerve damage due to an immune response to a single (infectious) event as well as treatment responsiveness. Unlike AIDP, CIDP typically has a more indolent course and published criteria for CIDP recognize time to greatest weakness of longer than 8 weeks as the defining feature that differentiates CIDP from AIDP <sup>19</sup>. CIDP disease presentation is usually classified into three subtypes. A progressive form in that the disease continues to worsen over time regardless of

immediacy and type of treatment. A recurrent form that has episodes of symptoms that starts and stops over time and lastly a monophasic form. The monophasic form is defined as a single bout of the disease that has a duration of one to three years, but does not ever recur <sup>22</sup>. CIDP is often misdiagnosed as Guillain-Barré Syndrome (GBS), the most common form of AIDP, and for this reason finding more robust diagnostic criteria is critical to proper disease diagnosis and prognosis.

### 1.3.3 Pathology of CIDP

The principal theory of CIDP pathogenesis is that cell-mediated and humoral mechanisms act synergistically to cause damage to the peripheral nerves. Several lines of evidence support the conclusion that CIDP is an autoimmune disease mediated by cellular immunity against yet to be undefined Schwann cell myelin protein antigens. Some patients have reported infections prior to onset of neurological symptoms, however no specific trigger for the autoimmune response has been identified and no infectious agent has been consistently linked with initiation of CIDP <sup>25</sup>. There have been some recent advances in the area of the pathophysiological significance of autoantibodies directed specifically towards the nodal regions of peripheral axons in patients with CIDP. It has become clear that the anatomical and the molecular complexity of the node of Ranvier affects the ability of antibodies to bind and is the likely pathogenicity of the immune response in CIDP. In a normal, healthy axon, the myelin sheath wraps around the axon and ion channels are clustered in the unmyelinated nodes of Ranvier. This enables Saltatory conduction down the length of the axon. In CIDP, there is systemic infiltration of T-cells, B-cells, plasma cells, and macrophages, which lead to a cascade of events including the release of pro-inflammatory cytokines and antibodies, which are

destructive to both the myelin and axons (Figure 1.3). Axonal damage and neurodegeneration occur simultaneously with focal inflammation. There is ongoing demyelination due to antibodies against myelin antigens. Demyelination leads to the redistribution of ion channels, which impairs conduction along the axon. It is a combination of these events, rather than one in particular that contributes to neurodegeneration and axonal damage in CIDP <sup>25,26</sup>.

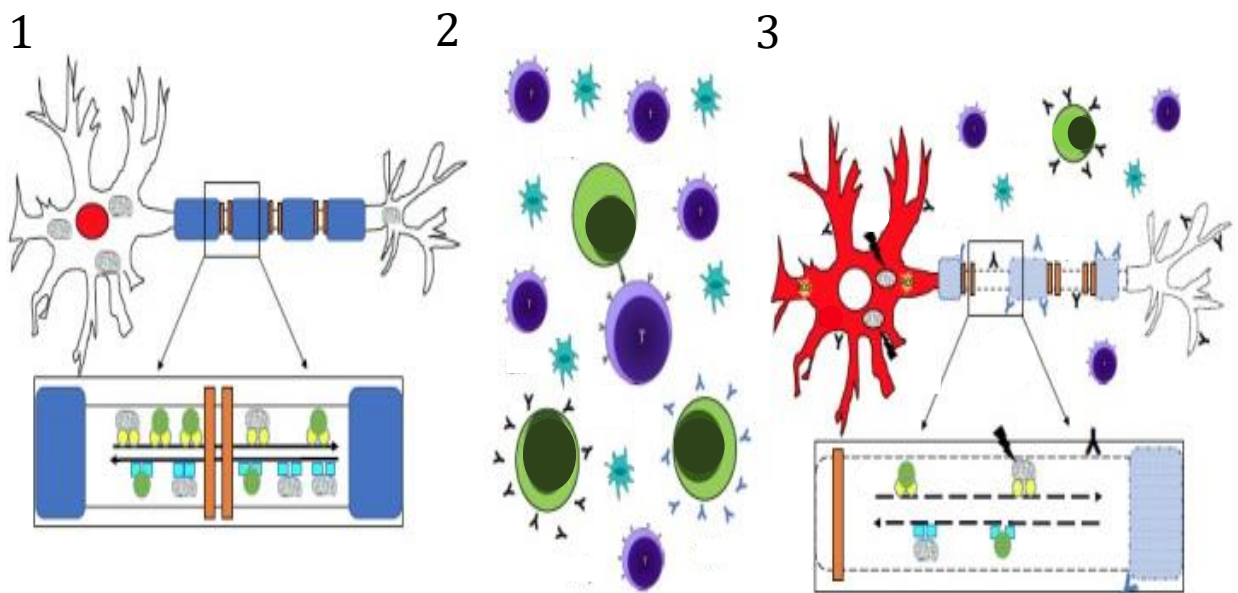


Figure 1.3 Axonal damage in CIDP

(1) Depiction of a healthy axon, the myelin sheath (blue) wraps around the axon and Na ion channels (orange) are clustered in the unmyelinated nodes of Ranvier. This enables saltatory conduction down the length of the axon. (2) Systemic infiltration of T-cells, B-cells, (purple cells) plasma cells (green cells), and macrophages (aqua cells) leading to a release of pro-inflammatory cytokines and antibodies (black and blue Y) that are destructive to both myelin and axons. (3) Ongoing demyelination due to antibodies against myelin antigens leads to the redistribution of ion channels that impairs action potential conduction along the axon. Adapted from: Salapa et al 2017 <sup>27</sup>

A combination of MRI, ultrasound and autopsy studies have established that the inflammatory lesions in CIDP arise predominantly in the spinal roots, proximal nerve

trunks and major plexuses and are often spread throughout smaller peripheral nerves <sup>25,26</sup>. However, due to the inaccessibility of proximal nerves and nerve roots for diagnostics, most clinical nerve biopsies are obtained from the sural nerve. Although the sural nerve is peripheral and located furthest from the most prominent inflammatory activity in the proximal nerve roots, pathophysiological changes in sural nerve biopsies reflect the broad spectrum of changes seen in CIDP. Pathological observations in sural nerve biopsies include demyelination, formation of onion bulbs, oedema, perivascular or endoneurial macrophage inflammatory infiltrates and T cells and axonal degeneration <sup>25,26</sup>. In blood and CSF of patients with CIDP studies have shown changes in the function and abundance of T cell subsets, altered expression of cytokines and other inflammatory mediators <sup>28,29,30</sup>. An animal model of CIDP called experimental autoimmune neuritis (EAN), demonstrates similar pathological changes to those observed in humans. This animal model of CIDP is induced in susceptible strains of rodents or rabbits by immunization with specific myelin proteins and is the result of an autoimmune attack on peripheral nerves mediated by macrophages and T-cells <sup>31</sup>.

#### 1.3.4 Treatment of CIDP

There are three conventional treatments prescribed for CIDP. Glucocorticoid drugs such as prednisone have proven effective in large patient trials. In many cases, individuals with CIDP may respond to glucocorticoid treatment alone <sup>32</sup>. However, individuals requiring high doses of glucocorticoid drugs may experience side effects that deter long-term therapy. Steroid drugs only act to reduce the inflammation and their long-term use in patients with CIDP has not been well-established <sup>32</sup>. Intravenous immunoglobulin (IVIG) has been also been proven to be effective and is often used as a treatment for

CIDP either alone or concurrently with glucocorticoids<sup>33,34</sup>. IVIG acts to suppress the proliferation of antigen-specific T cells, which diminishes the autoimmune insult on peripheral nerves. Lastly, plasma exchange (PE) has been shown in clinical trials to benefit individuals with CIDP<sup>33</sup>. The process of PE involves removing whole blood from an individual with CIDP and red blood cells are subsequently separated from plasma. The plasma is then replaced with healthy human plasma and the patient's blood cells are transfused back into the systemic circulation, thus removing only the plasma and its constituents. Importantly, IVIG and PE are effective only for a few weeks and may require chronic intermittent refresher treatments.

### 1.3.5 Functional Consequences of CIDP

Patients with CIDP can experience motor and or sensory disturbances and when combined can exacerbate functional consequences of the disease. Briefly, most individuals with CIDP experience some alterations of sensation causing sensory ataxia (loss of coordination) and paresthesia. Some patients only have sensory symptoms and signs but demonstrate typical abnormalities of nerve conduction and respond to treatment. This is considered the sensory variant of CIDP. Other common more severe systemic sensory symptoms include: chronic fatigue, pain, dysphagia, and diplopia. Importantly, gait will be abnormal and proprioceptive responses to various environmental sensory stimuli will be impaired. In cases of typical CIDP, motor decrements present symmetrically in a length dependent fashion with chronically progressive, stepwise or recurrent proximal and distal muscle weakness in all extremities. Although it is thought that the degree of muscle atrophy in CIDP is generally mild given the general severity and duration of weakness, some studies using computerized tomography (CT) have

shown patients to have muscle atrophy particularly in distal musculature <sup>36</sup>. Higher prevalence of muscle atrophy is reported amongst patients with longer disease durations or delayed treatment initiation. In patients with marked muscle atrophy, muscle weakness and atrophy primarily affect lower extremities, whereas in patients without marked muscle atrophy, the upper and lower limbs are equally affected <sup>37</sup>. Studies also establish that patient functional status (as determined by the MRS) are significantly worse in patients with discernable but not quantified muscle atrophy <sup>38</sup>. Overall, many individuals with CIDP are left with residual muscle weakness, tremors, fatigue, as well other symptoms that can lead to diminished quality of life and long-term morbidity.

#### 1.4 Motor Unit Number Estimations (MUNE) Using Decomposition-based Quantitative Electromyography (DQEMG)

Since the early days of neurophysiology research it has been recognized that the loss of motor units has been a crucial physiological process fundamental in various neuromuscular diseases <sup>39</sup>. Consequently, it has been of great interest to develop methodologies for *in vivo* quantification of functional motor units in a single muscle. Motor unit number estimate (MUNE) was developed to quantify the number of motor units in a specific muscle. Early MUNE techniques were developed to circumvent the limitations associated with standard clinical electrophysiological techniques, which only provided a qualitative physiological assessment of functional motor units. Since the original establishment of MUNE, the technique has been vastly improved <sup>39,40</sup>. In recent years, powerful digital signal processing capabilities have provided the impetus for developing new automated and semi-automated techniques designed to estimate the

number of functioning motor units *in vivo*<sup>41</sup>. MUNE is established upon the ratio between a maximal compound muscle action potential (CMAP) that is divided by a mean surface motor unit potential (SMUP)<sup>42</sup>. The CMAP signifies the absolute maximal electrophysiological size of the complete motor unit population within a muscle. The mean SMUP characterizes the absolute size of the average representative sample of a single motor unit<sup>34</sup>. Currently no gold standard methodology exists regarding counting human motor units or motor axons even with *in vitro* immunohistochemistry preparations.

Decomposition-based quantitative electromyography (DQEMG) is the quantitative *in vivo* assessment of motor unit action potentials from individual motor units and can provide valuable information in assessing the integrity of human motor units<sup>42</sup>. DQEMG incorporates a combination of intramuscular electromyography (EMG) and surface EMG to decompose complex EMG patterns into individual motor unit action potential trains<sup>41,43</sup>. This allows DQEMG software to deliver more detailed information for each motor unit train such as: motor unit size, shape, stability and most importantly the DQEMG software is used to acquire an estimate of the number of functioning motor units within a single muscle<sup>44,45</sup>. DQEMG uses two sources of EMG (micro and macro signals) to gain insightful information regarding specific motor unit characteristics<sup>45</sup>. Micro signals are gathered through intramuscular needle EMG electrodes. These micro EMG signals are usually collected via concentric needle electrodes during sustained 30-second volitional isometric contractions<sup>44,45</sup>. Originally this micro needle EMG signal, collected through low to moderate level muscle contractions, consists of complex EMG interference patterns from multiple simultaneously active motor units. DQEMG uses a series of



algorithms to decompose this complex micro EMG pattern into constituent individual motor unit action potential trains. Each action potential train belonging to a single motor unit is classified based on shape and firing rate variability <sup>43,44,45</sup>. Macro (surface EMG) signals are collected via surface electrodes, and provide EMG information regarding the overall size and spatial distribution of active individual motor units. By using each individual micro needle motor unit action potential train as a trigger for the macro signal, the macro signal is temporally aligned with the decomposed micro needle signal. Time locking of the macro EMG signal to the micro needle detected action potentials, allows for the derivation of SMUPs, which resemble the corresponding size of individual motor units within an active muscle and are used as the denominator in the MUNE calculation <sup>40</sup>.

Using DQEMG software to calculate a MUNE has been reported with high degrees of intra- and inter-rater reliability <sup>46,47,48,49</sup>. Numerous studies have shown that contraction intensity has a discernible effect on DQEMG derived MUNE calculations <sup>50</sup>. Studies executed in different muscles have found that with increasing contraction intensities mean SMUP size increases, which inversely decreases the MUNE for that specific muscle <sup>51</sup>. One study concluded that a contraction intensity of 25% of maximum voluntary contraction (MVC) in the tibialis anterior (TA) muscle, recruits a representative sample of low (type I) and high (type II) threshold motor units and thus provides the most representative motor unit number estimation in the TA muscle <sup>51,52</sup>. Importantly, DQEMG also conveys detailed electrophysiological data regarding the morphological characteristics of individual needle detected motor unit action potentials <sup>41,42</sup>. Morphological characteristics include: motor unit firing rates, motor unit firing rate

variability, motor unit action potential size (area and amplitude), motor unit action potential shape and complexity (turns, phases) and motor unit discharge stability (jitter, jiggle, and % blocking).

Increases in motor unit action potential complexity as well as increased action potential amplitude are electrophysiological indications of enlarged, collaterally reinnervated motor units, which have been associated with numerous neurological disease processes<sup>49</sup>. Motor unit action potential stability signifies the integrity of neuromuscular transmission, either at the neuromuscular junction (NMJ) or within the muscle fibre itself. This motor unit stability is examined through the detailed assessment of the variability in shape of each consecutively detected action potentials. There are two key motor unit stability properties associated with shape variability termed jitter and jiggle<sup>52,53,54</sup>. Jitter represents the variability in the time intervals between pairs of individual muscle action potentials from a single motor unit, and jiggle refers to the overall variability in motor unit action potential shape from one discharge to the next<sup>55,56</sup> (Figure 2.1). Abnormal neuromuscular stability, specifically increased jitter and jiggle have been detected in conditions that involve neuromuscular transmission interruptions and are indicative of early axonal denervation<sup>55,56</sup>. Lastly DQEMG provides a measure of the percentage of motor units that are blocked. Percent (%) blocking is a measure of unsuccessful motor unit action potential transmissions in a muscle fibre or axon and is a clinically prominent feature of many demyelinating diseases<sup>56</sup>. Most clinical diagnostic EMG studies are performed at minimal submaximal contraction intensities, which severely limit clinical needle EMG assessments to moderately few and entirely low threshold (type I) motor units, which inherently biases the motor unit data obtained<sup>56</sup>. Fundamentally, DQEMG

delivers an irreplaceable and appropriate paradigm in combination with needle detected motor unit action potential examination and MUNE measures to gain a more comprehensive understanding of the pathological changes to motor units that underlie nerve dysfunction in CIDP.

## 1.5 Intramuscular Needle Electromyography

During voluntary contractions, the central nervous system regulates muscle force by changing the number of motor units recruited. As discussed above additional force regulation is achieved by varying the individual motor neuron firing rates. Once maximum force has been established, no useful purpose is served by any further increase in motor neuron discharge frequency. In recent years, the precise measurement of individual motor-unit firing rates during voluntary contractions became possible using tungsten micro- electrodes <sup>57,58</sup>. Tungsten microelectrodes provide a high signal-to-noise ratio, allowing clear identification of single muscle fibre action potential trains even at the highest forces. Briefly the tungsten micro electrode consists of a 5 cm long, 0.2-mm diameter needle with an insulated tungsten shaft and a 10-15µm exposed tip. For successful recording of single muscle fibre action potentials with a high signal-to-noise ratio, an electrode impedance greater than 100 Ω is generally required <sup>59</sup>. The tungsten electrode is inserted through the skin until the tip is directly below the muscle surface. As a subject volitionally contracts, the needle is further slowly and progressively advanced (typically 1-3 mm at each contraction) such as to record trains of potentials from as many muscle fibres as possible (see Figure 3.1) <sup>59</sup>. The advantage of the tungsten technique over using conventional recording electrodes and DQEMG, is the isolation of single-unit firing rates during high-force contractions which is not possible with conventional

techniques since the potentials arising from single units are not clearly distinguished from each other at forces exceeding 75-80% MVC<sup>58,59,60</sup>. Numerous studies in neuromuscular diseases such as Amyotrophic Lateral Sclerosis (ALS) and Multiple Sclerosis (MS) have used this intramuscular tungsten technique to quantify motor unit firing rates resulting from targeted axonal damage<sup>61,62</sup>. Results from the tibialis anterior muscle in patients with ALS indicate that the physiological modulation of motor neuron firing rate is decreased as well the variability of MU discharges tends to be greater in this disease<sup>63</sup>. Only a minugia of clinical data exists regarding motor unit firing rates in CIDP, most of which only records from early recruited motor units and to date there have been no systematic studies investigating motor unit firing behaviour in individuals with CIDP especially at maximal firing rates.

## 1.6 Magnetic Resonance Imaging (MRI)

Magnetic resonance imaging (MRI) is a medical imaging technique used to form images of the internal structures and anatomy. MRI works by using the magnetization properties of the atomic nuclei. This imaging technique employs a uniformly powerful external magnetic field, which aligns the protons that are normally randomly oriented within water nuclei of the tissue under examination. This alignment called magnetization is then perturbed or disrupted by introducing energy from an external Radio Frequency (RF)<sup>64</sup>. After being perturbed the atomic nuclei return to their resting alignment through a relaxation processes, which emits RF energy that is measured for a specified period of time. The signal from the internal structures contain location information and are sorted in planes corresponding to intensity levels which appear as shades of gray in a matrix

arrangement of pixels. The sequence or frequency of RF pulses applied and collected can create different images.

Repetition Time (TR) is the amount of time between successive pulse sequences applied to the same slice of tissue and Time to Echo (TE) is the time between the delivery of the RF pulse and the receipt of the echo signal <sup>64,65</sup>. The different human tissue types can be characterized by two different relaxation times T1 and T2. T1 or longitudinal relaxation time is the time constant which determines the rate at which excited protons return to equilibrium. This is a measure of the time taken for spinning protons to realign with the external magnetic field. T2 or transverse relaxation time is the time constant, which determines the rate the excited protons reach equilibrium or go out of phase coherence. There has been a growing interest in MRI assessment of the peripheral nervous system in dysimmune or autoimmune neuropathies, especially in patients with CIDP <sup>66,67,68</sup>.

The first reported descriptions of nerve abnormalities, using conventional MRI was in the 1990s. Since then, higher strength and advanced MRI imaging sequencing techniques have enabled a better discrimination of the peripheral nervous system and a better characterization of nerve abnormalities. Typical MR findings in CIDP include nerve enlargement, T2 signal increase and enhancement of nerve roots, especially in the early stages of the disease when inflammation tends to be unmanaged <sup>67,68</sup>. Proximal nerve involvement is typical at the onset of CIDP and becomes more prominent and ubiquitous in the long-term. Imaging studies show nerve enlargement is positively correlated with disease duration <sup>67,68</sup>. However, correlation of MRI features with clinical disability seen in patients with CIDP, specifically functional losses of strength, are still lacking. Most previous work involving the MRI assessment of CIDP were focused on

the spinal nerve roots and proximal nerve trunks, and there is a paucity of work investigating the muscles that connect to these peripheral nerves. Importantly with the advancement in imaging techniques the distal extremities can be imaged with smaller surface coils reaching greater resolution. This allows direct and definitive visualization of skeletal musculature affected by demyelinated peripheral nerves seen in patients with CIDP. It is critical to investigate the degree of muscle atrophy associated with CIDP as well to quantify the infiltration of non-contractile tissue to help elucidate reasoning behind function muscle weakness in patients with CIDP.

## 1.7 Purposes and Hypotheses

The fundamental objective of the studies characterized within Chapters 2, 3, 4, and 5 was to examine the pathophysiological effects of CIDP on the human neuromuscular system. Previous investigations in CIDP have minimally explored the impacts of demyelination on axonal function and none to date has focused on the fundamental consequential changes to skeletal muscles innervated by chronically demyelinated nerves. In Chapter 2 the purpose was to determine if the loss of strength reported in patients with CIDP is related to a loss of motor units. Furthermore, I wanted to assess motor unit functional stability as quantified using DQEMG. It was hypothesized that patients with CIDP would have fewer and less stable motor units compared to healthy controls, and decreased MUNEs would be related to loss in strength observed in patients with CIDP.

The purpose of Chapter 3 was to investigate the specific motor unit firing patterns of demyelinated and remodelled motor units. Commonly, clinical data are recorded from small, low-threshold, early recruited motor units. However, it is not known how larger demyelinated motor units that are recruited at higher contraction intensities are affected

by disease demyelination and inflammation. If patients with CIDP have disruptions to motor unit firing patterns, that could further explain functional weakness. It was hypothesized that motor unit firing rates would be depressed at all levels of voluntary contractions in individuals with CIDP due to chronic peripheral nerve demyelination and conduction block.

To date, the vast majority of studies investigating nerve dysfunction focus on evidence of demyelination or nerve lesions detectable via imaging. Very few studies have focused on the repercussions of CIDP on the quantity and quality in the associated musculature. Therefore, the purpose of Chapter 4 was to determine how motor unit loss, instability and blocking affect the tibialis anterior musculature of patients using a general anatomical scan (T1) as well spin-echo (T2) MRI sequences. It was hypothesized that patients with CIDP would feature a greater degree of tibialis anterior muscle atrophy as well larger infiltrations of non-contractile tissue.

The purpose of Chapter 5 was to assess if nerves that supply the posterior leg muscles are affected by the demyelinating process to the same degree as the nerves supplying the anterior leg and if this leads to differences between compartments and muscles in overall composition. It was hypothesized that patients with CIDP would have uniform alterations both in the anterior and posterior musculature of the leg and proportions of non-contractile intramuscular tissue would be homogeneous in the two compartments.

## 1.8 References

1. Piccolino M. Luigi Galvani's path to animal electricity. *Journal of the History of Neuroscience*. **17** 3 335-348 (2006).
2. Seyfarth EA. Julius Bernstein (1839-1917): pioneer neurobiologist and biophysicist. *Biological Cybernetics*. **94** 2-8 (2005).
3. Finkelstein G. Mechanical neuroscience: Emil du Bois-Reymond's innovations in theory and practice. *Frontiers in Systems Neuroscience*. **9**, 33 (2015).
4. Ko CP. Neuromuscular system International Encyclopedia of Social and Behavior sciences. 10595-10600 (2001).
5. Henneman E, Somjen G, Carpenter DO. Functional significance of cell size in spinal motoneurons. *Journal of Neurophysiology*. **28** 3 560-580 (1965).
6. Henneman E. Relation between size of neurons and their susceptibility to discharge. *Science*. **12** 1345-1347 (1957).
7. Bigland B, Lippold OC. Motor unit activity in the voluntary contraction of human muscle. *Journal of Physiology*. **125** 322-335 (1954).
8. Polgar J, Johnson MA, Weightman D, Appleton D. Data on fibre size in thirty-six human muscles. *Journal of Neurological Sciences*. **19** 3 307-318 (1973).
9. Edgerton VR, Smith J, Simpson D. Muscle fibre type populations of human leg muscles. *The Histochemical Journal*. **7** 3 259-266 (1975).
10. Milner-Brown HS, Stein RB, Yemm R. The orderly recruitment of human motor units during voluntary isometric contractions. *Journal of Physiology*. **230** 2 359-370 (1973).
11. Eoka. R and Duchateau. Rate coding and the control of muscle force. *Cold Spring*



- Harbor Perspectives in Medicine.* **7** 10 1-12 (2012).
12. Ydens E, Lornet G, Smits V, Goethals S, Timmerman V, Janssens S. The neuroinflammatory role of Schwann cells in disease. *Neurobiology of Disease.* **55** 95–103 (2013).
  13. Bunimovich YL, Keskinov AA, Shurin GV, Shurin MR. Schwann cells: a new player in the tumor microenvironment. *Cancer Immunological Immunotherapy.* **66** 959–968 (2017).
  14. Kwa MS, van Schaik IN, De Jonge RR, Brand A, Kalaydjieva L, van Belzen N Vermeulen M, Baas F. Autoimmunoreactivity to Schwann cells in patients with inflammatory neuropathies. *Brain.* **126** 361–375 (2003).
  15. Hodgkin AL, and Huxley AF. A quantitative description of membrane current and its application to conduction and excitation in nerve. *Journal of Physiology.* **117** 4 500–544 (1952).
  16. Huxley AF, and Stämpfli R. Evidence for saltatory conduction in peripheral myelinated nerve fibres. *Journal of Physiology.* **108** 315–339 (1949).
  17. Renganathan M, Cummins T. R, and Waxman, SG. Contribution of Nav1. 8 sodium channels to action potential electrogenesis in DRG neurons. *Journal of Neurophysiology.* **86** 629–640 (2001).
  18. Rash JE, Vanderpool KG, Yasumura T, Hickman J, Beatty J, Nagy JI. KV1 channels identified in rodent myelinated axons, linked to Cx29 in innermost myelin: support for the electrically active myelin in mammalian salutatory conduction. *Journal of Neurophysiology.* **115** 4 1836-1859 (2016).

19. Rajabally YA, Simpson BS, Beri S, Bankart J, Gosalakkal JA. Epidemiologic variability of chronic inflammatory demyelinating polyneuropathy with different diagnostic criteria: study of a UK population. *Muscle and Nerve*. **39** 432–438 (2009).
20. Lunn MP, Manji H, Choudhary PP, Hughes RA, Thomas PK. Chronic inflammatory demyelinating polyradiculoneuropathy: a prevalence study in south east England. *Journal of Neurology, Neurosurgery and Psychiatry*. **66** 677–680 (1999).
21. Said G, Krarup C. Chronic inflammatory demyelinating polyneuropathy. *Handbook of Clinical Neurology*. 115 403–413 (2013).
22. Bergh FPYK Van Den, Hadden RDM, Bouche P. European Federation of Neurological Societies / Peripheral Nerve Society Guideline on management of chronic inflammatory demyelinating polyradiculoneuropathy : Report of a joint task force of the European Federation of Neurological Societies and the Peripheral Nerve Society — First Revision. 356–363 (2010).
23. Breiner A, Brannagan TH III. Comparison of sensitivity and specificity among 15 criteria for chronic inflammatory demyelinating polyneuropathy. *Muscle and Nerve*. **50** 40–46 (2014).
24. Rajabally YA, Fowle AJ, Van den Bergh PY. Which criteria for research in CIDP? An analysis of current practice. *Muscle and Nerve*. **51** 6 932-933 (2014).
25. Sommer C, Koch S, Lammens M, Gabreels-Festen A, Stoll G, Toyka KV. Macrophage clustering as a diagnostic marker in sural nerve biopsies of patients with CIDP. *Neurology*. **65** 12 1924–1929 (2005).

26. Bosboom WM, van den Berg LH, De Boer L, Van Son MJ, Veldman H, Fransson H, Logtenberg T, Wokke JH. The diagnostic value of sural nerve T cells in chronic inflammatory demyelinating polyneuropathy. *Neurology*. **53** 4 837–845 (1999).
27. Salapa HE, Lee S, Shin Y, Levin MC. Contribution of the degeneration of the neuro-axonal unit to the pathogenesis of multiple sclerosis. *Brain Science*. **6** 69-71 (2017).
28. Schmidt B, Toyka KV, Kiefer R, Full J, Hartung HP, Pollard J. Inflammatory infiltrates in sural nerve biopsies in Guillain-Barré syndrome and chronic inflammatory demyelinating neuropathy. *Muscle and Nerve*. **19** 4 474–487 (1996).
29. Chi LJ, Xu WH, Zhang ZW, Huang HT, Zhang LM, Zhou J. Distribution of Th17 cells and Th1 cells in peripheral blood and cerebrospinal fluid in chronic inflammatory demyelinating polyradiculoneuropathy. *Journal of Peripheral Nerve Systems*. **15** 4 345–356 (2010).
30. Rentzos M, Angeli AV, Rombos A, Kyrozis A, Nikolaou C, Zouvelou V, Dimitriou A, Zoga M, Evangelopoulos ME, Tsatsi A, Tsoutsou A, Evdokimidis I. Proinflammatory cytokines in serum and cerebrospinal fluid of CIDP patients. *Neurological Research*. **34** 9 842–846 (2012).
31. Linington C, Lassmann H, Ozawa K, Kosin S, Mongan L. Cell adhesion molecules of the immunoglobulin supergene family as tissue-specific autoantigens: induction of experimental allergic neuritis (EAN) by P0 protein-specific T cell lines. *European Journal of Immunology*. **22** 7 1813–1817 (1992).
32. van Lieverloo GGA, Peric S, Doneddu PE, Gallia F, Nikolic A, Wieske L, Verhamme C, van Schaik IN, Nobile-Orazio E, Basta I, Eftimov F. Corticosteroids in chronic inflammatory demyelinating polyneuropathy: A retrospective, multicentre study,

- comparing efficacy and safety of daily prednisolone, pulsed dexamethasone, and pulsed intravenous methylprednisolone. *Journal of Neurology*. **265** 9 2052–2059 (2018).
33. Kuwabara S, Mori M, Misawa S, Suzuki M, Nishiyama K, Mutoh T, Doi S, Kokubun N, Kamijo M, Yoshikawa H, Abe K, Nishida Y, Okada K, Sekiguchi K, Sakamoto K, Kusunok S, Sobue G, Kaji R, Glovenin I. Intravenous immunoglobulin for maintenance treatment of chronic inflammatory demyelinating polyneuropathy: a multicentre, open-label, 52-week phase III trial. *Journal of Neurology, Neurosurgery and Psychiatry*. **88** 1 832–838 (2017).
34. Lin CS, Krishnan AV, Park SB, Kiernan MC. Modulatory effects on axonal function after intravenous immunoglobulin therapy in chronic inflammatory demyelinating polyneuropathy. *Archives Neurology*. **68** 7 862– 869 (2011).
35. Dalakas MC. Advances in the diagnosis, pathogenesis and treatment of CIDP. *Nat Rev Neurol*. **7** 9 507–517 (2011).
36. Ohyama KH, Koike M, Katsuno M, Takahashi R, Hashimoto Y, Kawagashira M, Iijima H, Adachi H, Watanabe G, Sobue G. Muscle atrophy in chronic inflammatory demyelinating polyneuropathy: a computed tomography assessment. *European Journal of Neurology*. **21** 7 1002-1010 (2014).
37. Swash M, Brown MM, Thakkar C. CT muscle imaging and the clinical assessment of neuromuscular disease. *Muscle and Nerve*. **18** 7 708– 714 (1995).
38. Theodorou DJ, Theodorou SJ, Kakitsubata Y. Skeletal muscle disease: patterns of MRI appearances. *British Journal of Radiology*. **85** 1020 1298–1308 (2012).
39. Bromberg, MB. Updating motor unit number estimation (MUNE). *Clinical*

- Neurophysiology*. **118** 1 1–8 (2007).
40. McComas A J, Fawcett PR, Campbell MJ, Sica RE. Electrophysiological estimation of the number of motor units within a human muscle. *Journal of Neurology, Neurosurgery and Psychiatry*. **34** 2 121–131 (1971).
  41. Stashuk DW. EMG signal decomposition: how can it be accomplished and used? *Journal of Electromyography Kinesiology*. **11** 3 151–173 (2001).
  42. Doherty TJ and Stashuk DW. Decomposition-based quantitative electromyography: methods and initial normative data in five muscles. *Muscle and Nerve*. **28** 2 204–211 (2003).
  43. Stashuk DW. Decomposition and quantitative analysis of clinical electromyographic signals. *Medical Engineering and Physics*. **21** 6-7 389–404 (1999).
  44. Stashuk DW. Detecting single fiber contributions to motor unit action potentials. *Muscle and Nerve*. **22** 2 218–229 (1999).
  45. Boe S, Stashuk D, Doherty TJ. Within-subject reliability of motor unit number estimates and quantitative motor unit analysis in a distal and proximal upper limb muscle. *Clinical Neurophysiology*. **117** 3 596–603 (2006).
  46. Boe SG, Stashuk DW, Doherty TJ. Motor unit number estimation by decomposition-enhanced spike-triggered averaging: control data, test-retest reliability, and contractile level effects. *Muscle and Nerve*. **29** 5 693–699 (2004).
  47. Ives CT and Doherty TJ Intra- and inter-rater reliability of motor unit number estimation and quantitative motor unit analysis in the upper trapezius. *Clinical Neurophysiology*. **123** 1 200-205 (2012).
  48. Ives CT and Doherty TJ Intra-rater reliability of motor unit number estimation and

- quantitative motor unit analysis in subjects with amyotrophic lateral sclerosis *Clinical Neurophysiology*. **125** 1 170-178 (2014).
49. Boe SG, Stashuk DW, Brown WF, Doherty TJ. Decomposition-based quantitative electromyography: effect of force on motor unit potentials and motor unit number estimates. *Muscle and Nerve*. **31** 3 365–373 (2005).
50. Dalton BH, McNeil CJ, Doherty TJ, Rice CL. Age-related reductions in the estimated numbers of motor units are minimal in the human soleus. *Muscle and Nerve*. **38** 3 1108–1115 (2008).
51. McNeil CJ, Doherty TJ, Stashuk DW, Rice CL. The effect of contraction intensity on motor unit number estimates of the tibialis anterior. *Clinical Neurophysiology*. **116** 6 1342–1347 (2005).
52. Stalberg EV, Sonoo M, Assessment of variability in the shape of the motor unit action potential, “the jiggle,” at consecutive discharges. *Muscle and Nerve*. **17** 10 1135-1144 (1994).
53. Stålberg E. Jitter analysis with concentric needle electrodes. *Annals of the New York Academy of Sciences*. **1274** 1 77–85 (2012).
54. Benatar M, Hammad M, Doss-Riney H. Concentric-needle single-fiber electromyography for the diagnosis of myasthenia gravis. *Muscle and Nerve*. **34** 2 163–168 (2006).
55. Allen MD, Stashuk DW, Kimpinski K, Doherty TJ, Hourigan ML, Rice CL. Increased neuromuscular transmission instability and motor unit remodeling with diabetic neuropathy as assessed using novel near fiber motor unit potential parameters. *Clinical Neurophysiology*. **126** 4 794–802 (2015).

56. Allen MD, Choi IH, Kimpinski K, Doherty TJ, Rice CL. Motor unit loss and weakness in association with diabetic neuropathy in humans. *Muscle and Nerve*. **48** 2 298–300 (2013).
57. Bellemare F, Woods JJ, Johansson R, Bigland-Ritchie B. Motor-unit discharge rates in maximal voluntary contractions of three human muscles. *Journal of Neurophysiology*. **50** 6 1380-1392 (1983).
58. Bigland-Ritchie B, Johansson R, Lippold OC, Woods JJ. Changes in motoneuron firing rates during sustained maximal voluntary contractions. *Journal of Physiology*. **340** 1 335-346 (1983).
59. Bigland-Ritchie B, Dawson NJ, Johansson R, Lippold OC. Reflex origin for the slowing of motoneurone firing rates in fatigue of human voluntary contractions. *Journal of Physiology*. **379** 1 451-459 (1986).
60. Vucic S. Assessing motor unit firing rates in ALS: A diagnostic and pathophysiological prospect? *Clinical Neurophysiology*. **123** 11 2114-2115 (2012).
61. Dorfman LJ, Howard JE, McGill KC. Motor unit firing rates and firing rate variability in the detection of neuromuscular disorders. *Electroencephalography Clinical Neurophysiology*. **73** 3 215-224 (1989).
62. Dortch RD, Dethrage LM, Gore JC, Smith SA, Li J. Proximal nerve magnetization transfer MRI relates to disability in Charcot-Marie-Tooth diseases. *Neurology*. **83** 17 1545–1553 (2014).
63. Shibuya K, Sugiyama A, Ito SI, Misawa S, Sekiguchi Y, Mitsuma S, Iwai Y, Watanabe K, Shimada H, Kawaguchi H, Suhara T, Yokota H, Matsumoto H, Kuwabara S. Reconstruction magnetic resonance neurography in chronic

- inflammatory demyelinating polyneuropathy. *Annals of Neurology*. **77** 2 333–337 (2015).
64. Morrow JM, Sinclair CD, Fischmann A, Machado PM, Reilly MM, Yousry TA, Thornton JS, Hanna MG. MRI biomarker assessment of neuromuscular disease progression: a prospective observational cohort study. *Lancet Neurology*. **15** 1 65–77 (2016).
65. Kronlage M, Bäumer P, Pitarokoili K, Schwarz D, Schwehr V, Godel T, Heiland S, Gold R, Bendzus M, Yoon MS. Large coverage MR neurography in CIDP: diagnostic accuracy and electrophysiological correlation. *Journal of Neurology*. **264** 7 1434–43 (2017).
66. Lichtenstein T, Sprenger A, Weiss K, Slebocki K, Cervantes B, Karampinos D, Maintz D, Fink GR, Henning TD, Lehmann HC. MRI biomarkers of proximal nerve injury in CIDP. *Annals of Clinical Translational Neurology*. **5** 1 19–28 (2018).
67. Chhabra A, Madhuranthakam AJ, Andreisek G: Magnetic resonance neurography: current perspectives and literature review. *European Radiology*. **28** 2 698–707 (2018).
68. Ishikawa T, Asakura K, Mizutani Y, Ueda A, Murate KI, Hikichi C, Shima S, Kizawa M, Komori M, Murayama K, Toyama H, Ito S, Mutoh T. MR neurography for the evaluation of CIDP. *Muscle and Nerve*. **55** 4 483–489 (2017).



## Chapter 2

# 2 <sup>1</sup>Electrophysiological And Neuromuscular Stability Of Persons With Chronic Inflammatory Demyelinating Polyneuropathy (CIDP)

## 2.1 Introduction

Chronic inflammatory demyelinating polyneuropathy (CIDP) is a generalized neuropathy of immunological origin. It is as a heterogeneous disease of symmetrical muscle weakness, which includes sensory and motor deficits in both proximal and distal limbs that progressively increases for >2 months <sup>1</sup>. The condition is associated with absent or diminished tendon reflexes, signs of demyelination, elevated cerebrospinal fluid protein level, impaired sensation, slow nerve-conduction velocity, and distal muscle weakness <sup>2</sup>. In inflammatory polyneuropathies such as CIDP, early diagnosis and therapy may not only mitigate progression of demyelination but also prevent secondary motor unit (MU) loss, which is often responsible for persisting motor symptoms. Therefore, a better understanding of the degree and time course of loss and stability of functioning MUs due either to primary or secondary demyelination <sup>3</sup> in CIDP would provide more insight into the pathophysiology of the disease and possibly improve functional outcomes. CIDP affects men and women of all ages and has a population prevalence of 3 per 100,000 people <sup>4,5</sup>.

A version of this chapter has been published. Used with permission from John Wiley and Sons, Inc.

<sup>1</sup> Gilmore K.J, Doherty, T.J., Kimpinski, K., Rice, C.L. Electrophysiological And Neuromuscular Stability Of persons With Chronic Inflammatory Demyelinating Polyneuropathy. *Muscle and Nerve*. **56** 3 413-420 (2017).

Diagnosis is based on history, clinical examination including electromyography and nerve conduction studies, blood tests, cerebral spinal fluid, and in some cases nerve biopsies.

Further diagnosis of CIDP is confirmed by the elimination of other neurological diseases such as diabetic polyneuropathy and inherited demyelinating polyneuropathies. Although the electrophysiological and neuromuscular properties of persons with CIDP have been described above, details of undesirable alterations in motor unit structure and function that could explain weakness and related functional changes have not been quantified systematically. Although exact mechanisms are not understood entirely, limited evidence in autoimmune neuropathies indicates that disease related to pre or post-synaptic damage and muscle fiber atrophy lead to neuromuscular junction remodeling and impaired neuromuscular transmission <sup>6</sup>. It is presumed that in autoimmune neuropathies such as CIDP, MU death or axonal damage is followed by variable reinnervation by collateral sprouting and axonal outgrowth, both of which could add to neuromuscular transmission instability <sup>7</sup>. In routine clinical nerve conduction studies, a compound muscle action potential (CMAP) is recorded, but the CMAP features alone do not quantify the extent of motor unit loss or dysfunction because of the possible compensatory effect of reinnervation. The technique of decomposition-based quantitative electromyography (DQEMG), however, can be used to assess any loss of motor neurons and cardinally detect the increase of motor unit size due to collateral reinnervation. DQEMG has also been shown to be a reliable and valid tool for obtaining information regarding MU number, size, stability, and complexity in healthy subjects, older adults, and in some

other neuromuscular diseases and neuropathies, such as ALS and diabetic neuropathy<sup>8,9,10,11,12</sup>.

A few studies in CIDP, using single fiber EMG (SFEMG) in upper limb muscles have shown increased fiber density along with neuromuscular instability, but no studies have investigated lower limb muscles using the DQEMG technique in CIDP patients. This technique can extract beneficial information regarding the MU pool from simultaneously acquired surface and concentric needle-detected signals<sup>13</sup>. Furthermore, in conjunction with a maximal CMAP amplitude, DQEMG can be utilized to calculate a motor unit number estimate (MUNE). This measure provides critical insight about the innervation status of a muscle<sup>10,14</sup>. Near-fiber (NF) parameters such as jiggle, jitter, blocking, and area, derived from DQEMG also relate to the integrity or stability of neuromuscular transmission<sup>12,15,16</sup>, but these measures have not been applied to CIDP. Stability can be examined through assessment of the degree of variability in the shape and time of consecutively detected motor unit potentials (MUPs) termed “jiggle” and “jitter” respectively<sup>17</sup>.

Indeed, the assessment and understanding of these features could potentially be helpful for treatment monitoring to aid in disease understanding. MUP shape variability parameters and conduction blocking may provide valuable information regarding MU health in CIDP during disease progression. Using these techniques, we evaluated the magnitude of demyelination, collateral reinnervation following MU loss, and the stability of neuromuscular transmission in patients with CIDP. The purpose of this study was to assess the neuromuscular stability of the MUs in the tibialis anterior (TA) muscle of patients with CIDP using DQEMG compared with an age- and gender-matched healthy

control group. We chose to focus on the dorsiflexor muscle group, because there are comparative data available from several studies of MU properties in aging using this muscle group and these techniques<sup>18,19</sup>. In addition, adequate dorsiflexor function is critical for balance and gait and thus relate to falls risk<sup>18</sup>. When compared with controls, we hypothesized that patients with CIDP would feature reduced MUNE, as well significantly fewer stable MUs in the TA.

## 2.2 Methods

### 2.2.1 Subjects

Ten subjects (7 men, 3 women; ages 47–77 years) with CIDP volunteered for this study as well 10 healthy control subjects (7 men, 3 women; ages 57–75 years). History, clinical, and electrophysiological features confirming a diagnosis of CIDP were obtained by an experienced neurologist to exclude other causes of nerve dysfunction (i.e. radiculopathies, other polyneuropathies, or compressive mononeuropathies). Patients with any other neurological, metabolic (including diabetes) or vascular diseases (other than related to CIDP) were not included in this study (Table 1). All 10 patients underwent a clinical electrophysiological examination that assessed bilateral fibular, tibial, ulnar, and median motor nerves and bilateral sural, ulnar, and median sensory nerves. Limb temperature was monitored during standard electrodiagnostic testing and, if necessary limbs were warmed to a minimum of 32 degrees Celsius in the upper limb and 30 degrees in the lower limb. Additionally, all patients with CIDP underwent measures of nerve conduction velocities (CV), compound muscle action potentials (CMAP), and sensory nerve action potentials (SNAP) and compared to normal values. Patients had standard characteristics of acquired demyelination, including conduction block, temporal

dispersion, multifocal conduction velocity slowing, and F-wave prolongation. Moreover, CSF analysis revealed elevated protein in the absence of any other abnormality. Furthermore, all patients had a clinical presentation consistent with CIDP without evidence of alternative diagnosis (i.e. paraproteiniemic neuropathies, multifocal motor neuropathy or polyneuropathies). All 10 patients with CIDP received usual medical care and responded to treatment with intravenous immunoglobulin (IVIG), plasma exchange, or prednisone. The local university research ethics board approved the study, and informed written and oral consent were obtained from all participants preceding testing.

### 2.2.2 Dorsiflexor Strength and Tibialis Anterior DQEMG Data Acquisition

Subjects were seated in a custom isometric dynamometer designed to measure dorsiflexion and plantar flexion function<sup>20</sup>. The right leg was tested, and the ankle was positioned at 30° of plantar flexion, with both knee and hip angles maintained at 90°. A C-shaped brace was placed firmly over the distal aspect of the right thigh proximal to the patella to secure the leg and foot in the device for recording isometric contractions. Additionally, over the dorsum of the foot, inelastic Velcro straps were firmly fastened to secure the foot to the dynamometer<sup>19</sup>. Subjects first performed a total of 3 dorsiflexion maximal voluntary contractions (MVCs), with a minimum of 3 min of rest between each attempt. Each MVC was held for 3-5 s. Real time visual feedback was provided to the subjects via a 24 inch LCD monitor. Subjects were also strongly encouraged verbally during all contractions to ensure maximal effort. Voluntary activation during the second and third MVC efforts was assessed using the interpolated twitch technique<sup>21</sup>. This technique involves supramaximal (stimulus at 125% of peak CMAP amplitude)

percutaneous electrical stimulation of the common fibular nerve distal to the head of the fibula using a bar electrode. The peak amplitude of the interpolated torque electrically evoked from a single 100 $\mu$ s stimulus during the plateau of the MVC was compared with the torque produced using the same pulse delivered 1s following the MVC when the muscle was at rest. Voluntary activation was calculated as a percent using the following equation:  $[1 - (\text{interpolated twitch} / \text{resting twitch})] \times 100$ . The ITT provides an indication of the voluntary ability of subjects to produce maximal dorsiflexor activation during the MVC. Maximal torque for each participant was determined by the peak torque of the 3 MVC attempts. Torque signals were collected and sampled online at 500 Hz using Spike2 software (Version 7.11; Cambridge Electronic Design Ltd., Cambridge, United Kingdom) and subsequently analyzed off-line to establish voluntary and stimulated contractile properties.

Surface EMG signals were recorded from the TA using self-adhering Ag-AgCl electrodes (1 cm  $\times$  3 cm). The active electrode was positioned over the TA motor point, approximately 7 cm distal to the tibial tuberosity and 2 cm lateral to the anterior border of the TA. The active electrode placement was corrected as required to minimize the rise times and to maximize the TA CMAP negative peak amplitude. The reference electrode was placed on the distal aspect of the TA tendon. The ground electrode was positioned directly over the patella. DQEMG EMG data were obtained using the identical protocol described in detail elsewhere<sup>13,22</sup>. To record intramuscular EMG data, a disposable concentric needle electrode (Model N53153; Teca Corp., Hawthorne, NY) was inserted into the TA, 5–10 mm proximal or distal to the active surface electrode. Surface and concentric intramuscular EMG signals were bandpass filtered at 5 Hz to 1 kHz and 10 Hz

to 10 kHz, respectively. Intramuscular EMG signals were sampled at 30 kHz, and surface EMG signals were sampled at 3 kHz. In order to evoke a maximum TA CMAP, a bar electrode positioned distal to the fibular head delivered supramaximal electrical stimuli (i.e., 125% of the intensity required to achieve a plateau in amplitude) to the common fibular nerve. Subsequently, participants matched a dorsiflexor target line of 25% MVC for ~30 seconds using a real-time visual torque feed from the LCD monitor, while the intramuscular concentric needle electrode was manipulated gently in the muscle. This contraction intensity of 25% MVC of the dorsiflexors has been shown to be the most relevant level for obtaining a representative MUNE in the TA <sup>19</sup>. Intramuscular and surface EMG signals were recorded during these ~30s contractions. Between each 30-second contraction, the indwelling concentric needle electrode was repositioned to sample MUs from different regions of the muscle. These methods were repeated until a minimum of 20 suitable MUP trains and their respective surface-motor unit potentials (S-MUPs) were acquired.

### 2.2.3 Data Analyses

Dorsiflexor MVC torque was taken as the highest torque amplitude contraction of the 3 attempts, and the ITT was calculated as described in methods. In order to establish the acceptability of the extracted MUP trains and their corresponding S-MUPs, the decomposed intramuscular EMG signals were reviewed off-line. The MUP trains also were examined visually to guarantee that their MUP occurrence patterns were consistent with the anticipated electrical activity of a single motor unit (inter-discharge interval duration coefficient of variation of <0.3 and a consistent firing pattern). Invalid MUP trains and their associated S-MUPs were eliminated from subsequent analyses. The

DQEMG algorithm calculates a MUP and S-MUP template waveforms and automatically places markers linked to onset, negative peak, positive peak, and end positions with respect to the MUP template, and onset, negative peak onset, end, negative peak, and positive positions with respect to the S-MUP template. To ensure accurate marker placement, all MUP and S-MUP markers were reviewed visually by the operator. A motor unit number estimation (MUNE) was calculated by dividing the maximal negative-peak amplitude of the CMAP by the mean S-MUP negative peak amplitude<sup>14</sup>. These MUNE techniques have been reported previously for this muscle<sup>10</sup>. The DQEMG algorithms additionally provide mean-firing rates (Hz) of discrete motor units based on their extracted MUP trains. From these MU firings an overall mean firing rate per subject at the relative submaximal target level of contraction (25% of MVC) was estimated. Moreover, standard parameters of the MUP template, including peak-to-peak amplitude, duration, area, neuromuscular stability, and near-fiber parameters such as jiggle, jitter, and percent blocking were automatically computed by the DQEMG system (see below for details). MUPs that represent the isolated activity of a single motor unit were selected by the algorithms for assessment of MUP stability. The selected sets of isolated MUPs were inspected by an experienced operator, and any MUPs that were contaminated by activity of other motor units, were removed and replaced by uncontaminated MUPs. Test-retest and intra-rater and inter-rater reliability are reported to be high in control and clinical populations using these DQEMG measures<sup>9,11,23</sup>.

#### 2.2.4 Near-fiber Parameters

Neuromuscular transmission integrity was determined by evaluating the degree of variability in the shape of consecutively detected MUPs<sup>17</sup>. Two key properties related to



MUP shape variability are termed jiggle and jitter <sup>17</sup>. Near-fiber (NF) jiggle refers to the variability in overall MUP shape from 1 MUP discharge to the next. Jiggle is a statistic that measures the shape variability of MUPs produced by a single MU <sup>12,15</sup>. Successful MUP shape variability (jiggle) measurement requires the extraction of sets of “isolated” MUPs created by a single MU. The activity of MU fibers in close proximity to the concentric needle detection surface can be measured to determine MU stability. NF jitter refers to the variability of the time intervals between pairs of individual muscle fiber potentials from a single MUP <sup>19</sup>. Both jiggle and jitter have been reported to be increased under conditions of neuromuscular transmission disruption and axonal injury and therefore can reflect early axonal denervation <sup>24,25,26</sup>. Increases in MUP instability (assessed by jiggle and jitter) have been shown to be caused by variability in muscle fiber action potential velocity, a finding present in various myopathies <sup>17</sup>. Furthermore, % blocking was evaluated for all pairs of detected fiber contributions across the sets of isolated NF MUPs. This parameter is calculated by measuring the number of intermittent absences of an individual NF contribution to the NF MUPs from the set of isolated analyzed NF MUPs <sup>17</sup>. All of the abovementioned MUP and NF MUP parameters such as duration, dispersion, area, and fiber count were obtained using an intramuscular concentric needle electrode and decomposition-based quantitative electromyography (DQEMG) software <sup>13</sup>.

### 2.2.5 Statistics

Mean values  $\pm$  standard deviations are presented in the text and tables. All data were tested for normal distribution using the Shapiro-Wilk test. Data not be normally distributed were assessed using the Kruskal-Wallis 1-way analysis of variance, whereas

data that were normally distributed were analyzed using a 1-way ANOVA. The level of significance for all tests was set at  $P > 0.05$ . To represent the degree of differences between groups, effect sizes were calculated using the Cohen D.

## 2.3 Results

Participant characteristics are listed in Table 2.1. The two groups were well matched on gender, age, and anthropometric indices. Patient data indicate electrophysiologic and clinical features consistent with a diagnosis of CIDP (Table 2.2). There were no gender differences on any parameter measured in this study. Dorsiflexion strength, voluntary activation (ITT), standard MUP parameters, and MUNE values are listed in Table 2.3. NF MUP parameter values are presented in Table 3. NF jiggle values are listed as a percentage. During MVCs, both the patients and controls were able to achieve near-maximal (>95%) voluntary activation as assessed using the ITT. The patients with CIDP had smaller CMAPs compared to controls. Patients also had fewer motor units (-27%) and were weaker (-37%) than controls despite being fully activated during voluntary efforts. When assessing MU stability, the patients with CIDP had 90% more jiggle and 44% more jitter indicative of greater neuromuscular transmission instability when compared to controls (Table 2.4). Patients also had significant transmission blocking compared to controls (400% difference vs 0%, respectively). Patients with CIDP had greater: NF area (+26%), NF duration (+55%), NF dispersion (+106%), and maximal NF interval (+70%) compared to controls. Patients also had increased (+48%) fiber count. Figure 2.1 depicts exemplar data of near-fiber motor unit potential train (MUPT) data from control (a) and a subject with CIDP (b). The NF MUP rasters show sequential firings of motor unit potentials. The NF MUP shimmer plots are an overlay of MU firings

from a single MU. From these results, those with CIDP had significantly less strength but were fully activated during maximal voluntary efforts. Patients with CIDP also had substantially lower CMAP values and fewer numbers of MUs with increased neuromuscular instability and blocking compared with controls.

Table 2.1 Participant characteristics

<b>Anthropometric parameters</b>	<b>Controls (n = 10)</b>	<b>Patients with CIDP (n = 10)</b>
Men/Women	7/3	7/3
Age (years)	66.5 ± 9.2	60.5 ± 10.3
Height (cm)	170.0 ± 1.0	170.4 ± 1.2
Mass (kg)	79.3 ± 13.3	80.5 ± 11.5
BMI (kg/m <sup>2</sup> )	26.7 ± 2.9	27.8 ± 4.9

There were no significant differences ( $P>0.05$ ) in any parameter. BMI- Body mass index

Table 2.2 CIDP clinical classification

<b>Patient (M,F, age)</b>	<b>Duration of CIDP (y)</b>	<b>MRC score (out of 5)</b>	<b>CSF level (g/isolation)</b>	<b>C B</b>	<b>T D</b>	<b>F-Wave prolongati on/latency</b>	<b>Response to IVIG or Prednisone</b>
F, 59	8	3/5	3.3	√	√	√	75g/ 3weeks IVIG
M, 61	22	1/5	1.5	√	√	-	80g/ 4 weeks IVIG
M, 63	6	4/5	0.75	√	√	√	20g/ 3 weeks IVIG
M, 73	6	4/5	0.6	√	√	√	Plasma exchange/ 2 weeks, 125 mg prednisone daily
F, 62	5	3/5	0.85	√	√	-	55g/ 3 weeks IVIG
M, 68	3	4/5	0.7	√	-	-	20g/ 2weeks IVIG
M, 60	12	4/5	-	√	√	√	currently not treated
M, 45	20	2/5	-	√	√	√	20 mg prednisone daily
F, 59	10	5/5	2.9	√	√	√	5mg prednisone every other day
F, 58	12	4/5	6.6	√	√	√	55g/ 4weeks IVIG

CSF- Cerebral spinal fluid; IVIG- Intravenous immunoglobulin; - represents no value; √ - value observed;

CB - Conduction block; TD - Temporal dispersion, M-Male, F-Female

Table 2.3 Dorsiflexor strength and tibialis anterior MUP and MUNE parameters.

<b>Parameter</b>	<b>Controls (n = 10)</b>	<b>Patients with CIDP (n = 10)</b>	<b>% Difference</b>
Dorsiflexion MVC strength (Nm)	33.6 ± 7.7	21.2 ± 2.9*	-37%
Voluntary activation (%)	95 ± 3	95 ± 2	-
MU firing rates (Hz) at 25% MVC	12.10 ± 1.80	9.8 ± 0.9	-19%
MUP Vpp (μV)	811.8 ± 233.6	1081.3 ± 259.4*	+32%
MUP duration (ms)	12.6 ± 2.1	18.9 ± 4.6*	+47%
MUP area (μVms)	1443.2 ± 531.4	1636.4 ± 517.8	+13%
AAR (ms)	1.75 ± 0.2	2.2 ± 0.5*	+20%
Shape width (ms)	0.7 ± 0.1	0.7 ± 0.2	-
Turns (#)	2.6 ± 0.8	4.1 ± 1.2*	+58%
CMAP (mV)	6.9 ± 0.83	2.9 ± 0.9*	-57%
mSMUP (μV)	73.3 ± 12.8	84.0 ± 20.1	+13%
MUNE (#)	99 ± 15	72 ± 9.6*	-27%

MVC, maximal voluntary contraction; MU, motor unit; MUP, motor unit potential; Vpp, peak-to-peak voltage; AAR, area to amplitude ratio; CMAP, compound muscle action potential; mSMUP, mean surface

motor unit potential; MUNE, motor unit number estimate; -, no value. \* significant difference vs controls ( $P < 0.05$ ).

Table 2.4 Neuromuscular transmission stability and near-fiber parameters.

<b>Parameter</b>	<b>Controls (n = 10)</b>	<b>Patients with CIDP (n = 10)</b>	<b>% Difference</b>
Contractions (#)	4.2 ± 0.5	6.6 ± 1.0*	+57%
# of MUPTs/contraction	5.0 ± 0.4	4.1 ± 1.2	-18%
NF area (kV/s <sup>2</sup> ms)	6.9 ± 1.9	8.8 ± 1.3*	+26%
NF duration (ms)	3.8 ± 0.6	5.9 ± 1.4*	+55%
NF dispersion (ms)	1.7 ± 0.4	3.5 ± 1.0*	+106%
Max NF interval (ms)	1.0 ± 0.2	1.7 ± 0.5*	+70%
NF fiber count (#)	2.5 ± 0.4	3.7 ± 0.7*	+48%
NF jiggle (%)	34.3 ± 3.7	65.1 ± 7.2*	+90%
NF jitter (μs)	39.7 ± 9.5	57.1 ± 6.4*	+44%
% Blocking	0.0 ± 0.0	4.1 ± 1.4*	+400%

MUPT - motor unit potential train; NF - near-fiber. \* significant difference between patients with CIDP and controls ( $P < 0.05$ ). Conduction block in patients was 4 times greater than controls, represented by a 400% difference.

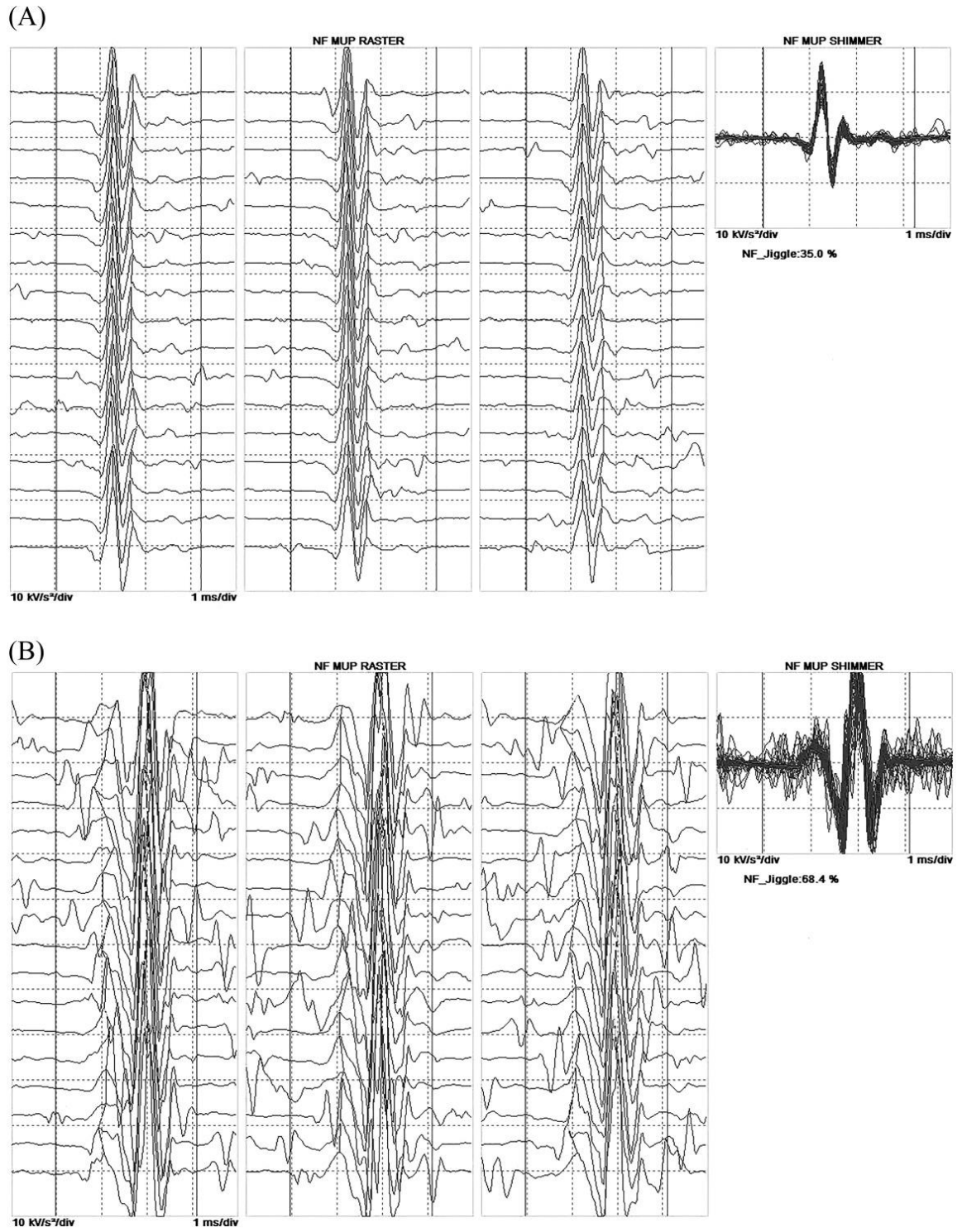


Figure 2.1 Motor unit potential train raster plots

Exemplar data of near-fiber MUPTs raster plots created from accelerated data from a control subject (A) and a patient with CIDP (B). The rasters show sequential firings of MUPs. The NF MUP shimmer plots are an overlay of MU firings from a single MU. NF jiggle values are shown as a percentage.

## 2.4 Discussion

In this study we found that individuals with CIDP showed marked differences in many neuromuscular measures in the tibialis anterior. Despite being age- and gender-matched and with equal voluntary activation abilities, dorsiflexor strength was 37% less in CIDP, and the TA in patients had 27% estimated fewer motor unit numbers which were considerably less stable with greater blocking compared to controls. Our results of MUNE and strength parameters are comparable to other studies of diseased neuromuscular systems. For example, Allen et al., (2015)<sup>10</sup> reported 60% fewer motor units and a 60% difference in strength in a diabetic polyneuropathy population compared to healthy controls. The number of motor units estimated by MUNE can be lower either because of axonal loss or because of loss of function of selected axons due to conduction block. Our data show fewer MUNE, greater NF jiggle, NF jitter and blocking in patients with CIDP in comparison to controls and may reflect the pathological alterations in neuromuscular transmission instability or decreased neuromuscular action potential propagation (Table 3). Greater neuromuscular transmission instability is believed to arise in conjunction with incomplete reinnervation occurring between orphaned muscle fibers and their adopted axonal sprouts throughout the course of collateral reinnervation, or with partial loss of innervation by a damaged motor axon,<sup>17</sup>. Additionally, our data quantified neuromuscular transmission failure (i.e., % blocking) in patients compared to controls (Table 2.3). This intermittent transmission failure indicates an underlying dysfunction related to neuromuscular transmission, and this would then lead to increased NF jiggle



and NF jitter. Furthermore % blocking is indicative of the rate at which an individual muscle fiber fails to propagate an action potential following activation of its motor neuron. However, it is not certain how potential dysfunction at any of these sites (the neuromuscular junction, muscle fiber action potential propagation, distal axonal branches, or a combination of factors) contribute to decreased neuromuscular stability in CIDP.

Studies using animal models suggest that neuromuscular instability could be due to a variety of factors including axon terminal dysfunction<sup>27</sup>, nerve demyelination or reduced axonal caliber<sup>28</sup>, structural changes in the muscle fiber<sup>27,29</sup>, ion channel alterations<sup>27,30,31</sup> and other possible mechanisms. Any of these proposed alterations in muscle fibers could potentially adversely impact muscle fiber action potential conduction velocity<sup>32</sup> and subsequently affect MUP shape stability. Our findings of increased NF dispersion, NF duration, fiber count, and max NF interval in CIDP likely indicate that prior compensatory reinnervation has occurred due to muscle fiber denervation<sup>12,33</sup>. MUNE techniques have been used in several studies of amyotrophic lateral sclerosis (ALS)<sup>34,35,36</sup>. However, there are very few studies conducted specifically on polyneuropathies<sup>40</sup>. Mostly these studies have focused on hereditary polyneuropathies<sup>38,39,40,41</sup>. Two studies in patients with CIDP that used single fiber EMG (SFEMG) in upper limb muscles reported abnormalities and increased fiber density<sup>42,43</sup> and transmission instability<sup>42</sup> compared with controls. Using stimulated SFEMG, another study reported that there was intermittent or persistent blocking in the nerve fibers in upper limb muscles of patients<sup>44</sup>. Moreover, Delmont et al (2016) showed that patients with CIDP have fewer motor units than controls in the TA using the motor unit number index (MUNIX)

technique <sup>45</sup>. They suggested the lower MUNIX was a sign of axonal loss or loss of functioning axons and an increase in the average motor unit size (SMUP and MUSIX) probably due to the compensatory effect of reinnervation. Lastly, another study that used MUNIX and multi-point stimulation showed that the MUNIX value was lower in the abductor pollicis brevis (APB) muscle when compared with healthy controls in CIDP <sup>7</sup>. It is not possible to compare directly various MUNE methods and MUNIX because of the specific differences in the technical and physiological aspects in each method. MUNIX is an “index” which reflects the number of motor units, using the power and area of CMAP and interference patterns, whereas DQEMG is more invasive but provides direct recordings of MU properties, including neuromuscular stability. Thus, by incorporating needle-detected signals our study provides further insight into factors that may affect MU function in relation to neuromuscular function and stability that may indicate the degree of disease involvement and disease severity.

Quantification of neuromuscular stability, specifically NF jiggle and NF jitter in patients with CIDP, has not been reported systematically. However, in other clinical conditions such as ALS, higher jiggle values were found in the small number of MUPs studied <sup>17</sup>, and in patients with myasthenia gravis higher jiggle values were reported <sup>26</sup>. Additionally, increased jiggle was found in patients with diabetic neuropathy <sup>12</sup>. Our findings of higher jiggle in CIDP align with these other studies, although the mechanisms responsible may be quite different (i.e diabetic polyneuropathy and CIDP). It has been shown that instability in the neuromuscular system negatively affects neuromuscular transmission propagation and can have corresponding detriments on strength <sup>12</sup>. Our finding that patients with CIDP have increased blocking is supported by Stalberg and Trontelj, who

showed increases in transmission blocking in myasthenia gravis using SFEMG <sup>46</sup>. Our data showing increased NF jiggle and NF jitter in patients relative to controls may reflect pathological alterations in neuromuscular action potential propagation or neuromuscular transmission instability, but it is difficult to ascertain a prime site. Our percent blocking results are also similar to Allen et al., (2015) <sup>10</sup>, in diabetic neuropathy and indicate failures in muscle fibers to propagate their signal after excitation of a spinal motor neuron <sup>12</sup>.

## 2.5 Conclusion

We have demonstrated the utility of concentric needle-derived DQEMG for detection of motor unit remodeling and differences in neuromuscular transmission instability when comparing patients with CIDP with age and gender-matched controls. This study highlights the value of DQEMG as a potential measure that is sensitive to changes not currently detectable by standard clinical nerve conduction studies associated with CIDP. The results of this study suggest that NF MUP parameters may have usefulness in tracking CIDP progression or the degree of physical impairment. The existence of neuromuscular transmission failure (i.e. blocking) in patients may have significant consequences regarding neuromuscular function under circumstances that stress the capacity of the neuromuscular system, such as contractions that are fatiguing. Finally, the outcomes of our study indicate that NF jiggle and NF jitter are valuable indices for identification of alterations in the early stages of neuromuscular disease, preceding the loss of motor units or onset of muscle atrophy. Further longitudinal studies of patients with CIDP undergoing treatment regimens using the stability parameters of jiggle and jitter may be helpful in improving the understanding of the disease.

## 2.6 References

1. Rajabally YA. Novel therapeutic avenues for chronic inflammatory demyelinating polyneuropathy: The difficulties of disease diversity. *EBioMedicine*. **6** 12–13 (2016).
2. Dimachkie MM, Barohn RJ. Chronic inflammatory demyelinating polyneuropathy. *Current Treat Options Neurology*. **15** 350–366 (2013).
3. Schaik IN van, Eftimov F. Chronic inflammatory demyelinating polyradiculoneuropathy - An overview of existing treatment options and prospects for the future. *European Neurology Reviews*. **6** 45-51 (2011).
4. Ritter C, Bobylev I, Lehmann HC, Chronic inflammatory demyelinating polyneuropathy (CIDP): change of serum IgG dimer levels during treatment with intravenous immunoglobulins. *Journal of Neuroinflammation*. **12** 1 148-157 (2015).
5. Vallat J-M, Sommer C, Magy L. Chronic inflammatory demyelinating polyradiculoneuropathy: diagnostic and therapeutic challenges for a treatable condition. *Lancet Neurology*. **9** 4 402–412 (2010).
6. Kraker J, Zivković SA. Autoimmune neuromuscular disorders. *Current Neuropharmacology*. **9** 3 400–408 (2011).
7. Paramanathan S, Tankisi H, Andersen H, Fuglsang-Frederiksen A. Axonal loss in patients with inflammatory demyelinating polyneuropathy as determined by motor unit number estimation and MUNIX. *Clinical Neurophysiology*. **127** 1 898–904 (2016).

8. Boe SG, Stashuk DW, Doherty TJ. Motor unit number estimation by decomposition-enhanced spike-triggered averaging: Control data, test-retest reliability, and contractile level effects. *Muscle and Nerve*. **29** 5 693–699 (2004).
9. Ives CT, Doherty TJ. Intra- and inter-rater reliability of motor unit number estimation and quantitative motor unit analysis in the upper trapezius. *Clinical Neurophysiology*. **123** 1 200–205 (2012).
10. Allen MD, Choi IH, Kimpinski K, Doherty TJ, Rice CL. Motor unit loss and weakness in association with diabetic neuropathy in humans. *Muscle and Nerve*. **48** 2 298–300 (2013).
11. Ives CT, Doherty TJ. Intra-rater reliability of motor unit number estimation and quantitative motor unit analysis in subjects with amyotrophic lateral sclerosis. *Clinical Neurophysiology*. **125** 1 170–178 (2014).
12. Allen MD, Stashuk DW, Kimpinski K, Doherty TJ, Hourigan ML, Rice CL. Increased neuromuscular transmission instability and motor unit remodeling with diabetic neuropathy as assessed using novel near fiber motor unit potential parameters. *Clinical Neurophysiology*. **126** 4 794–802 (2015).
13. Stashuk DW. Decomposition and quantitative analysis of clinical electromyographic signals. *Medical Engineering and Physics*. **21** 6-7 389–404 (1999).
14. Boe SG, Stashuk DW, Brown WF, Doherty TJ. Decomposition-based quantitative electromyography: Effect of force on motor unit potentials and motor unit number estimates. *Muscle and Nerve*. **31** 3 365–373 (2005).
15. Power GA, Allen MD, Gilmore KJ, Stashuk DW, Doherty TJ, Hepple RT, Taivassalo T, Rice CL. Motor unit number and transmission stability in octogenarian world class

- athletes: Can age-related deficits be outrun? *Journal of Applied Physiology*. **121** 4 1013-1020 (2016).
16. Hourigan ML, McKinnon NB, Johnson M, Rice CL, Stashuk DW, Doherty TJ. Increased motor unit potential shape variability across consecutive motor unit discharges in the tibialis anterior and vastus medialis muscles of healthy older subjects. *Clinical Neurophysiology*. **126** 12 2381–2389 (2015).
17. Stålberg E V, Sonoo M. Assessment of variability in the shape of the motor unit action potential, the “jiggle,” at consecutive discharges. *Muscle and Nerve*. **17** 10 1135–1144 (1994).
18. Connelly DM, Rice CL, Roos MR, Vandervoort AA. Motor unit firing rates and contractile properties in tibialis anterior of young and old men. *Journal of Applied Physiology*. **87** 2 843–852 (1999).
19. McNeil CJ, Doherty TJ, Stashuk DW, Rice CL. Motor unit number estimates in the tibialis anterior muscle of young, old, and very old men. *Muscle and Nerve*. **31** 4 461–467 (2005).
20. Marsh E, Sale D, McComas AJ, Quinlan J. Influence of joint position on ankle dorsiflexion in humans. *Journal of Applied Physiology*. **51** 1 160-167 (1981).
21. Belanger AY, McComas AJ. Extent of motor unit activation during effort. *Journal of Applied Physiology*. **51** 5 1131–1135 (1981).
22. Doherty TJ, Stashuk DW. Decomposition-based quantitative electromyography: Methods and initial normative data in five muscles. *Muscle and Nerve*. **28** 2 204–211 (2003).

23. Boe SG, Stashuk DW, Doherty TJ. Within-subject reliability of motor unit number estimates and quantitative motor unit analysis in a distal and proximal upper limb muscle. *Clinical Neurophysiology*. **117** 3 596-603 (2006).
24. Sanders DB, Howard JF. AAEE minimonograph #25 Single-fiber electromyography in myasthenia gravis. *Muscle and Nerve*. **9** 9 809–819 (1986).
25. Brill MH, Waxman SG, Moore JW, Joyner RW. Conduction velocity and spike configuration in myelinated fibers: computed dependence on internode distance. *Journal of Neurology, Neurosurgery and Psychiatry*. **40** 8 769–774 (1977).
26. Benatar M, Hammad M, Doss-Riney H. Concentric-needle single-fiber electromyography for the diagnosis of myasthenia gravis. *Muscle and Nerve*. **34** 2 163–168 (2006).
27. Fahim MA, Hasan MY, Alshuaib WB. Early morphological remodeling of neuromuscular junction in a murine model of diabetes. *Journal of Applied Physiology*. **89** 6 2235–2240 (2000).
28. Yagihashi S, Kamijo M, Watanabe K. Reduced myelinated fiber size correlates with loss of axonal neurofilaments in peripheral nerve of chronically streptozotocin diabetic rats. *American Journal of Pathology*. **136** 6 1365–1373 (1990).
29. Hegarty PV, Rosholt MN. Effects of streptozotocin-induced diabetes on the number and diameter of fibers in different skeletal muscles of the rat. *Journal of Anatomy*. **133** 205–211 (1981).
30. Kjeldsen K, Braendgaard H, Sidenius P, Larsen JS, Nørgaard A. Diabetes decreases Na<sup>+</sup>-K<sup>+</sup> pump concentration in skeletal muscles, heart ventricular muscle, and peripheral nerves of rat. *Diabetes*. **36** 7 842–848 (1987).

31. Nobe S, Aomine M, Arita M, Ito S, Takaki R. Chronic diabetes mellitus prolongs action potential duration of rat ventricular muscles: circumstantial evidence for impaired Ca<sup>2+</sup> channel. *Cardiovascular Research*. **24** 5 381–389 (1990).
32. Chisari C, D'Alessandro C, Manca ML, Rossi B. Sarcolemmal excitability in myotonic dystrophy: Assessment through surface EMG. *Muscle and Nerve*. **21** 4 543–546 (1998).
33. Hansen S, Ballantyne JP. Axonal dysfunction in the neuropathy of diabetes mellitus: a quantitative electrophysiological study. *Journal of Neurology, Neurosurgery and Psychiatry*. **40** 6 555–564 (1977).
34. Ahn S-W, Kim S-H, Kim J-E, Kim S-M, Kim SH, Park KS, Sung JJ, Lee KW, Hong YH. Reproducibility of the motor unit number index (MUNIX) in normal controls and amyotrophic lateral sclerosis patients. *Muscle and Nerve*. **42** 5 808–813 (2010).
35. Boekestein WA, Schelhaas HJ, van Putten MJ, Stegeman DF, Zwarts MJ, van Dijk JP. Motor unit number index (MUNIX) versus motor unit number estimation (MUNE): A direct comparison in a longitudinal study of ALS patients. *Clinical Neurophysiology*. **123** 8 1644–1649 (2012).
36. Furtula J, Johnsen B, Christensen PB, Pugdahl K, Bisgaard C, Christensen MK, Arentsen J, Frydenberg M, Fuglsang-Frederiksen A. MUNIX and incremental stimulation MUNE in ALS patients and control subjects. *Clinical Neurophysiology*. **124** 3 610–618 (2013).
37. Bromberg MB, Swoboda KJ, Lawson V.H. Counting motor units in chronic motor neuropathies. *Experimental Neurology*. **184** 53–57 (2003).



38. Lewis RA, Li J, Fuerst DR, Shy ME, Krajewski K. Motor unit number estimate of distal and proximal muscles in Charcot-Marie-Tooth disease. *Muscle and Nerve*. **28** 2 161–167 (2003).
39. Lawson VH, Gordon Smith A, Bromberg MB. Assessment of axonal loss in Charcot–Marie–Tooth neuropathies. *Experimental Neurology*. **184** 2 753–757 (2003).
40. Videler AJ, van Dijk JP, Beelen A, de Visser M, Nollet F, van Schaik IN. Motor axon loss is associated with hand dysfunction in Charcot-Marie-Tooth disease 1a. *Neurology*. **71** 16 1254–1260 (2008).
41. Van Dijk JP, Verhamme C, Van Schaik IN, Schelhaas HJ, Mans E, Bour LJ, Stegeman DF, Zwarts MJ. Age-related changes in motor unit number estimates in adult patients with Charcot-Marie-Tooth type 1A. *European Journal of Neurology*. **17** 8 1098–1104 (2010).
42. Oh SJ. The single-fiber EMG in chronic demyelinating neuropathy. *Muscle and Nerve*. **12** 5 371–377 (1989).
43. Gantayat M, Swash M, Schwartz MS. Fiber density in acute and chronic inflammatory demyelinating polyneuropathy. *Muscle and Nerve*. **15** 2 168–171 (1992).
44. Noto Y, Misawa S, Mori M, Kawaguchi N, Kanai K, Shibuya K, Isoses S, Nasu S, Sekiguchi Y, Beppu M, Ohmori S, Nakagawa M, Kuwabara S. Prominent fatigue in spinal muscular atrophy and spinal and bulbar muscular atrophy: evidence of activity-dependent conduction block. *Clinical Neurophysiology*. **124** 9 1893–1898 (2013).
45. Delmont E, Benvenuto A, Grimaldi S, Duprat L, Philibert M, Pouget J, Grapperon AM, Salort-Campana E, Sevy A, Verschueren A, Attarian S. Motor unit number index

(MUNIX): Is it relevant in chronic inflammatory demyelinating polyradiculoneuropathy (CIDP)? *Clinical Neurophysiology*. **127** 3 1891–1894 (2016).

46. Stålberg E, Trontelj J V. The study of normal and abnormal neuromuscular transmission with single fibre electromyography. *Journal of Neuroscience Methods*. **74** 2 145–154 (1997).

## Chapter 3

### 3 <sup>1</sup>Abnormal Motor Unit Firing Rates In Chronic Inflammatory Demyelinating Polyneuropathy

#### 3.1 Introduction

Chronic inflammatory demyelinating polyneuropathy (CIDP) is an immune mediated disorder of peripheral nerves, with predominant motor involvement and progression over several months. In some patients with CIDP the disease course is monophasic with complete recovery, and in others it can be slowly progressive, or relapsing-remitting resulting in prolonged morbidity and sometimes-permanent disability <sup>1</sup>. Even with appropriate treatment, CIDP usually results in multifocal and segmental demyelination that induces motor unit (MU) loss over time <sup>2</sup>. The primary goals of treatment management are to control the state of inflammation and thus reduce peripheral axonal loss and consequential atrophy, weakness and disability.

It is well established that functioning numbers of motor units as well as the motor unit firing rate characteristics influence the generation and control of muscle force, however this has not been systematically investigated in patients with CIDP. Skeletal muscle composition and some MU physiological properties have been described in Amyotrophic Lateral Sclerosis (ALS) including the finding that mean motor unit firing rates were higher in patients with dominant lower motoneuron (LMN) dysfunction compared to controls.

A version of this chapter has been accepted for publication in the Journal of the Neurological Sciences

<sup>1</sup> Gilmore K.J, Kirk E.A, Doherty T.J, Kimpinski K, Rice C.L. Abnormal Motor Unit Firing Rates In Chronic Inflammatory Demyelinating Polyneuropathy.

Conceivably this was due to compensatory mechanisms needed to achieve the desired force accounting for a loss of MUs<sup>3</sup>. MU firing rates were lower in patients with ALS with dominant upper motoneuron (UMN) features probably due to diminished central drive<sup>3</sup>. In addition to alterations in mean firing rates, it has been shown that patients with ALS have greater motor unit firing rate dysfunction and increased motor unit firing rate variability, specifically in ALS patients with dominant UMN dysfunction.

The few studies focused on MU function, demonstrated that individuals with CIDP have fewer MUs than control subjects in the tibialis anterior muscle<sup>2</sup>. Furthermore, severe disruptions in action potential propagation have been demonstrated by concentric needle detected jitter and jiggle values that were greater than controls, as well as the presence of neuromuscular junction blocking<sup>4,2</sup>. The losses in motor axons as well as the instability seen in the neuromuscular junctions of patients with CIDP may have precipitated the loss of total muscle mass and the infiltration of non-contractile tissue in the leg musculature<sup>5</sup>. Overall, these changes to the neuromuscular system likely contribute to functional weakness and disability in individuals with CIDP.

Functional impairment in patients with CIDP is primarily caused by conduction block and chronic denervation that leads to muscle atrophy and weakness. However, in addition to this, it is fundamental to study the motor unit firing characteristics to garner a fuller understanding of the etiology of muscle weakness in patients with a chronic peripheral demyelinating disease. Furthermore, because individuals with CIDP demonstrate a length dependency with regard to axonal loss, often affecting gait and balance, we chose to investigate a leg muscle, the tibialis anterior. Fewer motor units, skeletal muscle loss as well as neuromuscular blocking or slowed axonal transmissions have previously been

reported for this muscle <sup>2</sup> and therefore we expect firing rates to be impaired and recruitment of motor units to be the main strategy used for force gradation at higher contraction intensities in patients with CIDP.

## 3.2 Methods

## 3.3 Subjects

Seven control (4 male/3 female) subjects and eight (6 male/2 female) patients with CIDP were recruited for the study (Table 1). All control subjects were healthy, living independently and medication free. Control subjects were recreationally active but not trained systematically. Exclusion criteria included known neuromuscular or orthopaedic disorders of the lower limb, diabetes, excessive alcohol use, caffeine consumption prior to participation, and recreational drug use. This study was reviewed and approved by the local University's research ethics board for human experimentation and conforms to the latest revision of the Declaration of Helsinki.

### 3.3.1 Patient Electrodiagnostic Criteria

All individuals with CIDP were diagnosed based on the criteria established by the European Federation of Neurological Societies <sup>6</sup>. Patients with any metabolic (including diabetes), neurological, or vascular diseases (other than related to CIDP) were excluded from this study. Clinical electrodiagnostic evaluation included standard motor studies of the median, ulnar, tibial, and fibular nerves. All patients had electrodiagnostic testing and all patients demonstrated demyelinating features (increased temporal dispersion, or conduction block, onset latencies/conduction velocities in the demyelinating range) at the time of diagnosis (Table 3.2). Standard clinical measures of cerebral spinal fluid (CSF),

compound muscle action potential (CMAP) amplitudes, nerve conduction velocities, and sensory nerve action potential amplitudes (SNAP) were compared to normative values to substantiate a diagnosis of CIDP. Moreover, all patients with CIDP received standard medical care and responded to treatment with intravenous immunoglobulin (IVIG), oral prednisone or plasma exchange (Table 3.2).

### 3.3.2 Strength and Experimental Set-up

All data were collected during one testing session with one control subject returning for a second visit to collect a sufficient number of action potential trains for firing rate measures. To record voluntary strength of the dorsiflexors, subjects were seated upright in a dynamometer (Cybex HUMAC NORM; CSMi Medical Solutions, Stoughton, MA) with the right leg fixed to an adaptor arm with the right ankle positioned at 30° of plantar flexion, while both knee and hip angles were maintained at 90°. Inelastic fastenings were wrapped over the dorsum of the foot to secure it to the dynamometer ensuring no aberrant movement. Control and patients with CIDP performed three to five dorsiflexion MVCs, with at least five min of rest between each attempt. All subjects were instructed to contract as hard and as fast as possible to ensure maximal rate of torque were achieved. Each MVC was held for three to five seconds.

### 3.3.3 Electromyography

Surface electromyography (sEMG) signals were recorded from the TA using self-adhering Ag-AgCl electrodes (1 cm × 3 cm). The active electrode was positioned over the TA motor point, approximately seven cm distal to the tibial tuberosity and two cm lateral to the anterior border of the TA, with the reference was placed over the patella. All

sEMG signals were preamplified ( $\times 1,000$ ), wide-band filtered between 10 Hz and 10 kHz (Neurolog, NL844; Digitimer), and sampled at 2 kHz (Power 1401; Cambridge Electronic Design).

Intramuscular EMG signals were recorded during voluntary isometric contractions using two intramuscular tungsten electrodes<sup>7,8,9</sup>. The electrodes were commercially available insulated tungsten needles (123  $\mu\text{m}$  in diameter and 45 mm in length (FHC, Bowdoin, ME). After sterilization, these electrodes were inserted into the tibialis anterior muscle with one needle inserted distally in the TA muscle belly, and the other proximally (7-9 cm distal to the patella). The two intramuscular electrodes were connected to separate channels, and each needle was manipulated independently by an experienced operator. This allows the needle operator to sample at each contraction intensity from various discrete MUs, from different regions and depths of the muscle in order to build a representative MU profile. The intramuscular EMG signals were pre-amplified ( $\times 100$ ) and wide-band filtered between 10 Hz and 10 kHz and sampled at 20 kHz per channel. The surface ground electrodes for the intramuscular recordings were positioned over the patella of the tested limb. Live visual and audio feedback of intramuscular EMG signals were provided to each operator independently.

Multiple voluntary contractions were held for five to ten seconds at each of the three contraction levels (25%, 50%, 75%), whereas MVCs were held for three to five seconds. The order of contraction intensity was randomized. MU action potential trains were only included when sampled during the steady-state torque plateau of each voluntary contraction (Figure 3.1). To sample from many different isolated MUs over the series of voluntary contractions, the intramuscular tungsten electrodes were maneuvered and

advanced slowly through the muscle in increments of  $\sim 0.5$  cm or less per voluntary contraction. Verbal encouragement was provided, and live visual feedback of force was displayed to each subject during all voluntary contractions. Fatigue was minimized by providing adequate rest (3-5 minutes) between contractions and the session ended when an MVC contraction was  $>5\%$  lower than the baseline MVCs.

### 3.3.4 Data Analysis and Statistics

MU analyses were performed offline with Spike2 (Cambridge Electronic Design; Cambridge, UK) as described previously<sup>8,9,10,11</sup>. To confirm spikes belonged to the same specific MU, each MU was first analyzed using a template shape algorithm, and then visually inspected by an experienced operator<sup>7</sup>. To be accepted, rigorous inclusion criteria were applied and in addition to shape overlay of MU potentials a minimum of five consecutive contiguous action potentials (four inter-spike intervals) was required for each acceptable MU train. Additionally, a coefficient of variation of  $<30\%$  for the inter-spike intervals of each MU train was required for a train to be included in the analysis<sup>12</sup>. Any doublet firings ( $>100$  Hz) were not included in the MU analysis. An example of two discrete MU action potential trains extracted during an MVC from a control subject is provided (Figure 3.1). It should be noted that the needle electrode was slowly advanced during each contraction and thus there are small variations in the amplitude and shape of the successive action potentials and inherent small temporal differences in the timing of each firing. However, the characteristic unique ‘signature’ of each firing was the critical feature used to determine a single train of action potentials arising from one MU and independent from other units. To statistically compare MU trains between controls and patients, trains were grouped into four bins based on torque contraction level: a 25% bin



included units ranging from 12.5 - 37.5 % MVC, a 50% bin was from 37.5 % - 62.7%, a 75% bin was from 62.5% - 85%, and 100% bin contained torque levels between 85% – 100% of MVC<sup>9</sup>. To assess surface EMG, 1.5 second time epochs were measured during the steady-state torque portion of all four voluntary contraction intensities. The electromyographic root-mean-square (EMG-RMS) amplitude during MVC torque was used to normalize surface EMG for the 25, 50 and 75% contraction intensities. To determine statistical significance between CIDP and controls Chi square calculations were performed on contraction bins to measure how expected outcomes compare to observed data.

The R software program (version 3.6.1) was used for statistical analyses. Anthropometric data were compared using unpaired two-tailed t-tests. Pearson correlation coefficients were calculated for all mean MU firing rates dependent on MVC% for CIDP and control group. Random intercept mixed linear regression models were used to compare mean MU firing rates between control subjects and patients with CIDP for each voluntary contraction intensity bin using the *lme4* package<sup>13</sup>. To normalize data, mean MU firing rates were log-corrected, with null and full models with the subject as random effect estimates. The MVC%, MU train length, standard deviation of the firing rate means and the coefficient of variation of the mean firing rate were defined as fixed effect estimates. The models were a subset based on targeted contraction bins, with the Likelihood Ratio Tests performed to compare the effect of CIDP. Statistical significance was set to  $P \leq 0.05$ .

### 3.4 Results

Mean age and anthropometric indices were not different between groups (Table 3.1). Patients with CIDP were 33% weaker for dorsiflexor MVC strength when compared with controls (Table 3.1). The intramuscular EMG sampling of voluntarily activated MUs yielded a total of 1389 MU action potential trains, with 664 from individuals with CIDP and 725 from control subjects (Figure 3.2). There are apparent differences in the scatter plots, depicting each MU firing rate as a discrete sample between control and CIDP groups (Figure 3.2). Although rates are higher in the CIDP group at the lower (25% MVC) contraction intensity compared to controls, the mean firing rates of binned units were not higher at intensities of 75 and 100% MVC. This resulted in a weak negative correlation with %MVC ( $r = -0.20$  95% confidence interval =  $-0.27$ – $-0.13$ ,  $t = -5.37$ ,  $p$  value =  $1.08e-07$ ) for the CIDP group. Results from the control group contrasted with the findings in the CIDP group, and showed a strong positive correlation between MU firing rate and MVC% ( $r = 0.78$  95% confidence interval =  $0.75$ - $0.84$ ,  $t = 33.9$ ,  $p$  value <  $2.2e-16$ ).

When mean MU firing rates were grouped based on target contraction intensities, histograms show the distributions of sampled MU firing rates grouped by contraction intensity up to MVC (Figure 3.3). Notably, very few MU firing rates occurred above 30 Hz in the CIDP group. When the firing rate distributions at 75% and 100% of MVC were compared in the two groups, the rates in the CIDP group were significantly lower. At 25% of MVC, the patients with CIDP demonstrated a higher MU firing rate range and a shifted distribution to higher MU firing rates. To test the effect of CIDP on MU firing rates a mixed linear regression analysis was used to compare each targeted contraction

bin (Figure 3.2). Both groups were equally capable of targeting the various MVC intensities (Table 3.3) and mean MU firing rates of patients with CIDP were higher at the lowest contraction intensity bin of 25% MVC ( $X^2 = 15.9$ ,  $df = 8$ ,  $p$  value =  $6.6e-05$ ). Whereas, at the two highest contraction intensity bins, the firing rates in patients with CIDP were lower in comparison to controls (75 % of MVC;  $X^2 = 30.6$ ,  $df = 8$ ,  $p$  value =  $3e-08$ ; 100% of MVC  $X^2 = 42.2$ ,  $df = 8$ ,  $p$  value =  $8.1e-11$ ). There was no difference at 50% of MVC between the control group and the patients with CIDP and this finding is further supported by the similarity between mean values (Table 3.3) and distribution ranges (Figure 3.3). Surface EMG (normalized to MVC) indicated that both groups had a positive linear relationship between contraction intensity bins and sEMG. However, sEMG was lower ( $P < 0.05$ ) in patients with CIDP when compared with control subjects at 50 and 75% MVC (Table 3.3).

Table 3.1 Subject characteristics

<b>Anthropometric parameters</b>	<b>Controls (n = 7)</b>	<b>Patients with CIDP (n = 8)</b>
Men/Women	4/3	6/2
Age (years)	58.0 ± 8.3	59.2 ± 6.5
Height (cm)	152.0 ± 6.0	163.0 ± 4.0
Mass (kg)	73.5 ± 9.4	79.4 ± 11.3
BMI (kg/m <sup>2</sup> )	25.3 ± 2.8	27.8 ± 4.8
Dorsiflexion MVC strength (Nm)	44.2 ± 4.8	29.8 ± 3.4*

BMI- Body mass index, MVC- maximum voluntary contraction \* $P < 0.05$

Table 3.2 CIDP clinical features

Patient (M/F, age)	Duration of treatment (y)	MRC score (out of 5)	CSF protein level (mg/dL)	CB	TD	F-Wave prolongation/latency	Treatment IVIG or Prednisone
M, 61	22	1/5	150	√	√	-	80g/ 4 weeks IVIG
M, 63	6	4/5	75	√	√	√	20g/ 3 weeks IVIG
M, 73	6	4/5	60	√	√	√	Plasma exchange/ 2 weeks, 125 mg prednisone daily
M, 68	3	4/5	70	√	-	-	20g/ 2weeks IVIG
M, 45	20	2/5	-	√	√	√	20 mg prednisone daily
F, 59	10	5/5	290	√	√	√	5mg prednisone every other day
M, 60	12	4/5	660	√	√	√	55g/ 4weeks IVIG
F, 58	12	4/5	96	√	√	√	80g/3weeks IVIG, 10mg prednisone daily

MRC score of ankle dorsiflexion, CSF- Cerebrospinal fluid; IVIG- Intravenous immunoglobulin, M-Male, F-Female

Table 3.3 Motor unit data

Parameter	CIDP				Control			
	25	50	75	100	25	50	75	100
Targeted MVC %	25	50	75	100	25	50	75	100
MVC %	23.8 ± 3.8	46.8 ± 5.2	73.3 ± 5.5	94.3 ± 5.7	24.2 ± 5.4	47.2 ± 8.4	74.3 ± 6.6	96.2 ± 3.9
Discharge rate Hz	18.8 ± 1.1*	16 ± 6.3	18.1 ± 2.0*	17.1 ± 1.7*	13 ± 2.3	18.2 ± 4.4	31.6 ± 3.8	40.1 ± 2.3
No. MU trains	189	162	140	129	202	186	155	141
No. of ISIs per MU train	10.7 ± 5.4	13.2 ± 4.2	9.7 ± 2.5	8.5 ± 3.8	10.2 ± 3.6	10 ± 4.1	9.3 ± 3.3	9.9 ± 4.4
Coefficient of Variation %	10.2 ± 4.1	12.4 ± 3.1	13.8 ± 2.6	15.2 ± 3.6	10 ± 3.5	11.1 ± 2.4	13.2 ± 3.9	14.1 ± 2.8
sEMG %	23.2 ± 6.8	44.8 ± 8.9*	68.4 ± 9.5*	100 ± 0	26.4 ± 8.8	51.6 ± 10.2	77.4 ± 12.5	100 ± 0

Values are means ± SD. MVC, maximal voluntary isometric contraction, ISI- interspike interval, EMG-RMS- electromyography – root mean squared \* $P < 0.05$  for interactions between control and CIDP

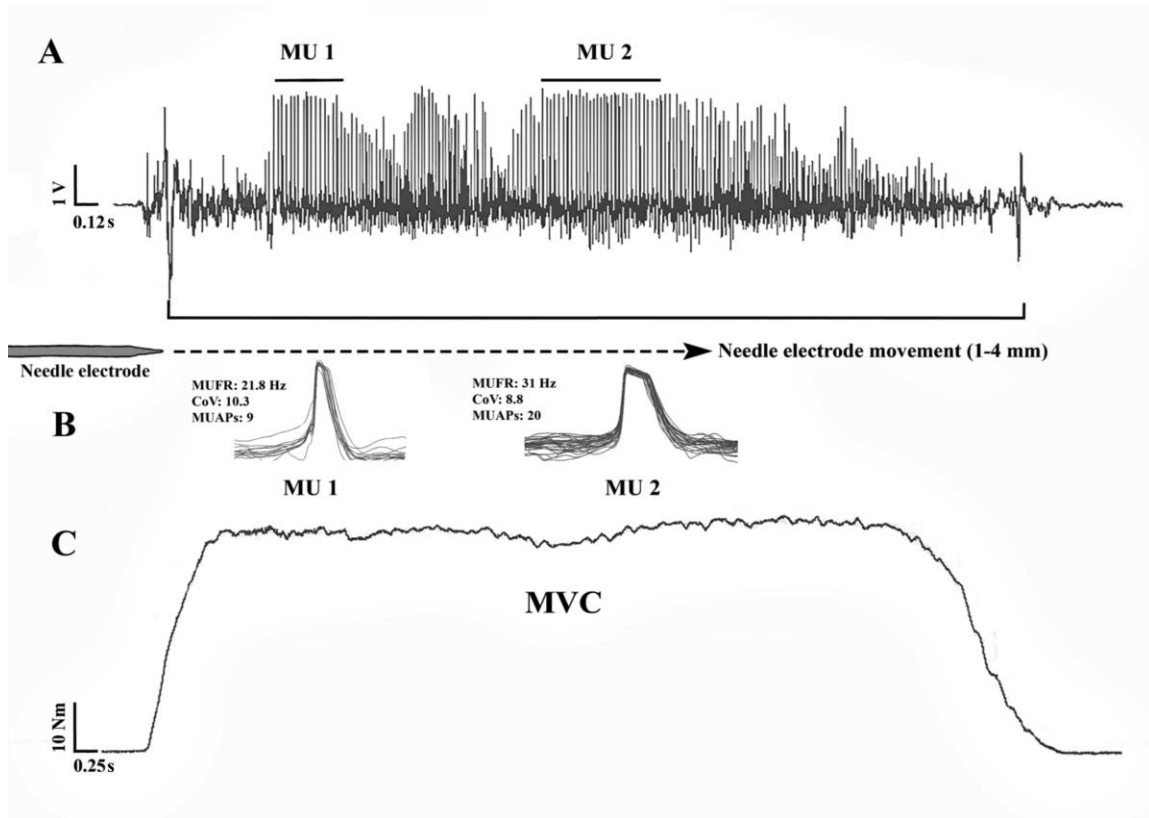


Figure 3.1 Example of tungsten needle recording during a contraction

**A:** Unprocessed tibialis anterior needle electromyography (EMG) recordings collected through tungsten electrodes from a healthy control subject. **B:** Examples of action potential shape and overlay of all action potentials from 2 identified motor unit (MU) trains. MU1 is an overlay of 9 action potentials with a coefficient of variation of 10.3, discharging at 21.8 Hz. MU2 is an overlay of 20 action potentials with a coefficient of variation of 8.8, discharging at 31 Hz. **C:** Raw torque tracing from a maximal voluntary contraction (MVC).

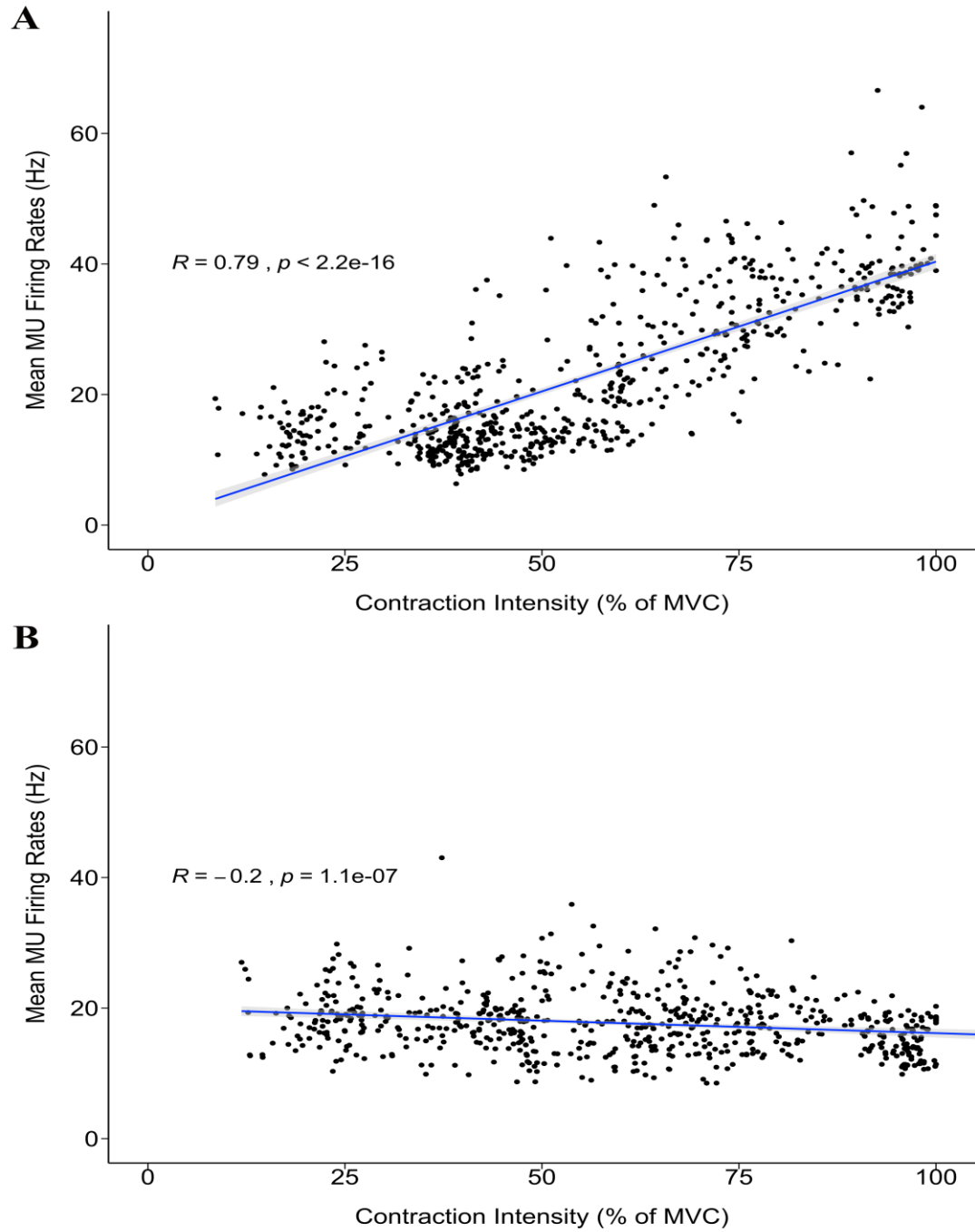


Figure 3.2 Scatter plot of MUF<sub>R</sub>

Scatterplots of 1,389 individual motor unit action potential trains with 725 from the control subjects (**A**) and 664 from patients with CIDP (**B**).



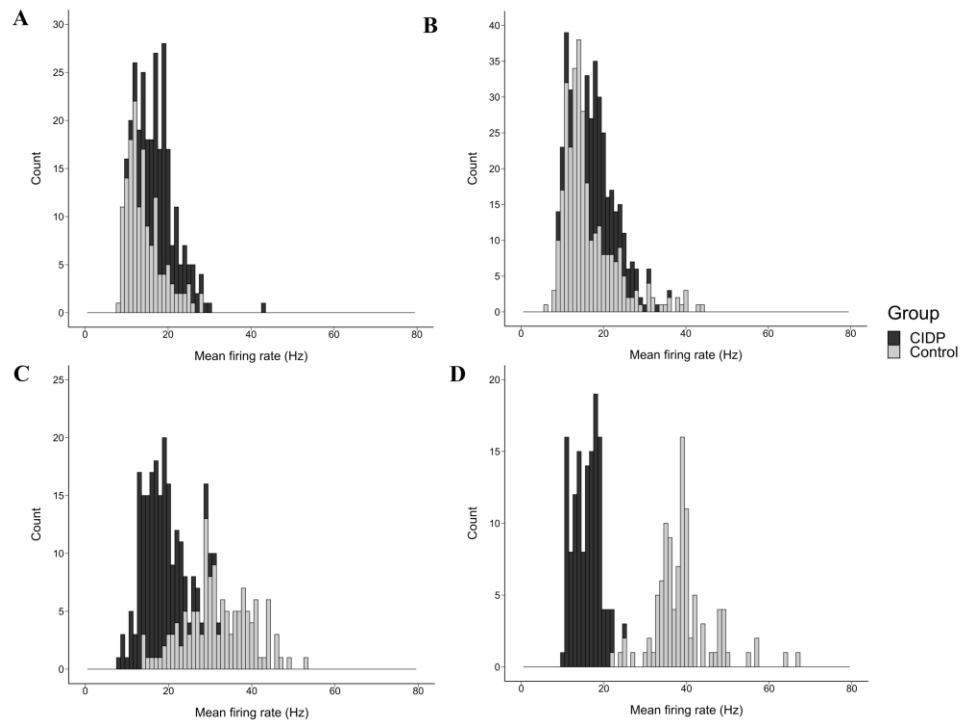


Figure 3.3 Histograms of MUFR means

Bars represent mean motor unit firing rates. Panel **A** is firing rates from a 25% contraction, **B** is 50%, **C** 75% and **D** are firing rates from maximum voluntary contractions (100%). Exact values are found in Table 3.3.

### 3.5 Discussion

In this study we demonstrate that individuals with CIDP, in comparison to an age- and sex-matched healthy group, are 33% weaker in dorsiflexor strength and show distinct alterations in MU firing rates of the tibialis anterior from low to maximal intensity voluntary dorsiflexion contractions. Patients with CIDP had significantly higher motor unit firing rates than controls at a low contraction intensity (25% MVC) and these MU firing rates remained minimally changed at higher contraction intensities (75, 100%

MVC). Conversely, the control group showed increasing rate modulation as contraction intensity was increased, and at MVC the MU firing rates were approximately 55% higher than patients with CIDP. Both control subjects as well as patients with CIDP, had linear increases in surface EMG with increased voluntary isometric contractions. This finding is in agreement with the literature in that there is usually a positive or approximate linear relationship between torque and surface EMG <sup>14</sup>. However, the patients with CIDP had significantly less normalized sEMG at 50 and 75% MVC compared with controls. Thus, for force gradation from lower to higher contraction intensities patients with CIDP may rely more on recruitment than rate coding. In conjunction, perhaps because patients with CIDP have an overall loss of MUs <sup>2</sup>, the patients have fewer units to recruit and thus have lower sEMG specifically at the higher contraction intensities when recruitment of larger MUs normally is required.

Our results are the first to investigate the firing characteristics of motor units in relation to a chronic peripheral demyelinating disease and may suggest that some degree of blocking of action potentials may be occurring along the axons, at the neuromuscular junction or potentially due to disruptions within the muscle fibers making the fibers unable to transmit high frequency (>30Hz) trains of action potentials. Studies using animal models suggest that neuromuscular blocking in patients with CIDP could be due to a variety of factors including reduced axonal caliber, axon terminal dysfunction, ion channel alterations, structural changes in the muscle fiber and other possible mechanisms all related to chronic nerve demyelination <sup>15,16</sup>. Any of these proposed alterations in muscle fibers could potentially adversely impact muscle fiber action potential conduction

propagation, velocity <sup>17</sup> and consequently affect MU firing rates of action potentials that do reach the muscle fibers.

Muscle weakness is a cardinal feature of patients with CIDP, and in prior studies we reported that muscle quantity and quality are lower compared with control subjects and may account for much of the weakness <sup>18,5</sup>. A component of lower skeletal muscle quantity and quality in patients with CIDP could be related to denervation and reinnervation from fewer numbers of MUs as shown previously <sup>2</sup>. Another study reported that when muscle from patients with CIDP was normalized to contractile cross-sectional area, individuals with CIDP still demonstrated weakness compared to healthy controls <sup>18</sup>. This indicates that despite accounting for non-contractile tissue from patients with CIDP, there remain inherent structural disruptions to the contracting proteins. Our results here indicate that lower firing rates in patients with CIDP at higher contraction intensities may also be a significant contributing factor to muscle weakness.

Two studies of patients with CIDP, that used single fiber electromyography (SFEMG) in upper limb muscles reported abnormalities including increased fiber density and transmission instability compared with control subjects <sup>15,16</sup>. Using stimulated SFEMG, it was determined that there was intermittent or persistent blocking in nerve fibers in the upper limb muscles of patients with CIDP <sup>16</sup>. A study by Gilmore et al., (2017) investigated the number of MUs as well the stability of these MUs in individuals with CIDP in the tibialis anterior muscle. That study demonstrated that individuals with CIDP had fewer motor units, with greater neuromuscular instability and motor unit discharge blocking in comparison to healthy aged and sex matched controls. As a consequence of peripheral nerve demyelination neuromuscular instability may reflect the pathological

alterations in neuromuscular transmission or decreased neuromuscular action potential propagation along the axon. Moreover, increased MU firing rates are often observed during routine needle EMG studies performed by clinicians in patients with peripheral neuropathies, however contraction intensities rarely exceed 25% in this setting, which does not allow for the observation of failure of rate modulation at higher contraction intensities <sup>19</sup>.

In addition to differences in mean firing rates, at low levels of contraction, patients with CIDP did not have MU firing rates (MUFR) above 30Hz whereas rates greater than 40Hz were observed in control participants at 75% and 100% of MVC. These results demonstrate that MUs that would normally be active at high force levels are absent due to MU loss, or conversely these later recruited larger MU have a physiological propagation block or have undergone intrinsic changes in the motor neuron properties resulting in the inability to fire at these highest rates.

Based on these observations it appears that force modulation beyond 25% MVC in patients with CIDP is mainly reliant on recruitment. However, these MUs that are later recruited may not have adequate firing rates to reach the necessary tetanic force.

### 3.6 Conclusion

These findings of altered motor unit firing rates and possible motor unit block in patients with CIDP may be fundamental in explaining some of the functional consequences related to weakness and atrophy. The inability of muscles to receive normal higher frequencies of excitation occurring over many years may have contributed to changes in muscle size and quality <sup>18</sup> ultimately contributing to some of the muscle weakness in

CIDP patients. Indeed, it is known that chronic low frequency muscle excitation will lead to dramatic detrimental changes on muscle properties<sup>20,21</sup>. Perhaps if muscles in patients with CIDP, stop receiving rates of excitation beyond 30 Hz the muscle will respond and change its properties accordingly. Importantly, studies examining microscopic muscle architecture in patients with CIDP would further elucidate the result of nerve demyelination on specific muscle composition.

### 3.7 References

1. Silwal A, Pitt M, Phadke R, Mankad K, Davison JE, Rossor A, DeVile C, Reilly MM, Manzur AY, Muntoni F, Munot P. Clinical spectrum, treatment and outcome of children with suspected diagnosis of chronic inflammatory demyelinating polyradiculoneuropathy. *Neuromuscular Disorders*. **28** 8 757-765 (2018).
2. Gilmore KJ, Allen MD, Doherty TJ, Kimpinski K, Rice CL. Electrophysiological and neuromuscular stability of persons with chronic inflammatory demyelinating polyneuropathy. *Muscle and Nerve*. **56** 3 413-420 (2017).
3. Zarei S, Carr K, Reiley L, Diaz K, Guerra O, Altamirano PF, Pagani W, Lodin D, Orozco J, China A. A comprehensive review of amyotrophic lateral sclerosis. *Surgical Neurology International*. **6** 2152-7806 (2015).
4. Vallat JM, Sommer C, Magy L. Chronic inflammatory demyelinating polyradiculoneuropathy: diagnostic and therapeutic challenges for a treatable condition. *Lancet Neurology*. **9** 402–412 (2010).
5. Ishikawa T, Asakura K, Mizutani Y, Ueda A, Murate KI, Hikichi C, Shima S, Kizawa M, Komori M, Murayama K, Toyama H, Ito S, Mutoh T. MR neurography for the evaluation of CIDP. *Muscle and Nerve*. **55** 4 483–489 (2017).
6. Bergh FPYK Van Den, Hadden RDM, Bouche P. European Federation of Neurological Societies / Peripheral Nerve Society Guideline on management of chronic inflammatory demyelinating polyradiculoneuropathy : Report of a joint task force of the European Federation of Neurological Societies and the Peripheral Nerve Society — First Revision. 356–363 (2010).

7. Bellemare F, Woods JJ, Johansson R, Bigland-Ritchie B. Motor-unit discharge rates in maximal voluntary contractions of three human muscles. *Journal of Neurophysiology*. **50** 1380–1392 (1983).
8. Connelly DM, Rice CL, Roos MR, Vandervoort A. Motor unit firing rates and contractile properties in tibialis anterior of young and old men. *Journal of Applied Physiology*. **87** 843-852 (1999).
9. Roos MR, Rice CL, Connelly DM, Vandervoort A. Quadriceps muscle strength, contractile properties, and motor unit firing rates in young and old men. *Muscle and Nerve*. **22** 1094-1103 (1999).
10. Dalton BH, Harwood B, Davidson AW, Rice CL. Triceps surae contractile properties and firing rates in the soleus of young and old men. *Journal of Applied Physiology*. **107** 1781-1788 (2009).
11. Graham MT, Rice CL, Dalton BH. Motor unit firing rates of the gastrocnemii during maximal brief steady-state contractions in humans. *Journal of Electromyography Kinesiology*. **26** 82-87 (2016).
12. Fuglevand AJ, Winter DA, Patla AE. Models of recruitment and rate coding organization in motor-unit pools. *Journal of Neurophysiology*. **70** 2470–2488 (1993).
13. Bates D, Maechler M, Bolker B, Walker S. Fitting Linear Mixed-Effects Models Using lme4. *Journal of Statistical Software*. **67** 1 1-48 (2015).
14. Enoka RM, Duchateau J. Rate Coding and the Control of Muscle Force. *Cold Spring Harbor Perspectives in Medicine*. **10** 7 (2017).
15. Gantayat M, Swash M, Schwartz MS. Fiber density in acute and chronic inflammatory demyelinating polyneuropathy. *Muscle and Nerve*. **15** 168–171 (1992).

16. Oh SJ. The single-fiber EMG in chronic demyelinating neuropathy. *Muscle and Nerve*. **12** 5 371–377 (1989).
17. Noto Y, Misawa S, Mori M, Kawaguchi N, Kanai K, Shibuya K, Iose S, Nasu S, Sekiguchi Y, Beppu M, Ohmori S, Nakagawa M, Kuwabara S. Prominent fatigue in spinal muscular atrophy and spinal and bulbar muscular atrophy: evidence of activity-dependent conduction block. *Clinical Neurophysiology*. **124** 893–898 (2013).
18. Gilmore KJ, Doherty TJ, Kimpinski K, Rice CL. Reductions in muscle quality and quantity in chronic inflammatory demyelinating polyneuropathy patients assessed by magnetic resonance imaging. *Muscle and Nerve*. **58** 396-401 (2018).
19. Dorfman LJ, Howard JE, McGill KC. Motor unit firing rates and firing rate variability in the detection of neuromuscular disorders. *Electroencephalography and Clinical Neurophysiology*. **73** 3 215-224 (1989).
20. Scott OM, Vrbová G, Hyde SA, Dubowitz V. Effects of chronic low frequency electrical stimulation on normal human tibialis anterior muscle. *Journal of Neurology Neurosurgery Psychiatry*. **48** 8 774–781 (1985).
21. Yagihashi S, Kamijo M, Watanabe K. Reduced myelinated fiber size correlates with loss of axonal neurofilaments in peripheral nerve of chronically streptozotocin diabetic rats. *American Journal of Pathology*. **136** 1365–1373 (1990).



## Chapter 4

### 4 <sup>1</sup>Reductions In Muscle Quality And Quantity In CIDP Patients Assessed By Magnetic Resonance Imaging

#### 4.1 Introduction

Chronic inflammatory demyelinating polyneuropathy (CIDP) is an inflammatory peripheral nerve disorder with sensory disturbances and progressive muscle weakness in both the proximal and distal extremities. Most studies on neuroinflammatory diseases, such as multiple sclerosis and inflammatory myelopathies, have focused on the detection of specific neurological lesions using MRI <sup>1,2</sup>. Indeed, nerve lesions in patients with CIDP have been shown by MR imaging in the lumbar nerve roots (L4 and L5), tibial nerve, and brachial plexus <sup>3,4</sup>. In one study the lumbar nerve roots using MRI were evaluated in both treated and untreated CIDP patients and in those with polyneuropathy due to other etiologies. They reported that MRI was useful in identifying nerve root hypertrophy, and as an adjunct test to identify CIDP in situations in which the diagnosis was uncertain <sup>5</sup>. Furthermore, using another MRI technique Sinclair et al <sup>6</sup> demonstrated that magnetization transfer ratio (MTR) in the posterior leg muscles of patients with CIDP was significantly lower than controls, indicating that hydration changes or subtle biochemical disparities within the leg musculature had occurred in the chronic degenerative disease stage of CIDP.

A version of this chapter has been published. Used with permission from John Wiley and Sons, Inc.

<sup>1</sup> Gilmore K.J, Doherty, T.J, Kimpinski, K, Rice, C.L. Reductions In Muscle Quality And Quantity in CIDP Patients Assessed By Magnetic Resonance Imaging. *Muscle Nerve*. **58** 3 396-401 (2018).

Moreover, this study also established that lower MTR values in the anterior compartment of the leg correlated strongly with diminished ankle dorsiflexion strength.

The loss of strength in muscles of those with CIDP is most severe distally, can be profound <sup>7</sup> and likely has a direct significance on functional impairments. However, very little data exists regarding the limb musculature in persons with CIDP, specifically muscle quantity and quality. A few studies have reported correlations between MRI detected nerve impairments and clinical findings (e.g., muscle strength and impairment) <sup>8,9</sup>. Although force (strength) is strongly associated with the quantity of muscle tissue that is accessible for measurement, there are essential qualitative muscle properties involved that may also severely affect muscle strength <sup>10</sup>. Muscle quality can be defined as strength per unit of muscle mass as assessed by MR imaging methods, and is usually assessed by normalizing strength to cross-sectional area <sup>11</sup> or to total muscle volume <sup>12,13</sup>. When muscle strength is normalized to tissue amount and strength deficits persist, this indicates deficiencies in contractile quality. Transverse magnetization (T2) relaxation time is a quantitative MRI sequence sensitive to small changes in proton density of a tissue. For example, when skeletal muscle atrophies with ageing or disease, a concurrent increase in non-contractile tissue, such as connective tissue and adipose tissue is deposited intramuscularly. Thus, in aging T2 relaxations times increase from 31ms in young adults to 42ms in those over 60 years <sup>14</sup>. Increased T2 relaxation times therefore can reflect reduced contractile muscle tissue density contributing to muscle weakness <sup>15</sup>. T2 weighted images and general anatomical MR scans are beneficial beyond calculating strength per unit mass, as they also provide a complementary understanding of tissue density and muscle protein structural integrity <sup>16</sup>. In CIDP, it is sensible to postulate that

muscle weakness may be caused by reductions in both quantity and quality of skeletal muscle, but to date, no studies have investigated these features comprehensively. Additionally, an enhanced understanding of muscle structure and function in CIDP would be very helpful to compare to the well-known electrophysiological alterations in the peripheral nervous system of patients with CIDP <sup>7</sup>. To address this, we chose to focus on the dorsiflexor muscle group, specifically the tibialis anterior (TA), because of its distal limb location. The TA has important functional roles in gait and balance, and has been extensively studied in health, disease and aging, to provide comparative data <sup>17,13,18</sup>. Accordingly, the purpose of the present study was to explore whether MRI is capable of detecting alterations in muscle quantity and quality relative to strength in those with CIDP when compared to a matched to a control group.

## 4.2 Methods

Subjects: Twelve patients (7 men, 5 women) with CIDP (mean age ~61 years) and ten age- matched (mean age ~60 years) control subjects (7 men, 3 women) were recruited to participate in this study. The local university research ethics board approved the study, and informed oral and written consent were obtained from both groups prior to testing. History, clinical, laboratory and electrophysiological features verifying a diagnosis of CIDP were obtained by an experienced neurologist, with specialty training in neuromuscular disorders and electrodiagnosis, to exclude other causes of nerve dysfunction (i.e. radiculopathies, other polyneuropathies, or compressive mononeuropathies). All patients with CIDP were diagnosed based on the criteria established by the European Federation of Neurological Societies (EFNS) <sup>19</sup>. Patients with any metabolic (including diabetes), neurological, or vascular diseases (other than

related to CIDP) were not included in this study (Table 4.1). Standard measures of compound muscle action potential amplitudes (CMAP) nerve conduction velocities, and sensory nerve action potential amplitudes (SNAP) were compared to normative values to confirm a diagnosis. Furthermore, all patients with CIDP received usual medical care and responded to treatment with either plasma exchange, intravenous immunoglobulin (IVIG), or oral prednisone (Table 4.2). All control subjects were healthy, living independently and medication free. All control subjects were screened by a neurologist to eliminate any indication of neuromuscular disease.

#### 4.2.1 MRI Measures

The MRI scans of the leg were acquired via serial axial plane scans in a 3.0-Tesla magnet (Magnetom Spectra 3T mMRBiograph; Siemens Healthcare, Erlangen, Germany). All MRI scans were completed during a single visit to the magnetic resonance imaging unit. Both CIDP and control subjects were inserted supine into the magnet feet first with the TA iso-centered to the bore of the magnet. Inelastic fastenings were used to secure firmly the legs and feet to the MR table to prevent subtle movements throughout the scanning procedure. The complete musculature of the left and right legs was imaged from the level of the tibial plateau to the distal malleoli. MRI for anatomical measures were acquired by means of a 3D FLASH sequence with the following parameters: 9.57-ms repetition time (TR); 2.46-ms echo time (TE); 320 x 240 matrix; 243 x 325-mm field of view; 384 slices; and 0.9mm slice thickness, with slice separation of 1 mm. Total scan acquisition time for the anatomical scan was approximately 13 min per subject. In a secondary scan during the same session, T2 relaxation time was determined by means of a spin–echo sequence with a TR of 3,500 ms. The first spin–echo echo was acquired at  $TE_1 = 13.2$  ms; the

subsequent echoes with 16 equidistant steps had an increment of  $\Delta TE = 13.2$  ms between 13.2 and 211.2 ms. Other parameters were: slice thickness = 5 mm; matrix = 128 x 128; field of view = 325 x 325; slices = 30; bandwidth = 601 HZ/Pixel. Total scan acquisition time for T2 was approximately 12 min per subject.

#### 4.2.2 TA Total Volume, Muscle Composition, and T2 Relaxation Times

Manual and semi-automated image analysis procedures were used offline to measure total TA muscle areas, volumes, composition (contractile versus non- contractile muscle tissue), and T2 relaxation times by means of imaging processing software (OsiriX version 8.2). The researcher was blinded to the group allocation of each subject. Total TA muscle volume was calculated by manually delineating regions of interest (ROIs) around the most proximal portion of the TA and at every third slice (2.6 mm) to the most distal slice comprising distinguishable muscle tissue. Connective tissue, blood vessels, and adipose tissue were eliminated during the manual tracing of the TA. Subsequently, all ROIs within the series were saved for further analysis of non-contractile tissue volume. In order to calculate TA non-contractile tissue volume, an ROI was created, indicative of muscle tissue only. We used the same method as Moore et al.<sup>10</sup> for non-contractile tissue volume. T2 relaxation time was calculated for each slice of the TA and a mean T2 relaxation time was calculated for each individual subject. TA ROIs were manually traced using the same method as described above in the anatomical scans. Pixel-by-pixel parametric color maps (magma) of T2 relaxation times were created from the signal intensity of 16 echo images of the TA. The T2 relaxation time was then calculated by means of the T2FitMap plug- in (version 1.4). The total amount of fat and non-contractile

tissue identified was subtracted from the total TA volume to achieve a volume of contractile tissue only. In addition, this fat corrected volume was used to normalize the MVC strength (strength per amount of contractile tissue).

### 4.2.3 Strength Assessment

On a separate appointment that occurred within 1-3 weeks of the MRI tests, voluntary strength and activation of the dorsiflexors were measured. Subjects were seated in a custom isometric dorsiflexion dynamometer <sup>20</sup> with the left ankle positioned at 30° of plantar flexion, while both knee and hip angles were maintained at 90°. Inelastic straps were wrapped over the dorsum of the foot to secure the foot to the dynamometer. Movement at the hip was disparaged by securing a padded, C-shaped brace to the distal aspect of the left thigh. <sup>21,16</sup>. Subjects performed three dorsiflexion MVCs, with at least 3 min of rest between each attempt. Subjects were instructed to contract as hard and as fast as possible to ensure maximal torque, and rate of torque development, was achieved. Each MVC was held for approximately 3–4 s. Voluntary activation during the 2nd and 3rd MVC attempts was assessed using the interpolated twitch technique <sup>22</sup>. All torque signals were collected and sampled online at 500 Hz using Spike2 software (Version 7.11; Cambridge Electronic Design, Cambridge, UK) and analyzed off-line to determine voluntary isometric torques (strength). Compound muscle action potential responses of the TA were obtained by supramaximal, percutaneous electrical stimulation of the fibular nerve, distal and posterior to the fibular head. Stimulation was performed through a bar stimulating electrode using single, 100- us square-wave pulses via a constant-voltage electrical stimulator (Digitimer stimulator, model DS7AH; Digitimer, Welwyn Garden City, UK).

#### 4.2.4 Statistics

Statistical analysis was performed using SPSS software (version 22). Normally distributed data were analyzed using an independent-samples *t*-test. The Levene test was used to determine homogeneity of variance. Non-normal distributions were assessed using the Shapiro–Wilk test of normality. The T2 relaxation times were not normally distributed and were assessed using Mann–Whitney non-parametric *t*-tests. The results were considered significant at  $P \leq 0.05$ . All data are presented as mean  $\pm$  standard deviation.

### 4.3 Results

There were no significant differences in age, height, weight and BMI between the patients and control subjects. Participant characteristics are presented in Table 4.1 and the clinical features of the patients with CIDP are listed in Table 4.2. Despite similar and equal high levels of voluntary activation (>95%), isometric strength when compared with controls was significantly lower in the subjects with CIDP (Table 4.3). Patients also had a lower compound muscle action potential (CMAP) amplitude compared to controls (Table 4.3). When normalized to total muscle volume, patients with CIDP strength was approximately 29% lower than controls (Table 4.3), and when normalized to fat corrected contractile tissue volume, CIDP strength was approximately 18% lower compared with controls. Overall, TA muscle volumes of patients with CIDP were significantly reduced compared to controls. As a relative percentage of total muscle volume, patients had significantly less contractile tissue compared with controls (Table 4.3). Consequently, non-contractile tissue quantities were significantly greater in CIDP when compared with controls (Table 4.3). Qualitatively, subcutaneous and intramuscular fat was more

abundant in patients with CIDP when compared with controls (Figure 4.1). Furthermore, as shown in Figure 4.2, T2 relaxation times were ~39% longer in duration in CIDP versus controls. Figure 4.3 shows the T2 map of the TA in a patient with CIDP compared with a control subject.

Table 4.1 Participant characteristics

<b>Anthropometric parameters</b>	<b>Controls (<i>n</i> = 10)</b>	<b>Patients with CIDP (<i>n</i> = 12)</b>
Men/Women	7/3	7/5
Age (years)	59 ± 7.6	60.8 ± 9.1
Height (cm)	167.0 ± 5.0	169.0 ± 8.0
Mass (kg)	71.5 ± 10.3	80.5 ± 10.1
BMI (kg/m <sup>2</sup> )	26.2 ± 3.1	27.5 ± 4.1

BMI- Body mass index



Table 4.2 CIDP clinical features

<b>Patient (M/F, age)</b>	<b>Duration of treatment (y)</b>	<b>MRC score (out of 5)</b>	<b>CSF protein level (mg/dL)</b>	<b>CB</b>	<b>TD</b>	<b>F-Wave prolongation /latency</b>	<b>Treatment IVIG or Prednisone</b>
M, 77	8	4/5	330	√	√	√	75g/ 3weeks IVIG
M, 61	22	1/5	150	√	√	–	80g/ 4 weeks IVIG
F, 62	6	4/5	75	√	√	√	20g/ 3 weeks IVIG
M, 73	6	4/5	60	√	√	√	Plasma exchange/ 2 weeks, 125 mg prednisone daily
M, 47	5	5/5	85	√	√	–	55g/ 3 weeks IVIG
M, 68	3	4/5	70	√	–	–	20g/ 2weeks IVIG
M, 45	20	2/5	-	√	√	√	20 mg prednisone daily

F, 59	10	5/5	290	√	√	√	5mg prednisone every other day
M, 60	12	4/5	660	√	√	√	55g/ 4weeks IVIG
F, 58	12	4/5	96	√	√	–	80g/3weeks IVIG, 10mg prednisone daily
F, 59	4	5/5	64	√	–	–	60g/2 weeks IVIG
F, 58	9	5/5	125	√	√	–	30g/2weeks IVIG

MRC score of ankle dorsiflexion, CSF- Cerebrospinal fluid; IVIG- Intravenous immunoglobulin, M-Male,

F-Female

Table 4.3 Strength, electrophysiology, and imaging parameters.

<b>Parameters</b>	<b>Controls (n = 10)</b>	<b>Patients with CIDP (n = 12)</b>	<b>Difference</b>
MVC strength (Nm)	42.1 ± 3.2	26.8 ± 3.5*	-36.3 %
TA CMAP Neg PK amplitude (mV)	7.1 ± 0.9	4.3 ± 0.8*	-39.4 %
Voluntary activation (%)	98	95	3%
Total muscle volume (cm <sup>3</sup> )	117.3 ± 25.2	97.8 ± 17.3*	-17.5 %
Total contractile TA volume (cm <sup>3</sup> )	110.2 ± 23.5	81.3 ± 15.7*	-26.2 %
Contractile volume (%)	93.2 ± 3.8	84 ± 2.2	-9.8 %
Non-contractile volume (%)	6.8 ± 2.2	16 ± 5.2*	58.2 %
MVC/total muscle volume (N·m/cm <sup>3</sup> )	0.38	0.27*	-29.0 %
MVC/contractile volume (N·m/cm <sup>3</sup> )	0.40	0.33*	-17.5 %

MVC- maximum voluntary contraction, CMAP- compound muscle action potential, Neg PK - negative peak amplitude; N·m- Newton meters. \*Significantly different than control ( $P < 0.05$ ). Values are expressed as mean ± standard deviation.

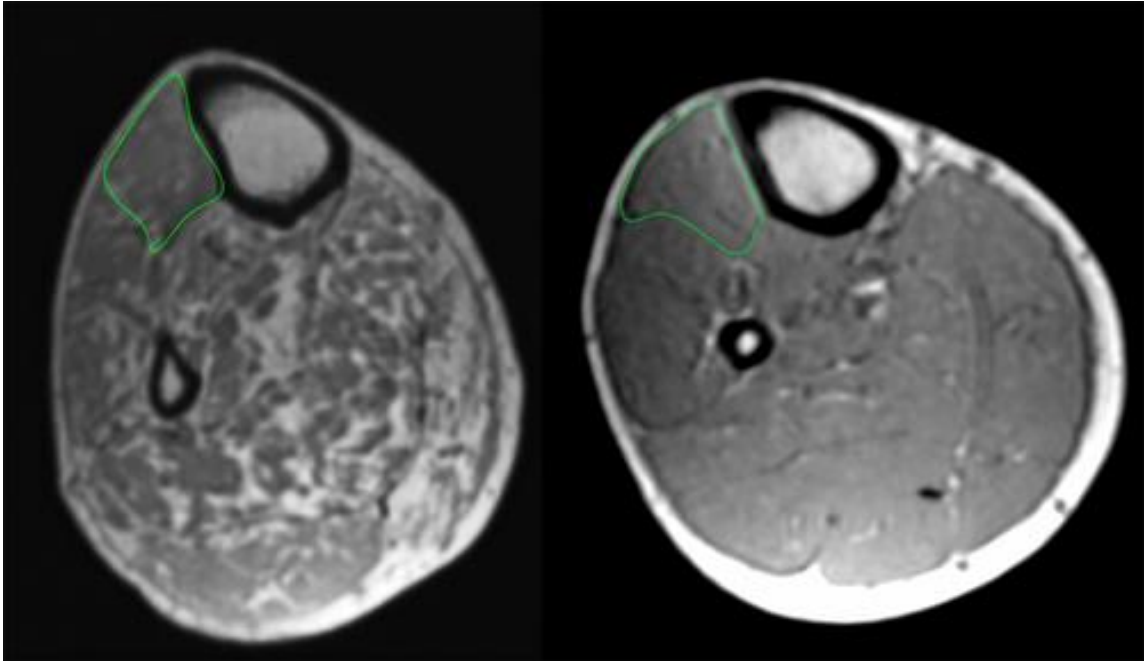


Figure 4.1 MRI cross section of left leg

MRI general anatomic scan: comparison of leg muscles of CIDP (left) vs. control (right) in 2 male participants. The patient with CIDP is 54 years old and the control subject is 55 years old. The TA muscle is outlined in green. Note the extensive intramuscular fat infiltration in the patient with CIDP throughout the leg.

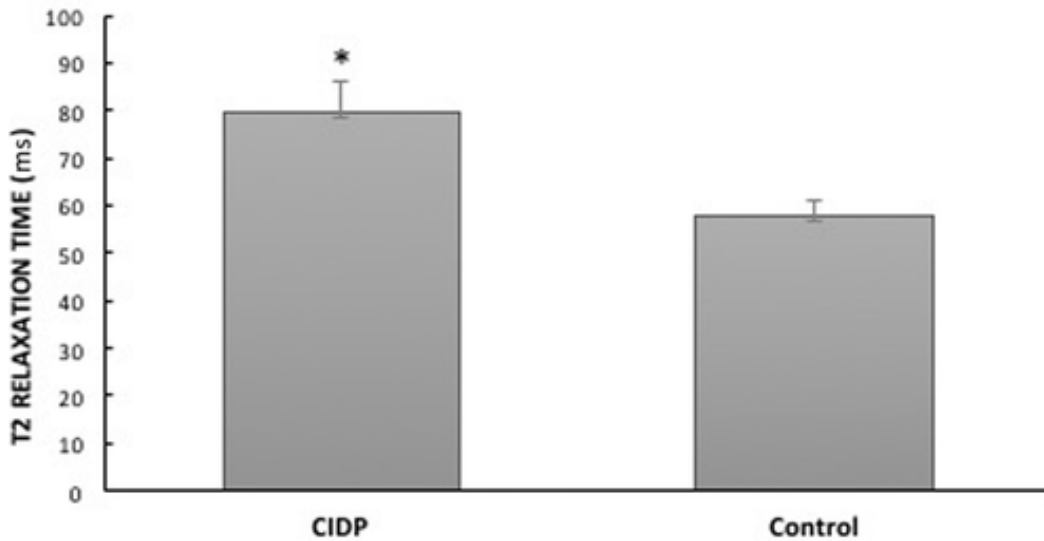


Figure 4.2 T2 relaxation times

T2 relaxation times of the tibialis anterior. \*Significantly longer than control ( $P < 0.05$ ). Values are expressed as mean  $\pm$  standard deviation.

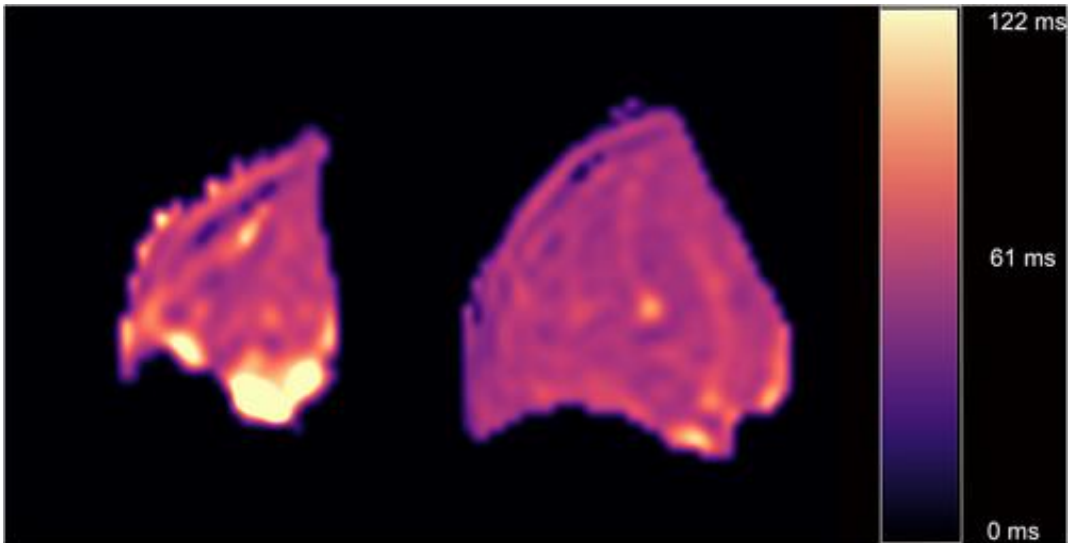


Figure 4.3 T2 maps

T2 maps (ms) of the tibialis anterior muscle: CIDP (left panel) and control (right panel). Purple: muscle (30–70 ms); orange to yellow: fat (>71 ms); black and blue: connective tissue (<30 ms). T2 maps displayed here are for the same participants as those depicted in Figure 4.1.

#### 4.4 Discussion

Using two MRI based techniques (T1 and T2 weighted scans) we have revealed quantitative and qualitative changes in muscle, indicating that compared with control subjects those with CIDP have structural alterations affecting the contractile capacity of muscle tissue. The most salient findings from this study are that patients with CIDP had lower total muscle protein quality and more non-contractile tissue infiltration in the TA, as indicated both by a greater amount of non-contractile tissue and elongated T2 relaxation times when compared to control subjects. Furthermore, CIDP muscles had lower normalized strength values than controls when related to corrected muscle volumes. Absolute dorsiflexion strength of patients with CIDP was ~36% less than the control subjects. This was not due to differences in voluntary activation of the dorsiflexors, as both groups produced >95% activation levels. When TA muscle volume

was expressed relative to strength (normalized strength), the difference between groups persisted at ~29% lower normalized strength for the CIDP group compared with controls. This difference denotes a large difference in muscle contractile quality between CIDP and control subjects indicating that weakness is not simply due to frank loss of tissue. This is further reinforced by the ~39% longer T2 relaxation times in the CIDP group when compared with controls. Consequently, beyond validating dorsiflexor muscle weakness in CIDP, our findings indicate a decrease in protein quality and a loss of total muscle tissue density in the TA of patients with CIDP. Our findings support and extend those of Sinclair et al (2012) who found that MTR in the calf muscles was significantly lower than controls in a group of patients with CIDP <sup>6</sup>.

CMAP amplitude, which provides an indication of excitable muscle mass was ~40 percent lower in the CIDP patient group. This finding aligns with our MRI results, which showed that CIDP patients had a smaller TA volume when compared to controls. Disease duration did not correlate with the amount of skeletal muscle loss in patients with CIDP. The muscle weakness in the patients, at the whole-muscle level, could be due to a quantitative loss of muscle due to denervation or impaired nerve innervation associated with CIDP, thus allowing replacement of functional muscle tissue with non-contractile tissues (adipose tissue). Indeed, it has been reported that dorsiflexion muscle weakness observed in patients with a peripheral neuropathy is correlated with proliferations in intramuscular adipose tissue, determined from T1-weighted MRI scans <sup>20,23</sup>. This indication has been further confirmed in our study by longer T2 relaxation times found for the patients with CIDP when compared to the T2 relaxation times of the control subjects. T2 relaxation times for healthy human skeletal muscle is reported to be between

30 and 70ms<sup>24</sup>, and the control subjects in our study showed a mean value of 59ms. Conversely, the T2 relaxation times of the patients with CIDP were 79ms, which was significantly longer than the controls. Longer T2 relaxation times are indicative of tissue that is less dense (lipid in structure) due in part to the slower motion of protons both in macromolecules as well as water molecules attracted to the surface of the macromolecule<sup>24</sup>.

Heterogeneous expansion of intramuscular non-contractile tissue and fatty infiltration<sup>23</sup> may not only reduce total muscle mass, but also could disrupt normal fascicular organization. Consequently, unfavorable changes in muscle tissue composition are likely key structural alterations that contribute to muscle weakness in CIDP. Findings from other MRI studies that assessed cross sectional area of peripheral nerves including L5 and cauda equina diameter, indicate that innervated muscle tissue would be affected<sup>2</sup>. Our findings are also supported by a study that found muscle disruptions in Charcot-Marie-Tooth neuropathy<sup>25</sup> and in another that showed declines in skeletal muscle function in patients with diabetic peripheral neuropathy<sup>26</sup>. Thus, reductions in muscle quantity and quality are likely driven by CIDP-related neural factors, such as motor axon loss<sup>7</sup> and impaired neural signaling perhaps related to nerve lesions as reported in prior studies that presumably lead to accelerated muscle atrophy<sup>3</sup>.

Importantly, we found that patients with CIDP were weaker relative to volume of muscle even when compared using fat corrected muscle volumes (normalized force). This indicates that the intrinsic force generating capacity of the presumed viable muscle tissue is lower in those with CIDP than controls supporting the concept that disruptions in neural innervation and function affect muscle tissue. We showed previously that patients

with CIDP have impaired neuromuscular stability (higher jitter and jiggle) and percent blocking compared to controls <sup>7</sup>. These nerve alterations therefore could lead to diminishments in muscle strength even when corrected for non-contractile tissue. Although motor unit or axon loss is a feature of CIDP <sup>7</sup> it is not known whether there is a preferential loss of for example Type II fibers and via collateral reinnervation of remaining Type I fibers found in ageing <sup>26</sup> and other neuropathies contributing to morphological changes within the muscle. Ultimately, due to a poorer quality of reinnervation, these muscle fibers may have intrinsic strength decrements as demonstrated in the present study by lower contractile force per cross sectional area (volume) <sup>27,28</sup>.

In using MRI sequences, T2 and the general anatomical scans, important insights have been gained into fundamental changes of skeletal muscle in patients with CIDP. Dorsiflexor weakness in CIDP is likely an outcome of numerous factors, including, but not limited to motor unit loss and accompanying muscle denervation and atrophy. Impaired neural signaling due to the primary site of lesions of the peripheral nerves also may indirectly contribute to poorer muscle tissue quality as reflected by lower normalized force compared with controls. Accordingly, T2 and the general anatomical scans can offer additional understanding into pathological and morphological disruptions to whole-muscle tissue composition that may contribute to diminished muscle function in CIDP. These results further support the utilization of MRI as a tool for muscle analysis and provide a better understanding of the impact of neuronal changes in CIDP on muscular characteristics. Finally, this information may be essential in targeting and evaluating treatment modalities in patients with CIDP.



## 4.5 References

1. Renowden S. Imaging in multiple sclerosis and related disorders. *Practical Neurology*. **14** 5 e3-e3 (2014).
2. Tsuchiya K, Honya K, Yoshida M, Nitatori T. Demonstration of spinal cord and nerve root abnormalities by diffusion neurography. *Journal of Computer Assist Tomography*. **32** 286–290 (2008).
3. Pitarokoili K, Schlamann M, Kerasnoudis A, Gold R, Yoon M-S. Comparison of clinical, electrophysiological, sonographic and MRI features in CIDP. *Journal of Neurological Science*. **357** 1-2 198–203 (2015).
4. Ishikawa T, Asakura K, Mizutani Y, Ueda A, Murate K-I, Hikichi C, Shima S, Kizawa M, Komori M, Murayama K, Toyama H, Ito S, Mutoh T. Magnetic resonance neurography for the evaluation of CIDP. *Muscle and Nerve*. **55** 4 483-489 (2016).
5. Vallat JM, Sommer C, Magy L. Chronic inflammatory demyelinating polyradiculoneuropathy: diagnostic and therapeutic challenges for a treatable condition. *Lancet Neurology*. **9** 4 402–412 (2010).
6. Sinclair CD, Morrow JM, Miranda MA, Davagnanam I, Cowley PC, Mehta H, Hanna MG, Koltzenburg M, Yousry TA, Reilly MM, Thornton JS. Skeletal muscle MRI magnetisation transfer ratio reflects clinical severity in peripheral neuropathies. *Journal of Neurology and Neurosurgery*. **83** 1 29–32 (2012).
7. Gilmore KJ, Allen MD, Doherty TJ, Kimpinski K, Rice CL. Electrophysiological and neuromuscular stability of persons with chronic inflammatory demyelinating polyneuropathy. *Muscle and Nerve*. **56** 3 413-420 (2017).

8. Grimm A, Schubert V, Axer H, Ziemann U. Giant nerves in chronic inflammatory polyradiculoneuropathy. *Muscle and Nerve*. **55** 285-289 (2016).
9. Lozeron P, Lacour M-C, Vandendries C, Théaudin M, Cauquil C, Denier C, Lacroix C, Adms D. Contribution of plexus MRI in the diagnosis of atypical chronic inflammatory demyelinating polyneuropathies. *Journal of Neurological Science*. **360** 170-175 (2016).
10. Moore CW, Allen MD, Kimpinski K, Doherty TJ, Rice CL. Reduced skeletal muscle quantity and quality in patients with diabetic polyneuropathy assessed by magnetic resonance imaging. *Muscle and Nerve*. **53** 5 726–732 (2016).
11. Allen MD, Kimpinski K, Doherty TJ, Rice CL. Length dependent loss of motor axons and altered motor unit properties in human diabetic polyneuropathy. *Clinical Neurophysiology*. **125** 4 836-843 (2014).
12. Power GA, Allen MD, Booth WJ, Thompson RT, Marsh GD, Rice CL. The influence on sarcopenia of muscle quality and quantity derived from magnetic resonance imaging and neuromuscular properties. *Age (Dordr)*. **36** 3 52-59 (2014).
13. Tracy BL, Ivey FM, Hurlbut D, Martel GF, Lemmer JT, Siegel EL, Metter EJ, Fozard JL, Fleg JL, Hurley BF. Muscle quality. II. Effects of strength training in 65- to 75-yr-old men and women. *Journal of Applied Physiology*. **86** 1 195–201 (1999).
14. Schwenzer NF, Martirosian P, Machann J, Schraml C, Steidle G, Claussen CD, Schick F. Aging effects on human calf muscle properties assessed by MRI at 3 Tesla. *Journal Citation Reports*. **29** 6 1346-1354 (2009).
15. Power GA, Dalton BH, Doherty TJ, Rice CL. If you don't use it you'll likely lose it. *Clinical Physiology and Functional Imaging*. **36** 6 497-498 (2015).

16. Dixon WT, Engels H, Castillo M, Sardashti M. Incidental magnetization transfer contrast in standard multislice imaging. *Magn Reson Imaging*. **8** 4 417-422 (1990).
17. McNeil CJ, Doherty TJ, Stashuk DW, Rice CL. Motor unit number estimates in the tibialis anterior muscle of young, old, and very old men. *Muscle and Nerve*. **31** 4 461–467 (2005).
18. Kent-Braun JA, Callahan DM, Fay JL, Foulis SA, Buonaccorsi JP. Muscle weakness, fatigue, and torque variability: Effects of age and mobility status. *Muscle and Nerve*. **49** 2 209-217 (2014).
19. Bergh FPYK Van Den, Hadden RDM, Bouche P. European Federation of Neurological Societies / Peripheral Nerve Society Guideline on management of chronic inflammatory demyelinating polyradiculoneuropathy: Report of a joint task force of the European Federation of Neurological Societies and the Peripheral Nerve Society — First Revision. 356–363 (2010).
20. Marsh E, Sale D, McComas AJ, Quinlan J. Influence of joint position on ankle dorsiflexion in humans. *Journal of Applied Physiology*. **51** 1 160–167 (1981).
21. Allen MD, Major B, Kimpinski K, Doherty TJ, Rice CL. Skeletal muscle morphology and contractile function in relation to muscle denervation in diabetic neuropathy. *Journal of Applied Physiology*. **116** 5 545–552 (2014).
22. Todd G, Gorman RB, Gandevia SC. Measurement and reproducibility of strength and voluntary activation of lower-limb muscles. *Muscle and Nerve*. **29** 6 834 –842 (2004).
23. Hilton TN, Tuttle LJ, Bohnert KL, Mueller MJ, Sinacore DR. Excessive adipose tissue infiltration in skeletal muscle in individuals with obesity, diabetes mellitus, and peripheral neuropathy: association with performance and function. *Physical Therapy*.

- 88** 11 1336–1344 (2008).
24. Bus SA, Yang QX, Wang JH, Smith MB, Wunderlich R, Cavanagh PR. Intrinsic muscle atrophy and toe deformity in the diabetic neuropathic foot: a magnetic resonance imaging study. *Diabetes Care*. **25** 8 1444–1450 (2002).
25. Pareyson D, Saveri P, Pisciotto C. New developments in Charcot-Marie-Tooth neuropathy and related diseases. *Current Opinion in Neurology*. **30** 5 471-480 (2017).
26. Parasoglou P, Rao S, Slade JM. Declining Skeletal Muscle Function in Diabetic Peripheral Neuropathy. *Clin Ther*. **39** 6 1085–1103 (2017).
27. McNeil CJ, Vandervoort AA, Rice CL. Peripheral impairments cause a <sup>[[[]]]</sup>progressive age-related loss of strength and velocity-dependent power in the dorsiflexors. *Journal of Applied Physiology*. **102** 5 1962–1968 (2007).
28. Buller AJ, Eccles JC, Eccles RM. Interactions between motoneurons and muscles in respect of the characteristic speeds of their responses. *Journal of Physiology*. **150** 2 417–439 (1960).

## Chapter 5

# 5 <sup>1</sup>Nerve Dysfunction Leads To Muscle Morphological Abnormalities In Chronic Inflammatory Demyelinating Polyneuropathy Assessed By MRI

### 5.1 Introduction

Chronic inflammatory demyelinating polyneuropathy (CIDP) is an autoimmune disease characterized primarily by demyelination and secondary axonal degeneration of peripheral nerves. Patients typically present with symmetrical motor deficits such as diffuse muscle weakness, as well as sensory impairments. Focal alterations in the lamellar pattern of myelin, which lead to segmental demyelination, are present in CIDP. The myelin sheath becomes discontinuous which has repercussions in relation to axonal conductance <sup>1</sup>. Studies related to neuromuscular function have mainly focused on the neuropathic aspects of CIDP and their involvement in motor impairment. However, changes in skeletal muscle quality and quantity maybe a consequence of motor nerve deficits, but these aspects have not been investigated extensively <sup>2,3</sup>. Nerve lesions in CIDP have been shown by magnetic resonance imaging in the lumbar nerve roots (L4 and L5), tibial nerve, and brachial plexus <sup>4,5</sup>. To date, the effect of nerve lesions in patients with CIDP has not been comprehensively explored in relation to quality and quantity of skeletal muscle. Only a few studies have describe dissociations between

A version of this chapter has been published. Used with permission from John Wiley and Sons, Inc.

<sup>1</sup> Gilmore K.J, Fanous J, Doherty, T.J., Kimpinski, K., Rice, C.L. Nerve Dysfunction Leads To Muscle Morphological Abnormalities In Chronic Inflammatory Demyelinating Polyneuropathy Assessed By MRI *Clinical Anatomy*. **33** 1 77-84 (2020).

MRI detected nerve impairments and clinical findings of decrements in muscle strength<sup>6,7</sup>. T2-weighted MRI and general anatomical MRI (T1) are advantageous beyond providing an overall assessment of muscle mass that can be used for example to normalize strength measures, as they also provide a complementary understanding of tissue density and muscle protein structural integrity<sup>8,9</sup>. Thus, muscle weakness in patients with CIDP may be related to reductions in both quantity and quality of skeletal muscle, however only one study has investigated muscle morphology in patients with CIDP<sup>10</sup>.

A previous study from our group found that overall tibialis anterior (TA) muscle volumes were lower in patients with CIDP compared with age and sex matched controls, and dorsiflexion strength was approximately 29% lower in the CIDP group<sup>10</sup>. Furthermore, non-contractile tissue quantities were roughly 60% greater in the TA muscle of patients when compared with controls. Thus, when strength was normalized to fat corrected contractile tissue volume, strength remained lower by approximately 18% in patients with CIDP compared with controls<sup>10</sup>. Although the dorsiflexors have functional importance in gait and balance, it remains to be determined whether these findings are unique to this muscle group for anatomical and functional reasons or whether other muscles of the leg would be affected similarly. Moreover, because CIDP affects distal musculature more severely<sup>11</sup> we investigated the triceps surae, including the soleus, medial head of gastrocnemius (MG), and lateral head of gastrocnemius (LG). Indeed, the triceps surae has important functional roles in gait and balance, and has been extensively studied in health and aging, to provide comparative data<sup>12,13,14</sup>.

Histochemical studies have shown that the TA contains 70–75% type II fibers <sup>15</sup> and similarly the soleus, is rather homogeneous, being composed of 80% type I muscle fibers <sup>14,15</sup>. However, unlike the TA, the soleus muscle has been shown to be spared from age-related muscle atrophy, contractile slowing, and a loss of motor units when compared to the TA <sup>16</sup>. Furthermore, when the soleus is compared with the gastrocnemii, which are composed of about 50% slow twitch (ST) fibers, the gastrocnemii show substantial anatomical loss when older individuals are compared with younger adults <sup>17</sup>. Thus, there may be anatomical or functional features among different muscles despite sharing the same spinal nerve root innervation that could be affected differently by the demyelination process of peripheral nerves. Given these deficiencies in the literature, a more comprehensive understanding of muscle structure and function from various muscle groups in CIDP would be advantageous in addition to the well-known electrophysiological and anatomical alterations in the demyelinated peripheral nerves of CIDP patients <sup>10</sup>. Accordingly, the purpose of the present study was to explore the large muscles of the posterior leg compartment to examine the degree to which plantar flexion strength and muscle quantity and quality are affected in those with CIDP when compared to matched controls. It was hypothesized that demyelinated peripheral nerves would lead to uniform reduction in all portions of the triceps surae in both quantity and quality of muscle of patients with CIDP.

## 5.2 Methods

Ten patients (six men, four women) with CIDP (mean age 62 years) and nine age-matched (mean age 60 years) control subjects (five men, four women) participated in this study (Table 5.1). The local university research ethics board approved the study, and both

groups provided informed oral and written consent prior to testing. A clinical history, as well as laboratory and electrophysiological descriptions verifying a CIDP diagnosis were obtained by an experienced neurologist, with specialty training in electrodiagnosis and neuromuscular disorders. All other causes of nerve dysfunction (i.e., radiculopathies, other polyneuropathies, or compressive mononeuropathies) as well patients with any metabolic (including diabetes), neurological, or vascular diseases (other than related to CIDP) were screened and these subjects were not included in this study. All patients were diagnosed based on the criteria established by the European Federation of Neurological Societies <sup>11</sup> (Table 5.2). Standard measures of nerve conduction velocities, compound muscle action potential amplitudes (CMAP) (Table 5.1) and sensory nerve action potential amplitudes (SNAP) were compared to normative values to establish a CIDP diagnosis. Furthermore, all patients with CIDP were receiving usual medical care and responded to treatment with intravenous immunoglobulin (IVIG), oral prednisone, or plasma exchange (Table 5.2). All control subjects were healthy, medication free, living independently and were screened by the same neurologist to eliminate any indication of neuromuscular or metabolic disease.

### 5.2.1 Strength Assessment

Within the same week as the MRI scans were acquired, voluntary strength of the right plantar flexors was measured. For strength assessments, subjects were seated in a plantar flexion isometric dynamometer with the right ankle positioned at 90° of plantar flexion and both knee and hip angles were maintained at 90°<sup>18</sup>. Movement at the hip was minimized by fixing a thinly padded, C-shaped support over the distal aspect of the right thigh. <sup>10,19</sup>. Two Velcro straps attached to the dynamometer footplate were secured across



the dorsum of the foot and the toes to secure the foot to the dynamometer footplate. Control subjects performed three plantar flexion maximum voluntary isometric contractions (MVCs), with 3–5 min of rest between each contraction. Patients with CIDP required three to five maximal isometric contractions, with two or more contractions of the contractions within 5% of each other. To mitigate fatigue in the group 5 min of rest was given between each maximal contraction. Both groups were given strong verbal encouragement and torque visual feedback. Each MVC was held for approximately three to four seconds. MVC torque was calculated as the highest torque value achieved from any of the three attempts. All torque signals were collected and sampled online at 500 Hz using Spike2 software (Version 7.11; Cambridge Electronic Design, Cambridge, UK) and analyzed offline to determine voluntary isometric torques (strength).

### 5.2.2 MRI Measures

All MRI scans were completed during a single visit to the MRI unit. Scans of the triceps surae were acquired via serial axial plane images in a 3.0-Tesla magnet (Magnetom Spectra 3T mMRBiograph; Siemens Healthcare, Erlangen, Germany). Control and CIDP subjects were inserted supine into the magnet, feet first with the triceps surae iso-centered to the bore of the magnet. Inelastic fasteners were used to secure tightly the legs and feet to the MR table to avoid subtle movements during the scanning process. The complete musculature of the left and right legs was imaged from the distal malleoli to the proximal tibial plateau. MRI for anatomical measures (T1) were acquired by means of a 3D FLASH sequence with the following parameters: 9.57-ms repetition time (TR); 2.46-ms echo time (TE); 320×240 matrix; 243×325-mm field of view; 384 slices; and 0.9 mm slice thickness, with slice separation of 1 mm. Total scan acquisition time for the

anatomical scan was approximately 13 min per subject. A secondary scan during the same session was performed to determine T2 relaxation times by means of a spin–echo sequence with a TR of 3,500 ms. The first spin–echo was acquired at TE =13.2 ms; the subsequent echoes with 16 equal distant steps had an increment of  $\Delta TE = 13.2$  ms between 13.2 and 211.2 ms. Other parameters were: slice thickness = 5 mm; matrix = 128×128; field of view = 325×325; slices = 30; bandwidth = 601 Hz/pixel. Total T2 scan acquisition time was approximately 12 min per subject.

### 5.2.3 Triceps Surae Total Volume, Muscle Composition, and T2 Relaxation Times

Before calculating MRI results, an inter- rater reliability test was completed to evaluate the reliability of two experimenters calculating muscle mass and subsequently quantifying contractile versus non-contractile tissues in the triceps surae complex. The results of this test indicated that both evaluators were within 95% confidence with each other. Manual and semi-automated image analysis procedures were used offline to measure the soleus, medial and lateral gastrocnemii muscle areas, volumes, composition (contractile versus non contractile muscle tissue), and T2 relaxation times by imaging processing software (OsiriX version 8.3). The researcher was single blinded to group allocation. Total soleus, medial and lateral heads of gastrocnemius muscle volumes were calculated by independently manually delineating regions of interest (ROIs) around the most proximal portion of each muscle and at every third consecutive slice (2.6 mm) to the most distal slice containing distinguishable muscle tissue. Connective tissue, adipose tissue and blood vessels were eliminated during the manual tracing of each of the three triceps surae muscles. All ROIs within the same muscle series were saved for further

analysis and calculation of non-contractile tissue volumes. In order to calculate non-contractile tissue volumes for all three muscles an ROI was created, indicative of only muscle tissue<sup>20</sup>. T2 relaxation time was calculated for each slice of the soleus, medial and lateral heads of gastrocnemius and a mean T2 relaxation time was calculated for each subject. The soleus, medial and lateral heads of gastrocnemius muscle ROIs were manually traced using the same method as described above in the (T1) anatomical scans. Pixel-by-pixel parametric color maps (magma) of T2 relaxation times were created from the signal intensity of 16 echo images of the three muscles. The T2 relaxation time was then calculated by means of the T2 Fit Map plug-in (version 1.5). The total amount of fat and non-contractile tissue identified was subtracted from the total volume of each muscle compartment to achieve a volume of contractile tissue only. In addition, this fat corrected volume was used to normalize the MVC strength (strength per amount of contractile tissue).

#### 5.2.4 Statistics

Statistical analysis was performed using SPSS software (version 22). Normally distributed data were analyzed using an independent-samples t-test. The Levene test was used to determine homogeneity of variance. Non-normal distributions were assessed using the Shapiro–Wilk test of normality. The T2 relaxation times that were not normally distributed were assessed using Mann–Whitney non-parametric t-tests. Cohen’s D effect sizes were calculated for group differences. The results were considered significant at  $P \leq 0.05$ . All data are presented as mean and standard deviation.

### 5.3 Results

There were no significant differences in age, height and weight between the patients with CIDP and control subjects. Participant characteristics are presented in Table 5.1 and the clinical features of the patients are listed in Table 5.2. Isometric plantar flexion strength was 28% lower in patients with CIDP when compared with controls (Table 5.1). Electrophysiological findings also indicated axonal dysfunction with patients having 50% lower CMAP amplitude of the tibial nerve compared to controls (Table 5.1). The total triceps surae volume of patients with CIDP was significantly lower by 19.3% compared to healthy controls. When eliminating the fat and other non-contractile tissue within the total volume of the triceps surae, the patients with CIDP had 47.5% less contractile tissue (Figure 5.1). Consequently, non-contractile tissue quantities were significantly greater (82%) in CIDP when compared with controls (Figure 5.2). Qualitatively, subcutaneous fat was more abundant in patients with CIDP when compared with controls. When normalized to total triceps surae muscle volume, strength was approximately 17% lower in CIDP than controls (Table 5.1) and when normalized to fat corrected contractile tissue volume, CIDP strength was approximately 30% lower compared with controls. Furthermore, as shown in Figure 5.3, T2 relaxation times in the soleus, medial and lateral heads of gastrocnemius were 36.8%, 37.3% and 26.0% longer induration (although not statistically significant) in CIDP versus controls. Figure 5.4 shows cross-sectional T1-weighted MRI scan comparing leg musculature of control versus CIDP with the soleus (SL), MG and LG outlined. Figure 5.5 shows the T2 map of the triceps surae (SL in blue, MG in orange, and LG in yellow) in a control subject compared to a patient with CIDP.

Table 5.1 Participant characteristics

<b>Subject characteristics</b>	<b>Controls (<i>n</i> = 9)</b>	<b>Patients with CIDP (<i>n</i> = 10)</b>
Men/Women	5/4	6/4
Age (years)	59 ± 6.2	61.8 ± 8.2
Height (cm)	167.0 ± 3.0	169.0 ± 8.0
Mass (kg)	73.5 ± 9.4	80.5 ± 8.4
MVC strength (Nm)	132.7 ± 12.2	95.3 ± 8.8*
Normalized strength to total triceps surae volume (Nm/cm <sup>3</sup> )	0.24 ± 0.03	0.15 ± 0.01*
CMAP (mV)	7.5 ± 0.34	3.7 ± 0.72*

MVC - maximum voluntary contraction; CMAP - compound muscle action potential of tibial nerve. There were only significant differences ( $P < 0.05$ ) in strength. Normalized strength is expressed as fat corrected triceps surae volume. Values are expressed as means ± standard deviations.

Table 5.2 CIDP clinical classification

<b>Patient</b>	<b>Duration of CIDP (y)</b>	<b>MRC score (out of 5)</b>	<b>CSF level (g/L isolation)</b>	<b>CB</b>	<b>TD</b>	<b>F-Wave prolongation /latency</b>	<b>Response to IVIG or Prednisone</b>
M, 77	8	3/5	3.3	√	√	√	75g/ 3weeks IVIG
M, 61	22	1/5	1.5	√	√	-	80g/ 4 weeks IVIG
F, 62	6	4/5	0.75	√	√	√	20g/ 3 weeks IVIG
M, 73	6	4/5	0.6	√	√	√	Plasma exchange/ 2 weeks, 125 mg prednisone daily
F, 60	7	4/5	0.75	√	√	-	45g/ 3 weeks IVIG
M, 63	3	4/5	0.7	√	-	-	20g/ 2weeks IVIG
M, 45	20	2/5	-	√	√	√	20 mg prednisone daily
F, 59	10	5/5	2.9	√	√	√	5mg prednisone every other day

M, 60	12	4/5	6.6	√	√	√	55g/ 4weeks IVIG
F, 58	12	4/5	0.96	√	√	√	80g/3weeks IVIG, 10mg prednisone daily

CSF- Cerebral spinal fluid; IVIG- Intravenous immunoglobulin; - represents no value; √ - value observed;  
CB-Conduction block; TD - Temporal dispersion, M-Male, F-Female

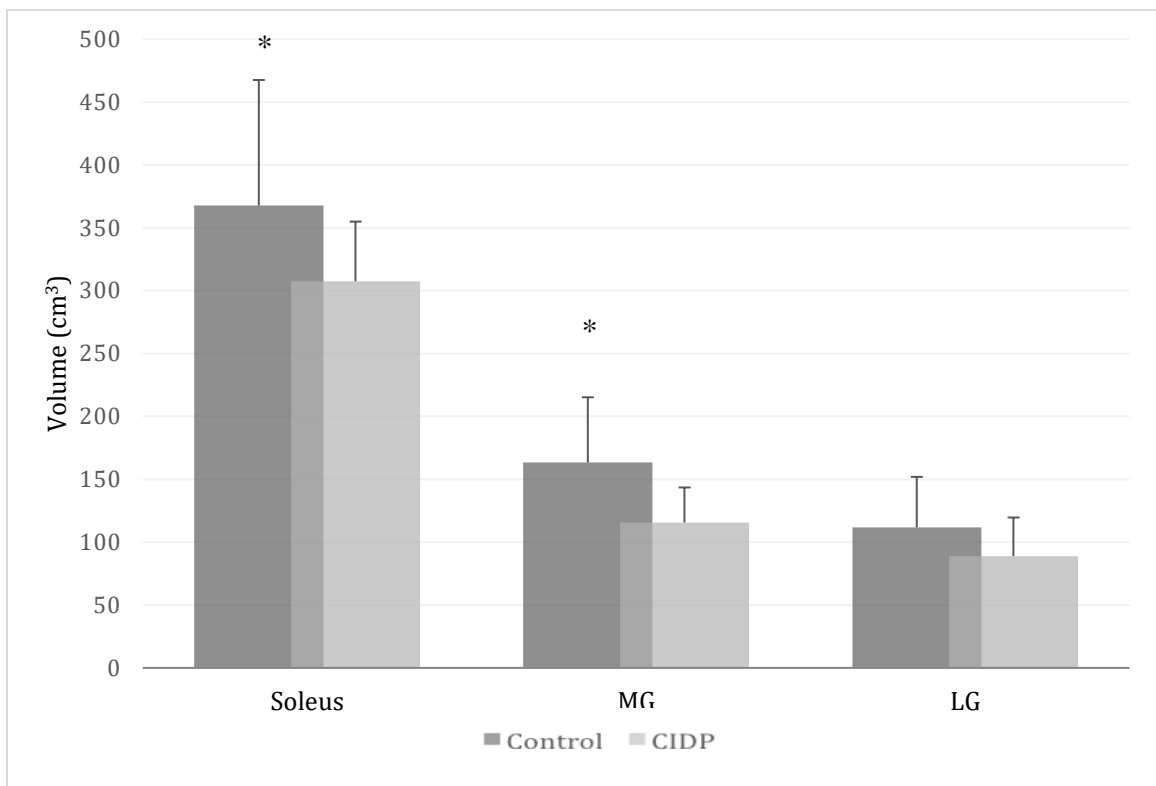


Figure 5.1 Total muscle volume of triceps surae

Total muscle volumes of the soleus, medial head of gastrocnemius (MG), and lateral head of gastrocnemius (LG). \*P < 0.05, significantly different than controls. Values are expressed as means ± standard deviations.

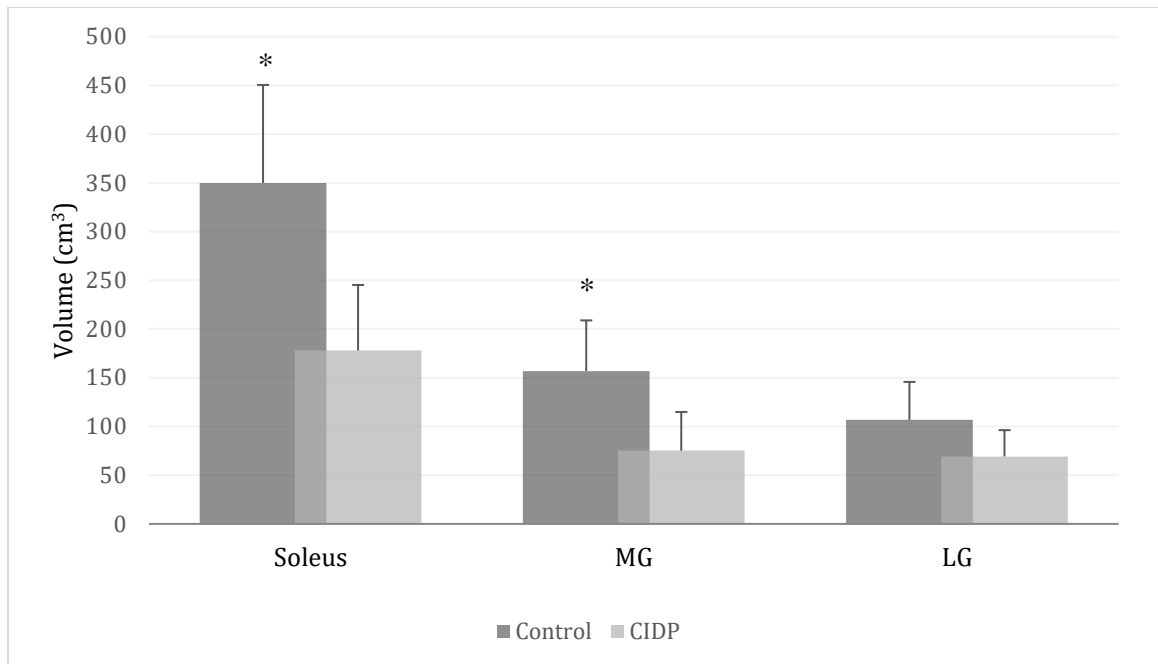


Figure 5.2 Total contractile volume triceps surae

Total triceps surae contractile volumes of the soleus, medial head of gastrocnemius (MG), and lateral head of gastrocnemius (LG). \* $P < 0.05$ , significantly different than controls. Values are expressed as means  $\pm$  standard deviations.



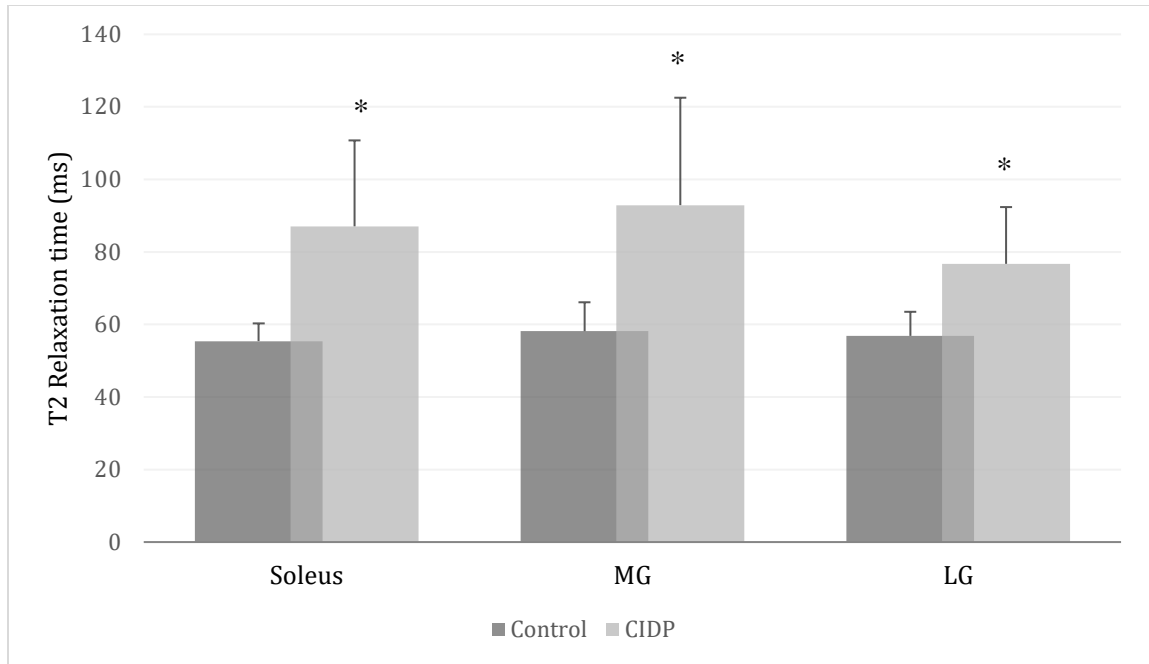


Figure 5.3 T2 relaxation times of triceps surae

T2 relaxation times of the soleus, medial head of gastrocnemius (MG), and lateral head of gastrocnemius (LG). \*P < 0.05, significantly longer than controls. Values are expressed as means  $\pm$  standard deviations.

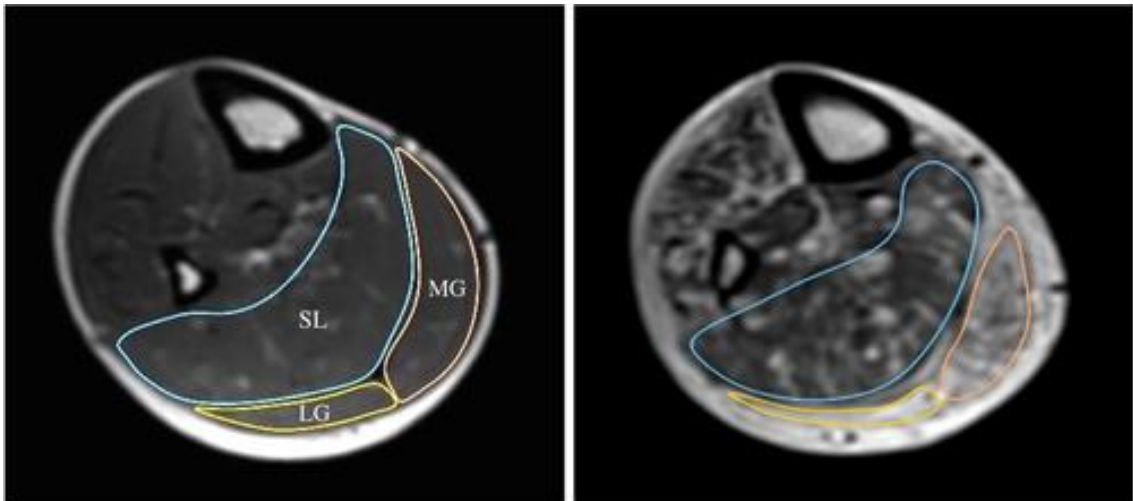


Figure 5.4 MRI T1 cross section of triceps surae

Cross-sectional T1-weighted MRI scan: comparing leg musculature of control (left) vs. CIDP (right). Soleus (SL), medial head of gastrocnemius (MG) and lateral head of gastrocnemius (LG) are outlined. Note the prominent marbled appearance of the leg muscles of the patient with CIDP due to extensive intramuscular fat infiltration.

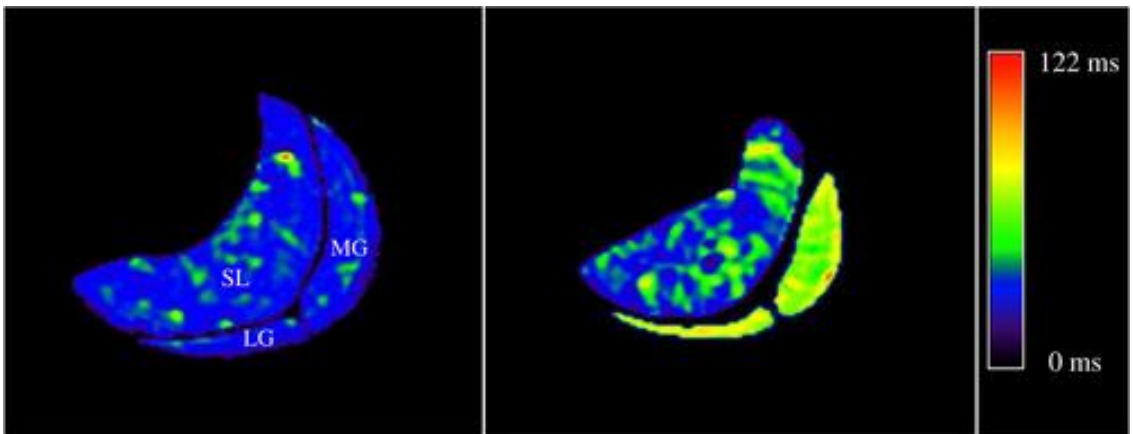


Figure 5.5 MRI T2 cross section of triceps surae

T2 maps (ms) of the soleus (SL), medial head of gastrocnemius (MG), and lateral head of gastrocnemius (LG) muscles: control (left panel) vs. CIDP (right panel). Muscle: purple, blue (30-70ms); fat green, yellow (>71 ms); connective tissue: black, purple (<30 ms). T2 ranges values from <sup>21</sup>. T2 maps displayed here are from the same participants shown in Figure 5.4.

## 5.4 Discussion

The present study aimed to establish the degree to which the posterior leg compartment, specifically the triceps surae is affected by the demyelinating nerve disease CIDP. Utilizing two MRI techniques, (T1 and T2-weighted scans), we discovered quantitative structural alterations in all portions of the triceps surae, demonstrating that patients with CIDP have significant atrophy and no contractile tissue infiltration that severely affect the contractile capacity of skeletal muscle tissue. Absolute plantar flexion strength of patients was roughly 28% less than the control subjects and when triceps surae muscle volume was expressed relative to strength (normalized strength), the difference between groups persisted with roughly 30% lower normalized strength for the CIDP group when compared to controls. The persistence of the strength difference is indicative of the lower muscle contractile quality in CIDP, which is further supported by the roughly 35% longer T2 relaxation times in all three muscles of CIDP individuals compared with controls. Thus, muscle weakness in patients with CIDP cannot be due to a loss of muscle tissue alone. Furthermore, disease duration was not related to the amount of skeletal muscle mass present in patients. Electrophysiological outcomes also indicated more prominent abnormalities that were suggestive of axonal dysfunction (e.g., CMAP amplitude) in the lower extremity. T2 relaxometry and water-fat separation techniques were not used in this study, thus we are not able to quantify total fat infiltration separated from water content or other non-contracting substances. The most important conclusions from this study are that patients with CIDP had significantly less total muscle volume indicated by T1 scans, as well lower total muscle protein quality as reflected by longer T2 relaxation times, and greater no contractile tissue infiltration found equally in the soleus, medial and

lateral heads of gastrocnemius and supported by longer T2 relaxation times when compared to control subjects. It is important to draw attention to the two possible contributing mechanisms at play in the patients. Not only are these patients disadvantaged by chronic nerve demyelination, but also the process of aging may compound these effects. Several studies using MRI techniques that have compared age-associated differences in muscle composition have shown that various muscles within the leg are affected to different degrees by aging. One study demonstrated that triceps surae muscle volume could be reliably calculated using maximal anatomical cross-sectional area values from MRI scans <sup>22</sup>. A subsequent study investigated changes in the architecture of the triceps surae muscle architecture in a group of young men ( $25.3 \pm 4.5$ ) and a group of old men ( $73.8 \pm 4.4$ ). Additionally, that study reported that the triceps surae in the old group was smaller in volume in all individuals compared with the young <sup>17</sup>. Our mean values for the control subjects fit closely with the volumes presented by this group. Furthermore, a study showed age-associated reductions in contractile tissue and subsequent increases in adipose and connective tissue composition using MRI in the triceps surae. These results further support our control group findings regarding force as well as muscle volume. In the older cohort, in addition to 39% lower isometric plantar flexion strength, total triceps surae volume was smaller by 17.5%, whereas the relative amounts of triceps surae intramuscular adipose tissue and gastrocnemii intramuscular connective tissue were larger by 55.1% and 48.9%, respectively <sup>23</sup>.

A study by Dalton et al (2009) supports that not all skeletal muscles are affected equally by the aging process and that the soleus in relation to both heads of the gastrocnemius may possess some type of neural protection as it was preserved to a greater degree in

aged individuals <sup>24</sup>. Indeed, it has been shown that sarcopenia is much more apparent in the LG and MG compared with soleus <sup>17</sup>. Heterogeneous increases of intramuscular adipose and non-contractile connective tissue may not only diminish total triceps surae muscle mass, but also could alter the usual fascicular fibre organization <sup>25</sup>. This may help explain the lower specific tension we found for this muscle group. Consequently, negative changes in skeletal muscle tissue amount and relative composition of contractile versus non contractile tissue lead to important structural modifications that contribute to plantar flexion muscle weakness in patients with CIDP. Thus, although disuse and age-related factors may play a role in the observed differences, it is likely that the primary cause is axonal dysfunction. In the past decade, numerous abnormal MRI findings in nerves of patients with CIDP have been reported.

Several studies have discovered abnormal hypertrophy of both ventral and dorsal spinal nerve roots in CIDP <sup>26,27,28,29,30,31</sup> which has also been demonstrated in Guillain–Barre syndrome <sup>32,33</sup>. Hypertrophy of spinal nerve roots has frequently been described in combination with abnormal nerve enhancement <sup>34,35,36</sup>. Increased signal intensity on T2-weighted images in the brachial plexus or nerve trunks has also been observed in some CIDP MRI studies <sup>37,38,39</sup>. Although nerve root enlargement is not specific for CIDP, several studies have demonstrated the frequencies of these abnormalities that are detected by MRI. For example, Midroni et al (1999) reported enhancement of the cauda equina in (69%) of patients with CIDP <sup>28</sup> and Duggins et al (1999) reported detection of cervical nerve root hypertrophy in (57%) of patients with CIDP <sup>27</sup>. Although these structural nerve abnormalities are apparent, few studies have explored the effect on skeletal muscles. In a few related studies, our findings are supported by one that found muscle disruptions in

Charcot–Marie-Tooth neuropathy <sup>40</sup> and some that have shown declines in skeletal muscle quantity and quality in patients with diabetic peripheral neuropathy <sup>17, 41</sup>. Thus, reductions in muscle quantity and quality are likely driven by CIDP-related neural factors, such as motor axon loss <sup>10</sup> and impaired neural signalling perhaps related to nerve lesions or segmental demyelination as reported in prior studies that presumably lead to accelerated muscle atrophy <sup>4</sup>.

Moreover, studies have shown proximal demyelination results in enlarged brachial and lumbar plexuses as well as enlargements in the cauda equina demonstrating segmental demyelination in nerves that have proximal roots. Findings from this study in combination with our previous results <sup>10</sup> indicate that both anterior and posterior leg compartments are affected to the same extent in CIDP. There does not seem to be any difference in muscle morphology specifically quantity and quality of skeletal muscle in the TA or within the constituent muscles of the triceps surae of patients with CIDP, and indeed muscles of the two major leg compartments seem to be equally affected. Thus, likely both the deep peroneal nerve as well as the tibial nerve has been affected to the same degree by the demyelinating process and subsequently the distal muscles have been compromised. This indicates that the insult to the nerve is more proximal possibly at its origin of the sciatic nerve and supports the finding of sacral plexus root enlargement reported previously <sup>35</sup>.

We were surprised by our initial findings in the TA muscle, which prompted us to explore whether another critical gait muscular group was affected by CIDP. In addition, the fiber type compositions of the main portions of the triceps surae are quite different and it was important to assess whether the soleus might be differently affected than the

gastrocnemii with support from studies on age-related changes as outlined above. Furthermore, a major concern for patients with CIDP is ambulation, and quantifying how several key leg muscles involved in gait are affected by a chronic nerve demyelination is very pertinent to the well being and quality of life of those with CIDP. Our results are further supported by Ohyama et al (2017) who, using computed tomography, showed significant atrophy to be more pronounced in the distal musculature compared to proximal muscles of patients with CIDP <sup>42</sup>. Thus, morphological alterations to distal skeletal muscle in patients seem to be uniform regardless of anatomical location or functional requirements. Furthermore, compositional changes within the muscle compartments, specifically infiltration by fat and connective tissue, may disrupt muscle architecture further diminishing effective functional capacity.

## 5.5 References

1. Bosboom WM, van den Berg LH, Franssen H, Giesbergen PC, Flach HZ, van Putten AM, Veldman H, Wokke HJ. Diagnostic value of sural nerve demyelination in chronic inflammatory demyelinating polyneuropathy. *Brain*. **124** 2427–2438 (2001).
2. Tsuchiya K, Honya K, Yoshida M, Nitatori T. Demonstration of spinal cord and nerve root abnormalities by diffusion neurography. *Journal of Computer Assisted Tomography*. **32** 2 286–290 (2008).
3. Renowden S. Imaging in multiple sclerosis and related disorders. *Practical Neurology*. **14** 5 e13-e13 (2014).
4. Pitarokoili K, Schlamann M, Kerasnoudis A, Gold R, Yoon M-S. Comparison of clinical, electrophysiological, sonographic and MRI features in CIDP. *Journal of Neurological Science*. **357** 1-2: 198–203 (2015).
5. Ishikawa T, Asakura K, Mizutani Y, Ueda A, Murate KI, Hikichi C, Shima S, Kizawa M, Komori M, Murayama K, Toyama H, Ito S, Mutoh T. MR neurography for the evaluation of CIDP. *Muscle and Nerve*. **55** 4 483–489 (2017).
6. Grimm A, Schubert V, Axer H, Ziemann U. Giant nerves in chronic inflammatory polyradiculoneuropathy. *Muscle and Nerve*. **55** 285-289 (2016).
7. Lozeron P, Lacour M-C, Vandendries C, Théaudin M, Cauquil C, Denier C, Lacroix C, Adms D. Contribution of plexus MRI in the diagnosis of atypical chronic inflammatory demyelinating polyneuropathies. *Journal of Neurological Science*. **360** 170-175 (2016).
8. Dixon WT, Engels H, Castillo M, Sardashti M. Incidental magnetization transfer contrast in standard multislice imaging. *Magnetic Resonance Imaging*. **8** 4 417-422



- (1990).
9. Kakuda T, Fukuda H, Tanitame K, Takasu M, Date S, Ochi K, Oshhita T, Kohriyama T, Ito K, Matsumoto M, Awai K. Diffusion tensor imaging of peripheral nerve in patients with chronic inflammatory demyelinating polyradiculoneuropathy: a feasibility study. *Neuroradiology*. **53** 12 955-960 (2011).
  10. Gilmore KJ, Allen MD, Doherty TJ, Kimpinski K, Rice CL. Electrophysiological and neuromuscular stability of persons with chronic inflammatory demyelinating polyneuropathy. *Muscle and Nerve*. **56** 3 413-420 (2017).
  11. Bergh FPYK Van Den, Hadden RDM, Bouche P. European Federation of Neurological Societies / Peripheral Nerve Society Guideline on management of chronic inflammatory demyelinating polyradiculoneuropathy: Report of a joint task force of the European Federation of Neurological Societies and the Peripheral Nerve Society — First Revision 356–363 (2010).
  12. Tracy BL, Ivey FM, Hurlbut D, Martel GF, Lemmer JT, Siegel EL, Metter EJ, Fozard JL, Fleg JL, Hurley BF. Muscle quality. II. Effects of strength training in 65- to 75-yr-old men and women. *Journal of Applied Physiology*. **86** 1 195–201 (1999).
  13. McNeil CJ, Doherty TJ, Stashuk DW, Rice CL. Motor unit number estimates in the tibialis anterior muscle of young, old, and very old men. *Muscle and Nerve*. **31** 4 461-467 (2005).
  14. Kent-Braun JA, Callahan DM, Fay JL, Foulis SA, Buonaccorsi JP. Muscle weakness, fatigue, and torque variability: Effects of age and mobility status. *Muscle and Nerve*. **49** 2 209-217 (2014).

15. Monster AW, Chan H, O'Connor D. Activity patterns of human skeletal muscles: relation to muscle fiber type composition. *Science*. **200** 314–317 (1978).
16. Dalton BH, Harwood B, Davidson AW, Rice CL. Triceps surae contractile properties and firing rates in the soleus of young and old men. *Journal of Applied Physiology*. **107** 6 1781-1788 (2009).
17. Morse CI, Thom JM, Reeves ND, Birch KM, Narici MV. In vivo physiological cross-sectional area and specific force are reduced in the gastrocnemius of elderly men. *Journal of Applied Physiology*. **99** 3 1050–1055 (2005).
18. Marsh E, Sale D, McComas AJ, Quinlan J. Influence of joint position on ankle dorsiflexion in humans. *Journal of Applied Physiology*. **51** 1 160–167 (1981).
19. Allen MD, Kimpinski K, Doherty TJ, Rice CL. Length dependent loss of motor axons and altered motor unit properties in human diabetic polyneuropathy. *Clinical Neurophysiology*. **125** 4 836-843 (2014).
20. Moore CW, Allen MD, Kimpinski K, Doherty TJ, Rice CL. Reduced skeletal muscle quantity and quality in patients with diabetic polyneuropathy assessed by magnetic resonance imaging. *Muscle and Nerve*. **53** 5 726–732 (2016).
21. Bus SA, Yang QX, Wang JH, Smith MB, Wunderlich R, Cavanagh PR. Intrinsic muscle atrophy and toe deformity in the diabetic neuropathic foot: a magnetic resonance imaging study. *Diabetes Care*. **25** 8 1444–1450 (2002).
22. Albracht K, Arampatzis A, Baltzopoulos V. Assessment of muscle volume and physiological cross-sectional area of the human triceps surae muscle in vivo. *Journal of Biomechanics*. **41** 10 2211–2218 (2008).
23. Csapo R, Malis V, Sinha U, Du J, Sinha S. Age-associated differences in triceps surae

- muscle composition and strength – an MRI-based cross-sectional comparison of contractile, adipose and connective tissue. *BMC Musculoskeletal Disorders*. **15** 209 (2014).
24. Dalton BH, McNeil CJ, Doherty TJ, Rice CL. Age-related reductions in the estimated numbers of motor units are minimal in the human soleus. *Muscle and Nerve*. **38** 3 1108–1115 (2008).
25. Hilton TN, Tuttle LJ, Bohnert KL, Mueller MJ, Sinacore DR. Excessive adipose tissue infiltration in skeletal muscle in individuals with obesity, diabetes mellitus, and peripheral neuropathy: association with performance and function. *Physical Therapy*. **88** 11 1336–1344 (2008).
26. Schady W, Goulding PJ, Lecky BR, King RH, Smith CM. 1996. Massive nerve root enlargement in chronic inflammatory demyelinating polyneuropathy. *Journal Neurology, Neurosurgery and Psychiatry*. **61** 6 636-640 (1996).
27. Duggins AJ, McLeod JG, Pollard JD, Davies L, Yang F, Thompson EO, Soper JR. Spinal root and plexus hypertrophy in chronic inflammatory demyelinating polyneuropathy. *Brain*. **122** 7 1383-1390 (1999).
28. Midroni G, de Tilly L.N, Gray B, Vajsar J. MRI of the cauda equina in CIDP: clinical correlations. *Journal of Neurological Science*. **170** 1 36-44 (1999).
29. Adachi Y, Sato N, Okamoto T, Sasaki M, Komaki H, Yamashita F, Kida J, Takahashi T, Matsuda H. Brachial and lumbar plexuses in chronic inflammatory demyelinating polyradiculoneuropathy: MRI assessment including apparent diffusion coefficient. *Neuroradiology*. **53** 1 3-11 (2011).
30. Matsuoka N, Kohriyama T, Ochi K, Nishitani M, Sueda Y, Mimori Y, Nakamura S,

- Matsumoto M. Detection of cervical nerve root hypertrophy by ultrasonography in chronic inflammatory demyelinating polyradiculoneuropathy. *Journal of Neurological Science*. **219** 1-2 15-21 (2004).
31. Tazawa K.I, Matsuda M, Yoshida T, Shimojima Y, Gono T, Morita H, Kaneko T, Ueda H, Ikeda S. Spinal nerve root hypertrophy on MRI: clinical significance in the diagnosis of chronic inflammatory demyelinating polyradiculoneuropathy. *Internal Medicine*. **47** 23 2019-2024 (2008).
32. Morgan GW, Barohn RJ, Bazan III C, King RB, Klucznik RP. Nerve root enhancement with MRI in inflammatory demyelinating polyradiculoneuropathy. *Neurology*. **43** 3 618-620 (1993).
33. Gorson KC, Ropper AH, Muriello MA, Blair R. Prospective evaluation of MRI lumbosacral nerve root enhancement in acute Guillain–Barré syndrome. *Neurology*. **47** 3 813-817 (1996).
34. De Silva RN, Willison HJ, Doyle D, Weir AI, Hadley DM, Thomas AM. Nerve root hypertrophy in chronic inflammatory demyelinating polyneuropathy. *Muscle and Nerve*. **17** 2 168-170 (1994).
34. Ginsberg L, Platts AD, Thomas PK. Chronic inflammatory demyelinating polyneuropathy mimicking a lumbar spinal stenosis syndrome. *Journal of Neurology Neurosurgery Psychiatry*. **59** 2 189-191 (1995).
35. Kitakule MM, McNeal A. Massive nerve root hypertrophy in chronic inflammatory demyelinating polyradiculoneuropathy. *Journal of the Association for Academic Minority Physicians*. **8** 3 55-57 (1997).
36. Crino PB, Grossman RI, Rostami A. Magnetic resonance imaging of the cauda equina

- in chronic inflammatory demyelinating polyneuropathy. *Annals of Neurology*. **33** 311-313 (1993).
37. Duarte J, Martinez AC, Rodriguez F, Mendoza A, Sempere AP, Claveria LE. Hypertrophy of multiple cranial nerves and spinal roots in chronic inflammatory demyelinating neuropathy. *Journal of Neurology Neurosurgery Psychiatry*. **67** 5 685-687 (1999).
38. Eurelings M, Notermans NC, Franssen H, Van Es HW, Ramos LM, Wokke JH, van den Berg LH. MRI of the brachial plexus in polyneuropathy associated with monoclonal gammopathy. *Muscle and Nerve*. **24** 10 1312-1318 (2001).
39. Pareyson D, Saveri P, Pisciotta C. New developments in Charcot-Marie-Tooth neuropathy and related diseases. *Current Opinion in Neurology*. **30** 5 471-480 (2017).
40. Parasoglou P, Rao S, Slade JM. Declining skeletal muscle function in diabetic peripheral neuropathy. *Clinical Therapy*. **39** 6 1085–1103 (2017).
41. Ohyama K, Koike H, Katsuno M, Takahashi M, Hashimoto R, Kawagashira Y, Iijima M, Adachi H, Watanabe H, Sobue G. Muscle atrophy in chronic inflammatory demyelinating polyneuropathy: a computed tomography assessment. *European Journal of Neurology*. **21** 7 1002–1010 (2017).

## Chapter 6

### 6 General Discussion and Summary

#### 6.1 General Discussion

This thesis provides considerable unique experimental evidence concerning the consequences of chronic inflammatory demyelinating polyneuropathy (CIDP) on the human neuromuscular system. The first half of this thesis concentrated on the motor axon changes that accompany CIDP. The results in this body of work indicate that patients with CIDP have a loss of motor units, neuromuscular transmission instability, abnormal firing rates of individual motor units and neuromuscular conduction block (Chapters 2, 3). The second half of this thesis focused on how these alterations to the motor axon and abnormal neuromuscular transmission behavior affect skeletal muscle mass and composition. The findings of the later chapters indicate that CIDP related motor unit loss, block and instability is associated with skeletal muscle atrophy as well as increased non-contractile intramuscular tissue infiltration (Chapter 4). Furthermore Chapter 4 elucidates an important finding that patients with CIDP are weaker when normalized to fat-corrected muscle volumes in the TA muscle of the anterior compartment that can be related to findings from the first two studies. This indicates there are intrinsic structural abnormalities within the contractile protein apparatus of the muscle fibers. The final Chapter (5) of this thesis investigates whether these distal symmetrical axonal losses and instability have homogeneous effects on the muscle tissue innervated. This was accomplished by using MRI to explore the portions of the triceps surae muscle group of the posterior compartment of the leg in patients with CIDP. Results show that regardless

of distal nerve loss and dysfunction, associated muscle undergoes uniform changes of atrophy and non-contractile tissue infiltration in all muscles regardless of functional differences or anatomical location. Combined, these findings provide a more comprehensive understanding of the current understanding of how CIDP affects the neuromuscular system as well mechanisms behind the functional limitations seen in patients with CIDP.

Although not well understood, there is a consensus that CIDP related demyelination causes neuromuscular dysfunction, and it has been presumed that part of this dysfunction is due to neuromuscular conduction block and the loss of motor axons<sup>1,2,3</sup>. However, studies to date have not quantified the losses of motor units or stability parameters associated with demyelinated motor axons in patients with CIDP. In this thesis, the results in Chapter 2 confirmed the suspected concept of motor unit loss by exhibiting reduced MUNE in the tibialis anterior (TA) of patients with CIDP versus healthy control subjects. This finding is important as it confirms that chronic motor axon demyelination to proximal nerve roots and plexuses can impact motor unit number and function in a distal muscle<sup>4</sup>. Chapter 2 also builds on this characterization by demonstrating increased neuromuscular jitter and jiggle in patients relative to controls, which reflects pathological alterations in neuromuscular action potential propagation or neuromuscular junction transmission instability. Importantly this Chapter demonstrates the utility of concentric needle derived DQEMG for the detection of motor unit loss and differences in neuromuscular transmission fidelity when comparing patients with CIDP to healthy controls. Furthermore, this Chapter highlights the significance of DQEMG as a valuable methodology that is sensitive to changes not currently detectable in standard clinical

nerve conduction studies. Finally, the neuromuscular stability outcomes of Chapter 2 indicate that jitter and jiggle are valuable indices for classifying axonal alterations in the early stages of disease, preceding the loss of motor units or the onset of muscle atrophy.

Chapter 3 of this thesis builds upon previous findings of axonal transmission failure via single fiber motor unit experimentation <sup>2</sup>. Numerous animal model studies using experimental autoimmune neuritis (CIDP equivalent in rodents) have demonstrated transmission disturbances in motor axons, neuromuscular junctions, and single muscle fibers, all of which culminate into failed action potential propagation in motor nerves or skeletal muscle fibers <sup>5</sup>. Surprisingly, patients with CIDP demonstrated abnormally high firing rates of early recruited low-threshold motor units at low volitional contraction intensities. These high firing rates observed in small, early recruited motor units may reflect a compensatory strategy to mitigate the overall motor unit loss. Findings from Chapter 3 also indicate that CIDP related demyelination, blockage and axon loss might be more prominent in larger, later recruited motor units. The surviving smaller type I motor units must discharge at faster rates to produce the necessary force in the absence or blockage of faster later recruited type II motor units. The finding of conduction failure (in the form of diminished motor unit firing rates or complete block) supports the concept that transmission failure occurs in human patients with CIDP. Moreover, this susceptibility of motor units to demonstrate transmission failure and abnormal firing rates could have functional implications, specifically regarding quantity and quality of the muscle tissue innervated by unhealthy nerves.

Indeed, MR imaging in the lumbar nerve roots and tibial nerve has shown nerve lesions in patients with CIDP <sup>6,7</sup>. The loss of strength in muscles of those with CIDP is most



severe distally, can be profound and likely has a direct significance on functional impairments. However, very little data exist regarding the morphological characteristics of the limb musculature in patients with CIDP, specifically muscle quantity and quality. In Chapters 4 and 5 of this thesis, two MRI based techniques (T1 and T2 weighted scans) are utilized to reveal CIDP related quantitative and qualitative changes in skeletal musculature. Results of Chapter 4 indicated that compared to control subjects those with CIDP have structural alterations that ultimately affect the contractile capacity of muscle tissue. The most important findings from Chapter 4 are that patients with CIDP have lower total muscle protein quality and more non-contractile tissue infiltration in the TA, as indicated both by a greater amount of non-contractile tissue and elongated T2 relaxation times, compared to healthy controls. This Chapter also demonstrates an interesting finding that patients with CIDP are weaker relative to volume of muscle even when compared using fat corrected muscle volumes normalized to force. This is significant because it indicates that patients with CIDP have disruptions to the intrinsic structural integrity at the molecular level of muscle proteins, supporting the concept that disruptions in neural innervation and function affect muscle protein quality. Consequently, these unfavorable changes to muscle tissue composition are likely key structural alterations that contribute to functional weakness in patients with CIDP. Chapter 5 investigates the homogeneity of the effects of chronic demyelination in a separate leg compartment. Findings from Chapter 5 in combination with results from Chapter 4 indicate that both anterior and posterior leg compartments are affected to the same extent in CIDP. There does not appear to be any difference in muscle morphology specifically quantity and quality of muscle tissue in the TA or within the constituent

muscles of the triceps surae in patients with CIDP. Findings from these two Chapters indicate that muscles of the two major leg compartments seem to be equally affected by the disease process. Thus, likely both the deep peroneal nerve as well the tibial nerve have been affected to the same gradation by the demyelinating process and subsequently the distal muscles have been compromised. This indicates that the focal insult to peripheral nerves is more proximal possibly at their origin of the sciatic nerve and supports the findings of sacral plexus root enlargement that has been previously reported<sup>6,7</sup>. In summary, the studies presented have elucidated many neuromuscular deficits in patients with CIDP and this information may be essential in disease management as well in directing and assessing treatment modalities.

## 6.2 Limitations

The first half of this dissertation uses EMG techniques that are not without limitations. The characteristics of an EMG signal are largely affected by the level of voluntary contraction, the anatomical and physiological properties of the muscle, the physical characteristics of the electrode used to detect the signal as well as the position of this electrode relative to the active muscle fibres. A specific limitation related to MUNE consists of the challenge in maintaining concentric needle electrode positioning during intramuscular recordings. Although the DQEMG software provides visual feedback and cueing, inconsistent needle electrode positioning may affect the sizes of detected action potentials recorded from active motor units. Intramuscular concentric needle depth has also been shown to have a significant effect on MUNE calculation<sup>8</sup>. Potential bias regarding depth and location of needle electrode intramuscular insertion was taken into account through careful needle manipulation or different insertion sites so that the

detection of motor units was representative of the population of motor units within the muscle.

There is clear evidence suggesting that that the level of force can have a significant impact on the sizes of both needle and surface detected motor unit action potentials sampled using DQEMG. The amplitude of the needle and surface detected motor unit action potentials increase as the level of force increases. Coupled with this change in action potential size is an increase in motor unit firing rate as well as a decrease in the magnitude of the MUNE values at higher force levels<sup>9</sup>. In order for DQEMG to maintain its accuracy and usefulness, methods of controlling for the level of force must be efficient and applicable to the study design. In order to reduce force variability the studies in this body of work used a consistent measure of torque and root-mean square EMG during signal acquisition to provide an indication of the absolute or relative level of force or muscle activation.

Motor unit number estimations and stability measures were conducted in the right leg (Chapters 2 and 3) and in the study calculating muscle quality and quantity the left leg (Chapter 4) was analyzed. This was done knowing that motor unit pathology is symmetrical in patients with CIDP<sup>4</sup>. This means that motor unit losses measured and detected in one side of the body should reflect losses in the opposite side to a similar degree. The left side was the non-dominant limb in 95% of all patients and controls tested and although not significant both plantar flexion and dorsiflexion strengths were slightly weaker in the non-dominant limbs of patients with CIDP. Additionally, the patient group studied throughout this thesis featured a more severe neuropathy, with a more extreme motor involvement than what would be expected in patients in the early stages of the

disease<sup>10,11,12</sup> .

Loss of cells from the motor system occurs during the normal aging process, leading to reduction in the complement of motor neurons and muscle fibers. This latter age-related decrease in muscle mass is termed sarcopenia and is often exacerbated with the detrimental effects of a sedentary lifestyle in older adults, leading to a significant reduction in the overall reserve capacity of the neuromuscular system<sup>13, 14, 15 16</sup>. The cellular processes that lead to age-related loss of spinal motor neurons in healthy adults are not well understood but it is widely agreed that nerve cell death is the precursor for the numerous neuromuscular adaptations seen with normal adult aging. These detrimental effects to the neuromuscular system manifest and are detectable by the six or seventh decade of life<sup>17</sup>. The mean ages of the patients and control subjects in this thesis were approximately 60 years old. Therefore it is reasonable to expect that the majority of patients with CIDP would not only be expressing CIDP related neuronal changes but also age-related changes to neurons. Thus, it was important to have age-matched controls. This may affect the generalizability of the results found in this thesis. Patients with CIDP may be differentially affected as they age, compared to how CIDP may influence a group of disease free younger adults.

Lastly, the patient and control experimental groups included a comparable number of males and females. The two groups were sex matched, however due to the rarity of the disease a sample size of 10-12 subjects was studied which did not provide enough statistical power to formally compare sex-based differences in CIDP.

### 6.3 Future Directions

The studies contained within this thesis provide a foundation from which further investigation can build upon. To further elucidate, quantify and expand the findings of Chapter 2, with a study investigating the loss of motor units in a more proximal muscle would be of value. CIDP has demonstrated detrimental affects to distal human musculature, however it is not known whether similar demyelinating effects are expected in proximal muscles of the body. Due to the length dependent nature of the disease it would be interesting to know if proximal muscles are preserved to a greater or lesser degree than distal muscles.

Quantification of isotonic muscle power generation, force-velocity relationship and maximal contractile velocity might considerably complement the understanding of Chapters 3, 4 and 5 regarding how CIDP impacts muscle function. Indeed, there is good evidence that voluntary isotonic (concentric and eccentric) contractions have different motor unit firing rates than voluntary isometric contractions <sup>18,19</sup>. Therefore, intramuscular fine wire recordings could be collected during dynamic contractions in a distal muscle to assess the firing characteristics of individual motor units during a dynamic task. To complement Chapter 3 repetitive nerve stimulation at different frequencies could also be used to test for neuromuscular transmission failure in order to quantify whether and at what frequency demyelinated motor neurons fail to propagate action potentials. Knowing that patients with CIDP have abnormal motor unit firing rates and overall neuromuscular block it would be important to know at what specific frequency peripheral axons demonstrate this failure to provide verification for the blockage in larger later recruited type II motor units.

Furthermore, certain inferences made in Chapters 4 and 5 could have been further supported or enhanced with the inclusion of skeletal muscle biopsies. The incorporation of muscle biopsies could have supported the ideas in Chapter 3 of neuromuscular remodeling (fiber type grouping) in patients with CIDP. Muscle biopsies could also give a superior molecular understanding of muscle quality by evaluating single myofibril morphology <sup>20</sup>. Nevertheless, the inclusion of muscle biopsies was not reasonable for these experiments as the majority of studies contained within this thesis concentrated on the dorsiflexor muscle groups, which are not considered suitable muscles to biopsy in comparison to muscles of the thigh for example. Obtaining and analyzing biopsies located in the quadriceps would provide insight for comparison with the TA, given the length-dependent nature of CIDP and the different fiber type proportions of these dissimilar muscle groups <sup>21</sup>. In combination with the procedures mentioned above, it would be advantageous to include standard clinical measures of mobility or functional capacity, such as balance and coordination tests. Moreover, subjective questionnaires that assess physical activity could offer evidence regarding the physical status of the subjects studied. The inclusion of these subjective measures may help delineate consequences of CIDP on the neuromuscular system.

Finally, a longitudinal study of patients with CIDP, as well a more detailed outline of patient's treatment regime could provide greater insight into the progression of CIDP related neuromuscular dysfunctions <sup>20</sup>. Concurrent assessments of the motor system and the changes reflected by the different treatments (IVIg, PE and prednisone) offered to patients with CIDP would be helpful in determining how this autoimmune neuropathy is affected by differing treatment modalities or the protective effects treatments have on

neuromuscular properties of patients with CIDP <sup>22,23,24,25</sup>. Conceivably, a longitudinal study would also provide an opportunity to assess the effects of aging on CIDP.

## 6.4 Summary and Significance

Chronic Inflammatory Demyelinating Polyneuropathy causes numerous detrimental physiological and functional alterations to the human neuromuscular system. This dissertation comprises an amalgamated collection of novel and foundational experiments in patients with CIDP. Firstly, it provides concrete evidence for the chronic loss of demyelinated motor units that underlie muscle atrophy and weakness in patients with CIDP (Chapter 2). Secondly, this body of work demonstrates that in addition to the loss of motor units, patients with CIDP display severe instability in remaining motor units (Chapter 2). Furthermore, for the first time experimentally, I illustrate that patients with CIDP have abnormal motor unit firing rates across a broad range of contraction intensities. Indeed, shown in this thesis the chronic loss of motor units, the detectable instability and conduction block of action potentials seem to be associated with skeletal muscle atrophy as well the intramuscular infiltration of non-contractile tissue (Chapters 4 and 5). Combined, the investigations contained within thesis provide a basis that will direct future experiments to further elucidate mechanisms that aid in the understanding of how CIDP influences the neuromuscular system.

## 6.5 References

1. Barohn RJ, Kissel JT, Warmolts JR, Mendell JR. Chronic inflammatory demyelinating polyradiculoneuropathy. Clinical characteristics, course, and recommendations for diagnostic criteria. *Archives of Neurology*. **46** 8 878–884 (1989).
2. Oh SJ. The single-fiber EMG in chronic demyelinating neuropathy. *Muscle and Nerve*. **12** 5 371–377 (1989).
3. Gantayat M, Swash M, Schwartz MS. Fiber density in acute and chronic inflammatory demyelinating polyneuropathy. *Muscle and Nerve*. **15** 2 168–171 (1992).
4. Bergh FPYK Van Den, Hadden RDM, Bouche P. European Federation of Neurological Societies / Peripheral Nerve Society Guideline on management of chronic inflammatory demyelinating polyradiculoneuropathy: Report of a joint task force of the European Federation of Neurological Societies and the Peripheral Nerve Society — First Revision. 356–363 (2010).
5. Linington C, Lassmann H, Ozawa K, Kosin S, Mongan L. Cell adhesion molecules of the immunoglobulin supergene family as tissue-specific autoantigens: induction of experimental allergic neuritis (EAN) by P0 protein-specific T cell lines. *European Journal of Immunology*. **22** 7 1813–1817 (1992).
6. Tazawa KI, Matsuda M, Yoshida T, Shimojima Y, Gono T, Morita H, Kaneko T, Ueda H, Ikeda S. Spinal nerve root hypertrophy on MRI: clinical significance in the diagnosis of chronic inflammatory demyelinating polyradiculoneuropathy. *Internal Medicine*. **47** 23 2019–2024 (2008).



7. Morgan GW, Barohn RJ, Bazan III C, King RB, Klucznik RP. Nerve root enhancement with MRI in inflammatory demyelinating polyradiculoneuropathy. *Neurology*. **43** 3 618-620 (1993).
8. Ives C, and Doherty TJ Influence of needle depth on DE-STA motor unit number estimation. *Muscle and Nerve*. **50** 4 587-592.
9. McNeil CJ, Doherty TJ, Stashuk DW, Rice CL. Motor unit number estimates in the tibialis anterior muscle of young, old, and very old men. *Muscle and Nerve*. **31** 4 461-467 (2005).
10. McCombe PA, Pollard JD, McLeod JG. Chronic inflammatory demyelinating polyradiculoneuropathy. A clinical and electrophysiological study of 92 cases. *Journal of Neurology* (Pt 6). **110** 6 1617–1630 (1987).
11. Draak THP, Gorson KC, Vanhoutte EK, van Nes SI, van Doorn PA, Cornblath DR, van den Berg LH, Faber CG, Merkies IS, PeriNomS Study Group. Correlation of the patient's reported outcome Inflammatory-RODS with an objective metric in immune-mediated neuropathies. *European Journal of Neurology*. **23** 7 1248–1253 (2016).
12. Vanhoutte EK, Faber CG, Merkies IS, PeriNomS study group. 196th ENMC international workshop: Outcome measures in inflammatory peripheral neuropathies. *Neuromuscular Disorders*. **23** 11 924–933 (2013).
13. Panaite P-A, Renaud S, Kraftsik R, Steck AJ, Kuntzer T. Impairment and disability in 20 CIDP patients according to disease activity status. *Journal of the Peripheral Nervous System*. **18** 3 241–246 (2013).
14. Salmons S & Vrbova G. The influence of activity on some contractile characteristics of mammalian fast and slow muscles. *Journal of Physiology*. **201** 3

535–549 (1969). [1]  
[SEP]

15. Allen MD, Stashuk DW, Kimpinski K, Doherty TJ, Hourigan ML, Rice CL. Increased neuromuscular transmission instability and motor unit remodelling with diabetic neuropathy as assessed using novel near fiber motor unit potential parameters. *Clinical Neurophysiology*. **126** 4 794–802 (2015).
16. Power GA, Allen MD, Gilmore KJ, Stashuk DW, Doherty TJ, Hepple RT, Taivassalo T, Rice CL. Motor unit number and transmission stability in octogenarian world class athletes: Can age-related deficits be outrun? *Journal of Applied Physiology*. **121** 4 1013-1020 (2016).
17. McNeil CJ, Doherty TJ, Stashuk DW, Rice CL. Motor unit number estimates in the tibialis anterior muscle of young, old, and very old men. *Muscle and Nerve*. **31** 4 461-467 (2005).
18. Vandervoort, AA. Aging of the human neuromuscular system. *Muscle and Nerve*. **25** 117– 25 (2002).
19. Harwood B, Davidson AW, Rice CL. Motor unit discharge rates of the anconeus muscle during high-velocity elbow extensions. *Experimental Brain Research*. **208** 1 103–13 (2011).
20. Harwood B, Choi IH, Rice C L. Reduced motor unit discharge rates of maximal velocity dynamic contractions in response to a submaximal dynamic fatigue protocol. *Journal of Applied Physiology*. **113** 12 1821–1830 (2012).
21. Rafuse VF and Gordon T. Self-reinnervated cat medial gastrocnemius muscles. II. analysis of the mechanisms and significance of fiber type grouping in reinnervated

- muscles. *Journal of Neurophysiology*. **75** 1 282–297 (1996). [L]  
[SEP]
22. Nobile-Orazio E, Gallia F, Terenghi F, Bianco M. Comparing treatment options for chronic inflammatory neuropathies and choosing the right treatment plan. *Expert Review of Neurotherapeutics*. **17** 8 755–765 (2017).
23. Hughes RAC, Donofrio P, Bril V, Dalakas MC, Deng C, Hanna K, Hartung HP, Latou N, Merkies IS, van Doorn PA, ICE Study Group. Intravenous immune globulin (10% caprylate-chromatography purified) for the treatment of chronic inflammatory demyelinating polyradiculoneuropathy (ICE study): a randomised placebo-controlled trial. *The Lancet Neurology*. **7** 2 136–144 (2008).
24. Kuwabara S, Mori M, Misawa S, Suzuki M, Nishiyama K, Mutoh T, Doi S, Kokubun N, Kamijo M, Yoshikawa H, Abe K, Nishida Y, Okada K, Sekiguchi K, Sakamoto K, Kusunoki S, Sobue G, Kaji R, Glovenin–I CIDP Study Group. Intravenous immunoglobulin for maintenance treatment of chronic inflammatory demyelinating polyneuropathy: a multicentre, open-label, 52-week phase III trial. *Journal of Neurology, Neurosurgery and Psychiatry*. **88** 10 832–838 (2017).
25. Harbo T, Andersen H, Overgaard K, Jakobsen J. Muscle performance relates to physical function and quality of life in long-term chronic inflammatory demyelinating polyradiculoneuropathy. *Journal of the Peripheral Nervous System*. **13** 3 208–217 (2008).



# Appendices

## Appendix A: CIDP Ethics approval



**Date:** 12 November 2019

**To:** Dr. Tim Doherty

**Project ID:** 105105

**Study Title:** Impacts of chronic inflammatory demyelinating polyneuropathy (CIDP) on the motor and sensory nervous systems

**Application Type:** Continuing Ethics Review (CER) Form

**Review Type:** Delegated

**REB Meeting Date:** 19/Nov/2019

**Date Approval Issued:** 12/Nov/2019

**REB Approval Expiry Date:** 04/Dec/2020

---

Dear Dr. Tim Doherty,

The Western University Research Ethics Board has reviewed the application. This study, including all currently approved documents, has been re-approved until the expiry date noted above.

REB members involved in the research project do not participate in the review, discussion or decision.

Western University REB operates in compliance with, and is constituted in accordance with, the requirements of the TriCouncil Policy Statement: Ethical Conduct for Research Involving Humans (TCPS 2); the International Conference on Harmonisation Good Clinical Practice Consolidated Guideline (ICH GCP); Part C, Division 5 of the Food and Drug Regulations; Part 4 of the Natural Health Products Regulations; Part 3 of the Medical Devices Regulations and the provisions of the Ontario Personal Health Information Protection Act (PHIPA 2004) and its applicable regulations. The REB is registered with the U.S. Department of Health & Human Services under the IRB registration number IRB 00000940.

Please do not hesitate to contact us if you have any questions.

Sincerely,

Daniel Wyzynski, Research Ethics Coordinator, on behalf of Dr. Joseph Gilbert, HSREB Chair

*Note: This correspondence includes an electronic signature (validation and approval via an online system that is compliant with all regulations).*

# Appendix B: License terms and conditions

## 1.1 Appendix B

### JOHN WILEY AND SONS LICENSE TERMS AND CONDITIONS

Dec 19, 2019

---

---

This Agreement between Kevin Gilmore ("You") and John Wiley and Sons ("John Wiley and Sons") consists of your license details and the terms and conditions provided by John Wiley and Sons and Copyright Clearance Center.

<b>License Number</b>	4732620154275
<b>License date</b>	Dec 19, 2019
<b>Licensed Content Publisher</b>	John Wiley and Sons
<b>Licensed Content Publication</b>	Muscle and Nerve
<b>Licensed Content Title</b>	Electrophysiological and neuromuscular stability of persons with chronic inflammatory demyelinating polyneuropathy
<b>Licensed Content Author</b>	Kevin Gilmore, Charles L. Rice, Kurt Kimpinski, Timothy J. Doherty
<b>Licensed Content Date</b>	Mar 23, 2017
<b>Licensed Content Volume</b>	56
<b>Licensed Content Issue</b>	3
<b>Licensed Content Pages</b>	8
<b>Type of use</b>	Dissertation/Thesis
<b>Requestor type</b>	Author of this Wiley article
<b>Format</b>	Print and electronic
<b>Portion</b>	Full article
<b>Will you be translating?</b>	No
<b>Title of your thesis / dissertation</b>	The effects of Chronic Inflammatory Demyelinating Polyneuropathy on the Neuromuscular System in Humans.
<b>Expected completion date</b>	Jan 2020
<b>Expected size (number of pages)</b>	180
<b>Publisher Tax ID</b>	EU826007151
<b>Total</b>	0.00 CAD

**JOHN WILEY AND SONS LICENSE  
TERMS AND CONDITIONS**

Dec 19, 2019

---

---

This Agreement between Kevin Gilmore ("You") and John Wiley and Sons ("John Wiley and Sons") consists of your license details and the terms and conditions provided by John Wiley and Sons and Copyright Clearance Center.

<b>License Number</b>	4732620485773
<b>License date</b>	Dec 19, 2019
<b>Licensed Content Publisher</b>	John Wiley and Sons
<b>Licensed Content Publication</b>	Muscle and Nerve
<b>Licensed Content Title</b>	Reductions in muscle quality and quantity in chronic inflammatory demyelinating polyneuropathy patients assessed by magnetic resonance imaging
<b>Licensed Content Author</b>	Kevin Gilmore, Charles L. Rice, Kurt Kimpinski, Timothy J. Doherty
<b>Licensed Content Date</b>	Sep 10, 2018
<b>Licensed Content Volume</b>	58
<b>Licensed Content Issue</b>	3
<b>Licensed Content Pages</b>	6
<b>Type of use</b>	Dissertation/Thesis
<b>Requestor type</b>	Author of this Wiley article
<b>Format</b>	Print and electronic
<b>Portion</b>	Full article
<b>Will you be translating?</b>	No
<b>Title of your thesis / dissertation</b>	The effects of Chronic Inflammatory Demyelinating Polyneuropathy on the Neuromuscular System in Humans.
<b>Expected completion date</b>	Jan 2020
<b>Expected size (number of pages)</b>	180
<b>Publisher Tax ID</b>	EU826007151
<b>Total</b>	0.00 CAD

**JOHN WILEY AND SONS LICENSE  
TERMS AND CONDITIONS**

Dec 19, 2019

---

This Agreement between Kevin Gilmore ("You") and John Wiley and Sons ("John Wiley and Sons") consists of your license details and the terms and conditions provided by John Wiley and Sons and Copyright Clearance Center.

<b>License Number</b>	4732620790261
<b>License date</b>	Dec 19, 2019
<b>Licensed Content Publisher</b>	John Wiley and Sons
<b>Licensed Content Publication</b>	Clinical Anatomy
<b>Licensed Content Title</b>	Nerve dysfunction leads to muscle morphological abnormalities in chronic inflammatory demyelinating polyneuropathy assessed by MRI
<b>Licensed Content Author</b>	Kevin J. Gilmore, Jacob Fanous, Timothy J. Doherty, et al
<b>Licensed Content Date</b>	Oct 30, 2019
<b>Licensed Content Volume</b>	33
<b>Licensed Content Issue</b>	1
<b>Licensed Content Pages</b>	8
<b>Type of use</b>	Dissertation/Thesis
<b>Requestor type</b>	Author of this Wiley article
<b>Format</b>	Print and electronic
<b>Portion</b>	Full article
<b>Will you be translating?</b>	No
<b>Title of your thesis / dissertation</b>	The effects of Chronic Inflammatory Demyelinating Polyneuropathy on the Neuromuscular System in Humans.
<b>Expected completion date</b>	Jan 2020
<b>Expected size (number of pages)</b>	180
<b>Publisher Tax ID</b>	EU826007151
<b>Total</b>	0.00 CAD



# Curriculum Vitae

**Kevin J. Gilmore**

PhD Candidate

School of Kinesiology, Faculty of Health Sciences

The University of Western Ontario

London, Ontario N6K 3K7

Canada

## **EDUCATIONAL EARNED DEGREES**

### **Doctorate of Kinesiology (Ph.D.)**

The University of Western Ontario (London ON, Canada)

January 2014- March 2020. (Fast Tracked to from Masters to PhD Program)

### **Bachelor of Health Sciences (B.H.Sc Hons) Specialization in Rehabilitation Sciences**

The University of Western Ontario (London ON, Canada)

September 2009-2014

## **AWARDS and HONOURS**

2019	FHS Western Travel Award
2018	FHS Western Travel Award
2017	NSERC Alexander Graham Bell Scholarship CGS –D 3 year (\$105,000)
2017	Ontario Graduate Scholarship (declined)
2017	FHS Graduate Tri-Council Scholarship Incentive (\$1000)
2017	FHS Western Travel Award
2016/2017	Western Graduate Research Scholarship (WGRS)
2016/2017	Ontario Graduate Scholarship (accepted)

2016 scholarship) in	The American Physiological Society Select (distinction in the Journal of Applied Physiology)
2015/2016 (\$17,500)	NSERC Alexander Graham Bell Scholarship CGS-M 1 year
2015/2016	Ontario Graduate Scholarship (declined)
2015/2016	Western Graduate Research Scholarship (WGRS)
2015	Canadian Society of Exercise Physiology (poster Award)
2015	FHS Western Graduate Travel Award
2014/2015	Western Graduate Research Scholarship (WGRS)
2013	Dean's Honor Roll The University of Western Ontario
2012	Dean's Honor Roll The University of Western Ontario
2011	Dean's Honor Roll The University of Western Ontario
2011	Founders Award The University of Western Ontario

## **PUBLICATIONS**

1. **Gilmore K.J**, Kirk E.A, Doherty T.J Kimpinski K, Rice C.L. (2019). Abnormal motor unit firing rates in chronic inflammatory demyelinating polyneuropathy. (submitted to Journal of Neurological Sciences Dec 6, 2019)
2. **Gilmore K.J**, Fanous J, Doherty T.J, Kimpinski K, Rice C.L. (2019). Nerve dysfunction leads to muscle morphological abnormalities in chronic Inflammatory demyelinating polyneuropathy assessed by MRI. Clinical Anatomy (CA-19-0336) In Press Sept 15<sup>th</sup>, 2019
3. Kirk E.A, **Gilmore K.J**, Stashuk D.W, Doherty T.J, Rice C.L. (2019). Human motor unit characteristics of the superior trapezius muscle with age-related comparisons. Journal of Neurophysiology. 122 (2): 823-832

4. **Gilmore K.J**, Doherty T.J, Kimpinski K, Rice C.L. (2018). Reductions in muscle quality and quantity in chronic inflammatory demyelinating polyneuropathy patients assessed by magnetic resonance imaging. *Muscle and Nerve*. 58 (3): 396-401
5. **Gilmore K.J**, Kirk E.A, Doherty T.J, Rice C.L. (2018). Effect of very old age on anconeus motor unit loss and compensatory remodeling. *Muscle and Nerve*. 57 (4): 659-663
6. Power G.A, Dalton B.H, **Gilmore K.J**, Allen M.D, Doherty T.J, Rice C.L. (2017). Maintaining motor units into old age: running the final common pathway. *European Journal of Translational Myology*. 1 (27): 71-73
7. Kirk E.A, **Gilmore K.J**, Rice C.L. (2017). Neuromuscular changes of the aged human hamstrings. *Journal of Neurophysiology*. 120 (2): 480-488
8. Power G.A, Allen M.D, **Gilmore K.J**, Stashuk D.W, Doherty T.W, Hepple R.T, Taivassalo T, Rice C.L. (2016). Motor unit numbers and transmission stability in octogenarian world class athletes: can age related deficits be outrun? *Journal of Applied Physiology*. 121 (4): 1013-1020
9. **Gilmore K.J**, Morat T, Doherty T.J, Rice C.L. (2016). Motor unit number estimations and neuromuscular fidelity in three stages of sarcopenia. *Muscle and Nerve*. 55 (5): 676-684
10. **Gilmore K.J**, Allen M.D, Doherty T.J, Kimpinski K, Stashuk D.W, Rice C.L. (2016). Electrophysiological and neuromuscular properties of persons with chronic inflammatory demyelinating polyneuropathy (CIDP). *Muscle and Nerve*. 56 (3): 413-420
11. Morat T, **Gilmore K.J**, Rice C.L. (2016). Neuromuscular function in different stages of sarcopenia. *Journal of Experimental Gerontology*. (81): 28-36
12. Xu S.X, **Gilmore K.J**, Szabo P, Zeppa J.J Baroja M.L, Haeryfar S.M.M, McCormick J.K. (2014). Superantigen-mediated CD11b+Ly6G+ neutrophil influx into the liver enhances abscess formation to promote *Staphylococcus aureus* survival in vivo. *Infection and Immunity*. 82 (9): 3588-98

## **PUBLISHED JOURNAL REPLIES**

1. Kirk EA, **Gilmore K.J**, Rice C.L. (2018). An objective criterion for stimulation intensity may be necessary to properly assess muscle contractile properties. *Journal of Neurophysiology*. 6 (120): 3288
2. **Gilmore K.J**, Morat T, Doherty T.J, Rice C.L. (2017). Reply to motor unit number estimations and neuromuscular fidelity in three stages of sarcopenia. *Muscle and Nerve*. 930-931

## **PUBLISHED AND PRESENTED ABSTRACTS**

1. **Gilmore K.J**, Kimpinski K, Rice C.L (2019) Microscopic muscle architecture in chronic inflammatory demyelinating polyneuropathy. *Canadian Society for Exercise Physiology (CSEP) Appl. Physiol. Nutr. Metab.* 44(10): S75. (**Oral presentation**)
2. Jacqueline Chevalier, Hao Yin, John-Michael Arpino, Caroline O'Neil, Zengxuan Nong, **Kevin Gilmore**, Jason Lee, Emma Prescott, Matthew Hewak, Charles L Rice, Luc Dubois, Adam H Power, Douglas W Hamilton, Geoffrey Pickering (2019) Microvascular stenosis in end-stage peripheral artery disease: role of partial endothelial to mesenchymal transition submitted Abstract to 2019 Canadian Vascular and Lipid Summit. (**Poster presentation**)
3. Chevalier J, Arpino J-M, Yin H, Prescott E, O'Neil C, Nong Z, **Gilmore K.J**, Lee J, Hewak M, Rice C.L, Dubois L, Power A, Hamilton D, Pickering G (2019) - Microvascular stenosis in end-stage peripheral artery disease: role of partial endothelial to mesenchymal transition *Arteriosclerosis, Thrombosis, and Vascular Biology*; 39: A242 (**Oral presentation**)
4. Fanous J, **Gilmore K.J**, Kimpinski K, Rice C.L (2018) An MRI investigating of the lower limb musculature in patients with chronic inflammatory demyelinating (**Poster presentation**) *The FASEB J.* vol. 33 no.1 Supplement 2

5. Kirk, E.A, **Gilmore K.J**, Rice, C.L (2018) Motor unit firing rates during dynamic isokinetic fatiguing contractions in young and old men (**Poster presentation**) Appl. Physiol. Nutr. & Metab. 43: 10 (Suppl. 2): S69
6. Kirk, E.A, **Gilmore K.J**, Doherty, T.J, Stashuk, D.W, Rice, C L (2018) Ageing. It's a trap! Neuromuscular properties of the superior trapezius. (**Poster presentation**) Proceedings of the XXii Congress of the International Society of Electrophysiology & Kinesiology (ISEK), PII.47, p.130
7. Fanous J, **Gilmore K.J**, Kimpinski K, Rice C.L (2018) Investigating the triceps surae in chronic inflammatory demyelinating polyneuropathy patients using magnetic resonance imaging. Experimental Biology Annual Meeting (**Poster presentation and award**) The FASEB J. vol. 32 no. 1 Supplement 641.2
8. **Gilmore K.J**, Kirk E.A, Kimpinski K, Rice C.L (2017) Chronic inflammatory demyelinating polyneuropathy: weakness associated with reductions in motor unit discharge rates. Canadian Society for Exercise Physiology (CSEP) (**Poster presentation**) Appl. Physiol. Nutr. & Metab. 42: 10 (Suppl.): S76
9. **Gilmore K.J**, Kirk E.A, Rice C.L (2017) Is there a cessation of motor unit remodeling as a compensatory strategy to age-related motor unit loss? American College of Sports Medicine (**Poster presentation**) Med. Sci. Sports and Ex. (Suppl 1. Vol. 49, No. 5) p. 1031
10. **Gilmore K.J**, Kimpinski K, Doherty T.J, Rice C.L (2016) Chronic inflammatory demyelinating polyneuropathy weakness is associated with reduced muscle mass and motor unit loss. Society for Neuroscience, (**Poster presentation**) Program No. 441.11/ ZZ3 Neuroscience Meeting Planner
11. **Gilmore K.J**, Kimpinski K, Stashuk D.W, Doherty T.J, Rice C.L (2016) Chronic inflammatory demyelinating polyneuropathy: muscle atrophy associated with denervation and neuromuscular transmission instability. Experimental Biology Annual Meeting (**Poster presentation**) The FASEB J. vol. 30 no. 1 Supplement 991.7

12. **Gilmore K.J**, Doherty T.J, Kimpinski K, Stashuk D.W, Rice C.L (2015) Electrophysiological and neuromuscular properties of persons with chronic inflammatory demyelinating polyneuropathy (CIDP). CSEP Annual Meeting (**Poster presentation & poster award**) Appl. Physiol. Nutr. & Metab. 40: (9 (Suppl. 1): S25
13. **Gilmore K.J**, Allen M.D, Stashuk D.W, Rice C.L (2015) Neuromuscular transmission stability in very old world-class master's athletes. 62<sup>nd</sup> ACSM Annual Meeting (**Poster presentation**) **Med. Sci. Sport and Exercise**. (Suppl 1. 47, No. 5) p.864

#### **UNPUBLISHED PRESENTED ABSTARCTS**

1. **Gilmore K.J**, Kimpinski K, Rice C.L (2019) Microscopic muscle architecture in chronic inflammatory demyelinating polyneuropathy. Exercise Neuroscience Group Meeting Hamilton ON (**Oral presentation**)
2. **Gilmore K.J**, Kimpinski K, Doherty T.J, Rice C.L (2018) The effects of demyelination in chronic inflammatory demyelinating polyneuropathy (CIDP) on neuromuscular properties, muscle quantity and quality. First International Motor Impairment meeting Sydney Australia (**Oral presentation**)
3. **Gilmore K.J**, Kirk E.A, Kimpinski K, Doherty T.J, Rice C.L (2018) Alterations in motor unit firing rates in patients with chronic inflammatory demyelinating polyneuropathy. International Motorneuron Society (IMS) Boulder Colorado (**Poster presentation**)
4. **Gilmore K.J**, Kimpinski K, Stashuk D.W, Doherty T.J, Rice C.L (2015) chronic inflammatory demyelinating polyneuropathy: muscle atrophy associated with denervation and neuromuscular transmission instability. London Health Research Day: TOFS (**Oral presentation**)

5. **Gilmore K.J.**, Doherty T.J, Kimpinski K, Stashuk D.W, Rice C.L (2015) Electrophysiological and neuromuscular properties of persons with chronic inflammatory demyelinating polyneuropathy (CIDP). Exercise Neuroscience group meeting Guelph ON (**Oral Presentation**)
6. Xu S.X, **Gilmore K.J.**, Szabo P, Baroja M.L, Haeryfar S.M, McCormick J.K (2012) Superantigens promote abscess formation and bacterial survival in the liver during Staphylococcus aureus sepsis. London Health Research Day (**Poster Presentation/Oral Presentation**)
7. **Gilmore K.J.**, McCormick J.K. (2013) Polarizing invariant natural killer T cells towards a Th2 phenotype reduces disease severity in intra-abdominal sepsis. The American College of Surgeons Clinical Congress, Washington, D.C. (**Poster presentation**)
8. Anantha RV, Mazzuca D, Xu S.X, **Gilmore K.J.**, Shrum B, Mele T, Fraser D, Martin C, Haeryfar S.M, McCormick J.K. (2013) Polarizing invariant natural killer T cells towards a Th2 phenotype reduces disease severity in intra-abdominal sepsis. The Canadian Surgical Forum, Ottawa, ON (**Oral presentation**)
9. Anantha R.V, Mazzuca D, Xu S.X, **Gilmore K.J.**, Shrum B, Mele T, Fraser D, Martin C, Haeryfar S.M, McCormick J.K. (2013) Th2-polarized invariant natural killer T cells reduce disease severity in intra-abdominal sepsis. Clinician Investigator Trainee Association of Canada/Canadian Society for Clinical Investigation Annual Meeting, Ottawa, ON (Second Place Winner). (**Poster presentation**)
10. Anantha R.V, Mazzuca D, Xu S.X, **Gilmore K.J.**, Shrum B, Mele T, Fraser D, C Martin C, Haeryfar S.M, McCormick J.K. (2013) Polarizing invariant natural killer T cells towards a Th2 phenotype reduces disease severity in intra-abdominal sepsis. Clinician Investigator Training Association of Canada Young Investigators Forum, Ottawa, ON (**Oral presentation**)
11. Anantha R.V, Mazzuca D, Xu S.X, **Gilmore K.J.**, Shrum B, Mele T, Fraser D, Martin C, Haeryfar S.M, McCormick J.K. (2013) Polarizing invariant natural killer T

cells towards a Th2 phenotype reduces disease severity in intra-abdominal sepsis.  
The Annual Robert Zhong Department of Surgery Research Day, London, ON  
**(Poster presentation)**

12. Anantha R.V, Mazzuca D, Xu S.X, **Gilmore K.J**, Shrum B, Mele T, Fraser D, Martin C, Haeryfar S.M, McCormick J.K. (2013) Polarizing invariant natural killer T cells towards a Th2 phenotype reduces disease severity in intra-abdominal sepsis. General Surgery Residents Research Day, Division of General Surgery, London, ON. **(Oral presentation)**

13. Xu S.X, **Gilmore K.J**, Baroja M.L, Summers K, Haeryfar S.M, McCormick J.K. (2013) ‘Superantigen-mediated immune suppression in the liver during Staphylococcus aureus sepsis’ 8<sup>th</sup> Annual Infection and Immunity Research Forum London, ON, Canada, **(Oral presentation)**

14. Xu S.X, **Gilmore K.J**, Baroja M.L, Summers K, Haeryfar S.M, McCormick J.K. (2013) ‘Superantigen-mediated immune suppression in the liver during Staphylococcus aureus sepsis’ Staphylococcal Disease Gordon Research Conference **(Poster presentation)**

15. Xu S.X, **Gilmore K.J**, Baroja M.L, Summers K, Haeryfar S.M, McCormick J.K. (2013) ‘Superantigen-mediated immune suppression in the liver during Staphylococcus aureus sepsis’ 26<sup>th</sup> Annual Canadian Student Health Research Form **(Poster presentation)**

### **INVITED SEMINARS AND LECTURES**

Memorial University - Invited seminar speaker: Biomedical Sciences division in the Faculty of Medicine St. Johns Newfoundland (March 24<sup>th</sup>, 2019)

Western University - Guest lecturer in an undergraduate class Anatomy and Cell Biology ACB 2221(Oct 18<sup>th</sup>, 2018)

Los Angeles Biomedical Research Institute - Invited seminar speaker: Divisional Research Group at Harbor- UCLA Medical Center: Motor Unit Number Estimations In Different Populations, Including Disease. (April 27<sup>th</sup> 2018)



Invited - Motor Impairment blog posting lead author  
<https://motorimpairment.neura.edu.au>

Laurier University - Invited guest lecturer for a graduate course: Selected topics in Neuromechanics of Human Movement (KP 697) 12 July 2017 Decomposition based Quantitative Electromyography (DQEMG) (MSc/PhD) workshop

Western University - Mentored a visiting Master's student to learn a neuromuscular technique (Decomposition based Quantitative Electromyography) (DQEMG) (Sept-Oct, 2016)

Western University - Guest Lecturer: undergrad/graduate Neuromuscular Physiology course KIN4421 (Oct 16, 2016)

### **CERTIFICATIONS**

Accessibility at Western (AODA)	09/12/2019
Supervisor Health and Safety Awareness	09/12/2019
Comprehensive WHMIS	09/12/2019
Laboratory-Environmental Waste Management Safety Training	09/12/2018
Biosafety Training	09/12/2018
Safe Campus Community	09/12/2016
Certified Phlebotomist	08/17/2016
Community First Aid	04/30/2014
Basic CPR-Red Cross	06/22/2014

### **ACVS Animal care and use**

Basic Rodent Handling  
Basic Mouse or Rat Workshop  
Mouse or Rat Anesthesia  
Gas Anesthesia  
Blood Collection Techniques in Mouse or Rat  
Techniques in Mouse or Rat  
Recovery Mouse or Rat Surgery Room Methodology I and II  
Surgical Pack Preparation  
Microtome training (tissue prep and sectioning)  
Light Microscope training (Fluorescent Light Microscopy)  
Cryostat Training (tissue prep and sectioning)  
Monitoring Assessment and Intervention

### **VOLUNTEER EXPERIENCE**

Student Academic Orientation session leader (Western University) 2012-2018

Let's Talk Science instructor (grades 4 and 5) 2013  
Student Volunteer at University Hospital, Victoria Hospital, Parkwood Hospital (London ON) and Strathroy Middlesex General Hospital (Strathroy ON) 2010-2014  
Addictions Treatment Center OATC (London ON) 2010-2012

### **REASERCH Related WORK EXPERIENCE**

**Teaching Assistant-** Anatomy and Cell Biology 2<sup>nd</sup> year gross cadaveric anatomy:  
Conducted weekly laboratory sessions in gross anatomical dissection, 2018

**Teaching Assistant-** Health Science 2<sup>nd</sup> year gross anatomy: Conducted weekly  
laboratory sessions in anatatorium, 2014-2015

**Junior Research Histologist- Company Sernova Inc.** (Supervisor: Delfina Siroen)  
Research Project: Cell pouch histological examinations. Phase III clinical study in  
subjects with diabetes; 2013-2014

**Work-Study Student** (Supervisor: Dr. John K. McCormick)  
Research Project: Superantigen-mediated immune suppression in the liver during  
Staphylococcus aureus sepsis'. 2011-2013

**Junior Research assistant- Company Sernova Inc.** (Supervisor: Delfina Siroen)  
Research Project: Cell pouch histological examinations. Phase I/II clinical study in  
subjects with diabetes; measuring of safety and efficacy. 2010-2012

**Work-Study Student** (Supervisor: Dr. John K. McCormick)  
Research project: Staphylococcal superantigens in colonization and disease. 2010-2011

**Summer Student** (Supervisor: Dr. John K. McCormick)  
Research project: Staphylococcal superantigens in colonization and disease. 2009-2010